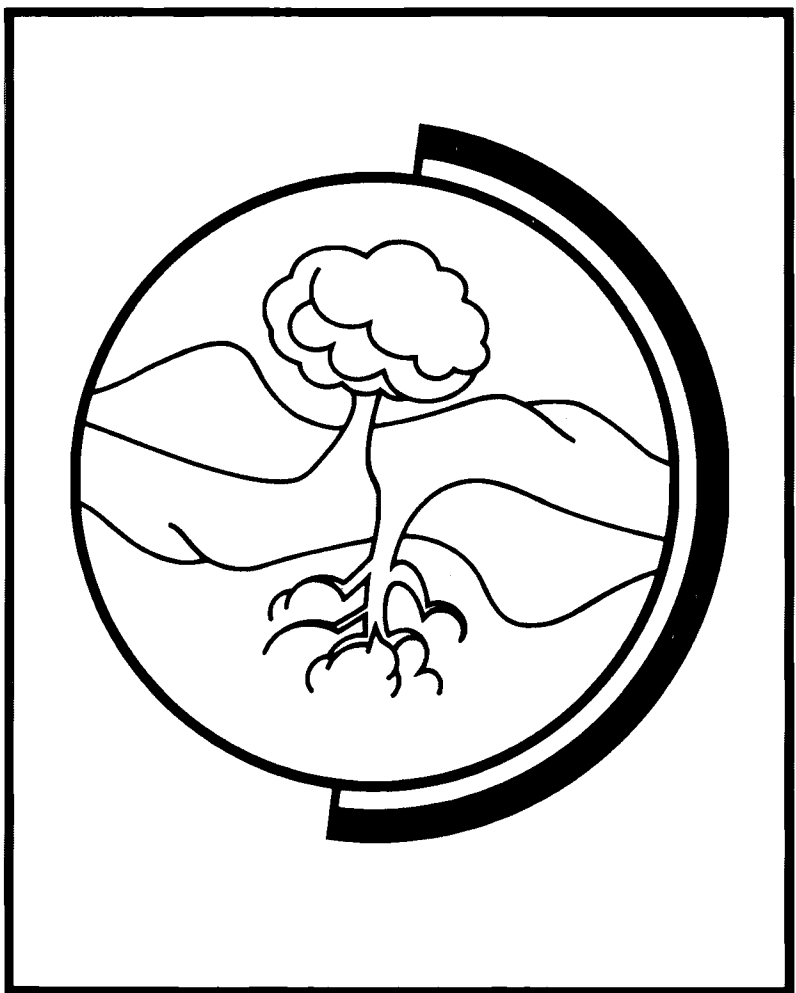# Design, Performance and Analysis of an Aquifer Thermal Energy Storage Experiment Using the Doublet Well Configuration

September 1983

❀❀Battelle

DISCLAIMER

DESIGN, PERFORMANCE AND ANALYSIS
OF AN AQUIFER THERMAL ENERGY
STORAGE EXPERIMENT USING THE DOUBLET
WELL CONFIGURATION

F. J. Molz
J. G. Melville
O. Güven
A. D. Parr

Department of Civil Engineering
Auburn University, Alabama 36849

September 1983

Pacific Northwest Laboratory
Richland, Washington 99352

FOREWORD

Seasonal thermal energy storage (STES) involves storing thermal energy, such as winter chill, summer heat, and industrial waste heat, for future use in heating and cooling buildings or for industrial processes. Widespread development and implementation of STES would significantly reduce the need to generate primary energy in the U.S. In fact, 1980 data indicate that STES is suitable for providing 5 to 10% of the nation's energy with major contributions in the commercial, industrial, and residential sectors.

Aquifer thermal energy storage (ATES) is predicted to be the most cost-effective technology for seasonal storage of low-grade thermal energy. Approximately 60% of the U.S. is underlain with aquifers potentially suitable for underground energy storage. Under sponsorship of the U.S. Department of Energy, Pacific Northwest Laboratory (operated by Battelle Memorial Institute) has managed numerical modeling, laboratory studies, evaluation of environmental and institutional issues, and field testing of ATES at several sites.

This report describes a series of ATES experiments undertaken by Auburn University under contract to Pacific Northwest Laboratory. The experiments were performed to characterize the key technical issues affecting performance of medium temperature ATES under conditions favorable to lower temperature ATES. The report describes and presents analyses of the last three, nominal 80°C test cycles, and briefly documents earlier testing at the site. The thermohydraulic performance of the aquifer as well as the geochemical and water quality aspects of the testing are discussed.

Although testing has been terminated at this site due to research funding reductions, the results indicate that, for high permeability aquifers, relatively sophisticated multiwell supply and injection

configurations and well field operations will be required to obtain acceptable performance at moderate temperatures. Testing of such multiwell configurations has not been undertaken in the U.S. and is not planned for the near future.

<div align="right">
Landis D. Kannberg, Manager
Underground Energy Storage Program
September 1983
</div>

SUMMARY

In March 1980 Auburn University began a series of aquifer thermal energy storage (ATES) experiments using the doublet well configuration. The test site, developed under prior DOE contracts, was in Mobile, Alabama. The objectives of the three experimental cycles were to demonstrate the technical feasibility of the ATES concept, to identify and resolve operational problems, and to acquire a data base for developing and testing mathematical models.

Pre-injection tests were performed and analyses of hydraulic, geochemical, and thermodynamic data were completed. Three injection-storage-recovery cycles had injection volumes of 25,402 m³, 58,010 m³, and 58,680 m³ and average injection temperatures of 58.5°C, 81.0°C, and 79.0°C, respectively. The first cycle injection began in February 1981 and the third cycle recovery was completed in November 1982.

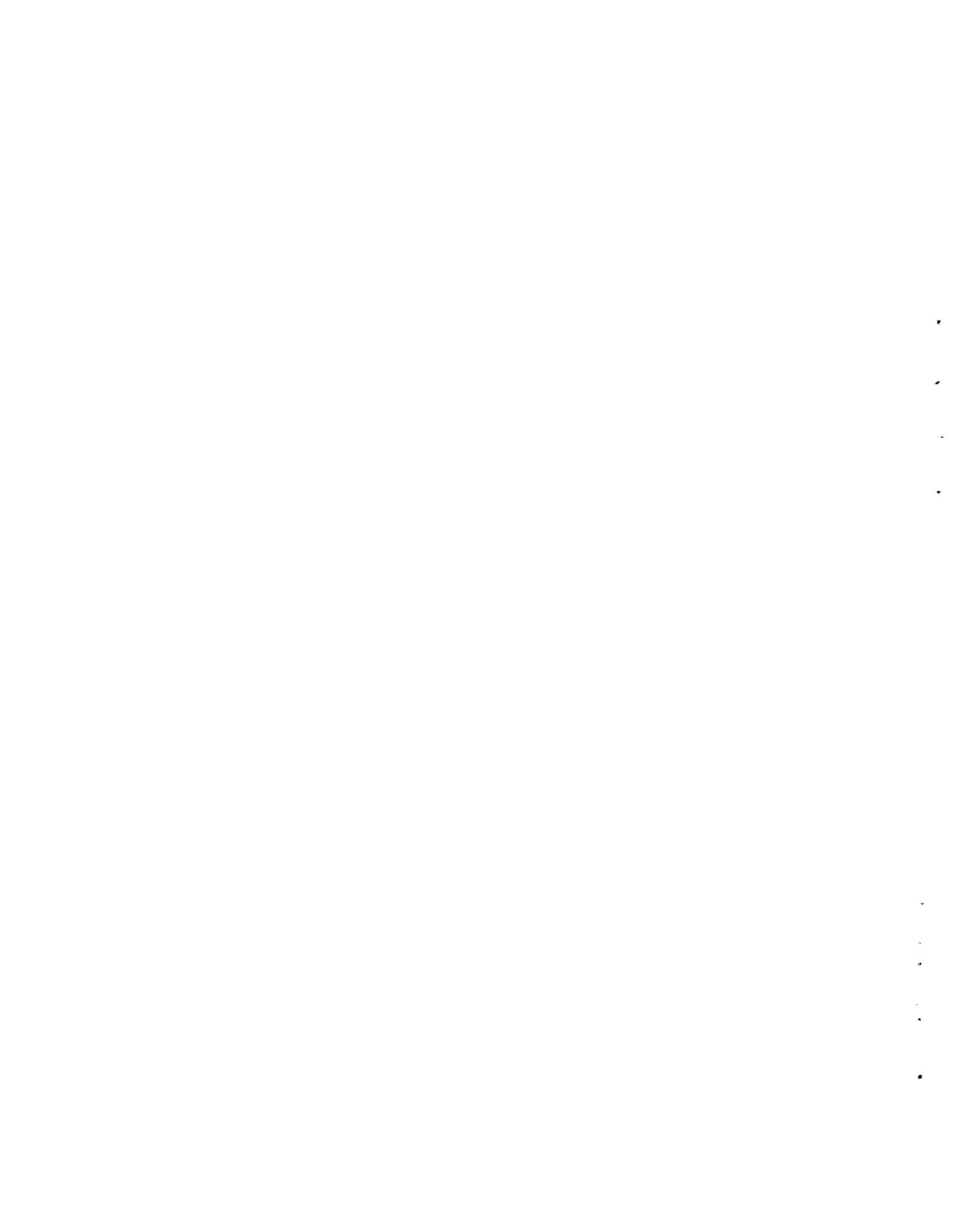Attributable to the doublet well configuration no clogging of injection wells occurred. Energy recovery percentages based on recovery volumes equal to the injection volumes were 56, 45, and 42%. Thermal convection effects were observed. Aquifer nonhomogeneity, not detectable using standard aquifer testing procedures, was shown to reduce recovery efficiency.

ACKNOWLEDGMENTS

CONTENTS

FIGURES

TABLES

NOMENCLATURE

A $A = Q/2\pi bn$

b   aquifer thickness, m

b'   aquitard thickness, m

c_w volumetric heat capacity of water, kcal/m^3/°C

c_{va} volumetric heat capacity of aquifer, including solid and liquid, kcal/m^3/°C

c_s specific heat of solid, kcal/m^3/°C

c   tracer concentration, mg/ℓ

c_o injection tracer concentration, mg/ℓ

d   length of pumping well casing in the aquifer from the top of the aquifer to the top of the screen, Figure 3.1, m

erf(u)   error function

erf$_c$(u)   complimentary error function

f   dimensionless drawdown deviation due to anisotropy

f_{tc} match point value for type curve

f_{dc} match point value for data curve

Δf   correction factor

inverf   inverse of error function

K_z vertical permeability, m/day

K_r horizontal permeability, m/day

K'   aquitard vertical permeability, m/day

K_o modified Bessel function of second kind and order zero

n   aquifer porosity

Q   pumping rate, m^3/day

r	distance from pumped well, m
r_1	distance from observation well to image well, m
r_c	$r = K_z/K_r$, m
S	storage coefficient
S_c	calculated storage coefficient
S'_s	aquitard specific storage, m^{-1}
s	drawdown, m
Δs	finite change in drawdown for change in logarithm of time, m
δ_s	drawdown deviation due to anisotropy, m
T	transmissivity, m^2/day
t	time; days, hours, or minutes
t_o	time when s = 0; days, hours, or minutes
t_D	$t_D = Tt/Sr^2$
t'_D	$t'_D = K't/S'_s z^2$
Δt	time interval, day
u	$u = r^2 S/4Tt$, pumping tests
u	$u = (r^2/2 - At)/(4\alpha r^3/3)^{1/2}$, dispersivity test
$\bar{v}$	pore velocity, m/day
$W(u)$	well function
z	vertical coordinate, m
z_w	distance from top of aquifer to bottom of screen for pumped well in the anisotropy test, Figure 3.1, m
α	longitudinal dispersivity, m or cm

α' aquitard hydraulic diffusivity (coefficient of consolidation), m^2/day

ρ_w density of water, kg/m^3

ρ_s density of solid, kg/m^3

DESIGN, PERFORMANCE, AND ANALYSIS OF
AN AQUIFER THERMAL ENERGY STORAGE
EXPERIMENT USING THE DOUBLET
WELL CONFIGURATION

1.0 INTRODUCTION

An underground rock formation that both stores and transmits water is called an aquifer. Aquifers can be composed of many different materials such as limestone, fractured granite, sandstone or, quite commonly, loose sand (Bouwer 1978). If hot or chilled water is pumped into an aquifer, stored for a period of time, and then recovered, one has an example of an aquifer thermal energy storage (ATES) system. The major purpose of such a system is to store energy and thereby correct a mismatch between the availability and demand for heat or chill. Often this mismatch occurs on a seasonal basis.

The three main components of an ATES system for heating are the heat source, the storage aquifer, and the heat sink. Subsystems include the supply and injection wells, pumps, heat exchangers and piping. A typical duty cycle would be as follows. During a time of surplus heat, water is pumped from the supply well, heated in the heat exchanger, and reinjected into the storage aquifer. The water then remains stored for a period of weeks or months until a net demand for heat occurs. At this time, the hot water would be recovered from the aquifer, used to heat water going to the heat sink, such as a district heating system, and returned to the supply zone of the storage aquifer. After an optimal portion of the stored heat is utilized, the system would be ready for another injection-storage-recovery cycle. For the first several cycles, efficiency increases somewhat because of heat left behind in the storage zone from previous cycles. The temperature of the supply water increases also because not all heat removed from the aquifer is transferred to the heat sink.

Commercial use of ATES is uncommon but has existed for a number of decades at various locations in the world (Meyer 1982). Only recently, however, has an international effort been organized with the goal of developing dependable ATES design procedures. In the United States, this effort is funded largely by the U.S. Department of Energy (DOE) and managed by the Pacific Northwest Laboratory (PNL), operated for DOE by Battelle Memorial Institute. Research is motivated by the possibility that widespread development and implementation of ATES could significantly reduce the need to generate primary energy in the U.S. In fact, 1980 data indicate that ATES may be suitable for providing about 7% of the nation's energy with major contributions in the commercial, industrial, and residential sectors (Reilly 1980).

Many potential energy sources exist for use in an aquifer thermal energy storage system. These include solar heat, power plant cogeneration, winter chill, and industrial waste heat sources such as aluminum plants, paper and pulp mills, food processing plants, garbage incineration units, cement plants, and iron and steel mills. Energy sources ranging from 50°C to over 250°C are availabale for heating. Potential energy uses include space heating on a large individual building or district scale, heating for industrial or institutional plants and heat for processing/manufacturing.

Studies indicate that low temperature (<100°C) ATES has the greatest potential for near-term application. Furthermore, many geologists and ground-water hydrologists believe that heated and chilled water in the 0 to 100°C temperature range can be injected, stored, and recovered from aquifers. Geologic materials are good thermal insulators and potentially suitable aquifers are distributed throughout the world. However, technical and economic problems and uncertainties with ATES inhibit development and application of the technology in energy conservation programs. Aquifer responses to long-term injection, storage and recovery of heated and cooled water has not been adequately categorized. In addition, problems can occur such as permeability reduction due to physical and chemical effects, water quality degradation and loss of stored energy.

This report describes a series of ATES experiments undertaken to solve some of the technical problems and move ATES closer to useful applications. Section 2.0 presents background information on previous experiments conducted at the Mobile site. The data and observations from those earlier tests provide the rationale for the more current experiments discussed in subsequent sections. Section 3.0 describes the hydraulic, thermodynamic and chemical tests performed at the Mobile site. In section 4.0, the first and second injection-storage-recovery experiment cycles are documented and aquifer storage problems encountered with 80°C injection temperatures are discussed. Section 5.0 describes the third experimental cycle in which a selective recovery configuration was used and evaluated.

2.0 SCIENTIFIC AND TECHNICAL BACKGROUND FOR CURRENT EXPERIMENTS

Aquifer thermal energy storage (ATES) continues to receive international attention as a possible means for storing large amounts of energy at low cost and with little heat loss. There are experiments recently completed or presently underway in Canada, Denmark, France, Germany, Japan, Sweden, Switzerland and the United States. Many of these projects are concerned with practical application of the ATES concept for either heating or cooling. Current information on the international effort may be obtained from the proceedings of the October 1981 symposium on seasonal thermal energy storage (STES) organized by the Pacific Northwest Laboratory (U.S. Department of Energy 1981) and from the various quarterly issues of the STES Newsletter published by the Lawrence Berkeley Laboratory (Tsang 1981, 1982, 1983).

In the United States, experimental study of the ATES concept was started by Auburn University in 1975 at a test site in Mobile, Alabama (Molz, Warman and Jones 1978). Power station condenser cooling water at a temperature of about 36°C was injected into a confined aquifer, stored for one month and then recovered. The data generated by this experiment enabled the U.S. Geological Survey and others to make a preliminary test of several mathematical models designed to simulate the coupled transport of water and heat in an aquifer (Papadopulos and Larson 1978). However, the volume of water used in the experiment was too small (only 7,570 m^3) to adequately test the storage well concept. Nevertheless, the relatively high recovery factor[a] of 0.53 was promising.

In March 1978, a second round of experiments was begun at the Mobile test site (Molz et al. 1979, 1981). Two 6-month injection-storage-recovery cycles were performed. Using the supply-injection well configuration shown in Figure 2.1, 54,784 m^3 of water were pumped from a shallow supply

---

[a]The recovery factor is defined as the ratio of the energy recovered to the energy injected in a volume of water equal to the injection volume.
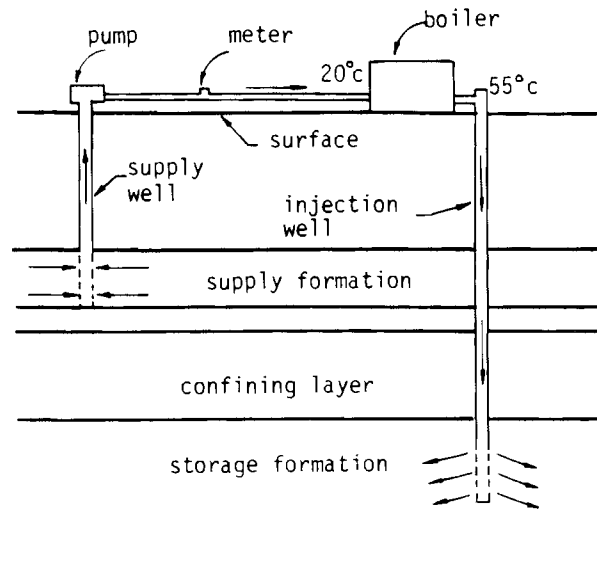
FIGURE 2.1. System for Supplying, Heating, and Injecting Water into the Storage Aquifer During the 1978-79 Experiments at the Mobile Test Site

aquifer heated to an average temperature of 55°C, and injected into a deeper confined aquifer where the ambient temperature was 20°C. After a 51-day storage period, 55,345 m^3 of water were produced from the confined aquifer. Throughout the experiment, which lasted approximately six months, groundwater temperatures were recorded at six depths in each of 10 observation wells, and hydraulic heads were recorded in five observation wells. To prevent errors due to thermal convection, most of the observation wells recording temperature had to be backfilled with sand. During the 41-day production period, the temperature of the produced water varied from 55°C to 33°C, and 66% of the injected thermal energy was recovered. At no time was an appreciable amount of free thermal convection observed in the storage formation. The dominant heat dissipation mechanisms appeared to be hydrodynamic thermal dispersion and possible mixing of cold and hot water induced by clogging and unclogging of the injection-production well.

On the basis of laboratory and field studies, it was concluded that clogging of the injection well, which constituted the major technical problem during the experiment, was caused by the freshwater-sensitive nature of the storage aquifer. The relatively low concentration of cations in the supply water caused clay particles to swell, disperse, and migrate until they become trapped in the relatively small pores connecting the larger pores (Brown and Silvey 1977, van Olphen 1963). Surging the pump and backwashing the injection well dislodged the clogging particles and temporarily improved the storage formation permeability. The phenomenon is apparently largely independent of temperature because it was reproduced in the laboratory with unheated water. However, it may depend on pore velocity.

The second cycle injection, performed in a manner similar to the first, began on September 23, 1978 and continued until November 25, 1978, when 58,010 m^3 of water had been pumped into the storage aquifer. The major problem experienced during the first cycle, a clogging injection well, was reduced by regular backwashing. This backwashing was done eight times during injection and resulted in a 24% average injection rate increase compared to the first cycle. A 63-day storage period ended on January 27, 1979 and production of hot water began with an initial temperature of 54°C. By March 23 this temperature had dropped to 33°C, with 66,400 m^3 of water and 76% of the injected thermal energy recovered. This compares to 66% recovery during the first cycle over the same drop in production temperature. Production of hot water continued until April 20, at which time 100,100 m^3 of water and 89% of the injected thermal energy were recovered at a final production temperature of 27.5°C. During the second cycle, relative land subsidence and rebound were measured to a precision approaching 0.1 mm. It was found that the surface elevation near the injection well rose 4 mm during injection, fell slowly during storage, and dropped more rapidly toward its original elevation during production. This movement was due to thermal expansion and contraction rather than head changes in the storage aquifer.

The observations summarized above indicate that clogging of the injection-production well during injection was an important negative result of past experiments. Molz, Warman and Jones (1978) and others have suggested that using water from the storage aquifer as supply water for the boiler or other heating system would minimize clogging problems. In this case, the major difference between the water to be stored and the water displaced in the formation would be temperature, which would suppress geochemical phenomena that could lead to clogging.

Drilling the supply well and the injection-production well in the same formation leads to what is called the doublet configuration. This scheme, shown in Figure 2.2, has advantages in addition to those related to geochemistry. Residual heat left in the production water is partially saved by reinjecting it into the supply well. After several injection-storage-recovery cycles, a warm ground-water zone builds up around the supply well and a hotter zone around the injection-production well. This leads to more efficient system operation. Over time, there is no significant addition or subtraction of ground water from any aquifer in the vicinity of the thermal energy storage site. Thus, little or no land subsidence should occur due to pressure changes in aquifers. However, some rising and falling of the land surface could occur from thermal expansion and contraction of saturated clays (Molz et al. 1979).

The doublet configuration has at least two potential disadvantages. Because the supply well is also used as an injection well for spent recovery water, two injection processes will occur simultaneously. Thus, there is a potential clogging problem at both the supply well and the injection-production well. In addition, the supply and injection wells must be sufficiently separated so that "short circuiting" does not occur. This requires using relatively more extensive land area.

If aquifer storage of thermal energy becomes feasible on a commercial scale, however, it seems likely that a system based on the doublet configuration will offer distinct advantages. Therefore, a real need exists to study the concept experimentally so that potential advantages and

SEASONAL THERMAL ENERGY STORAGE

HEAT RECOVERY CYCLE
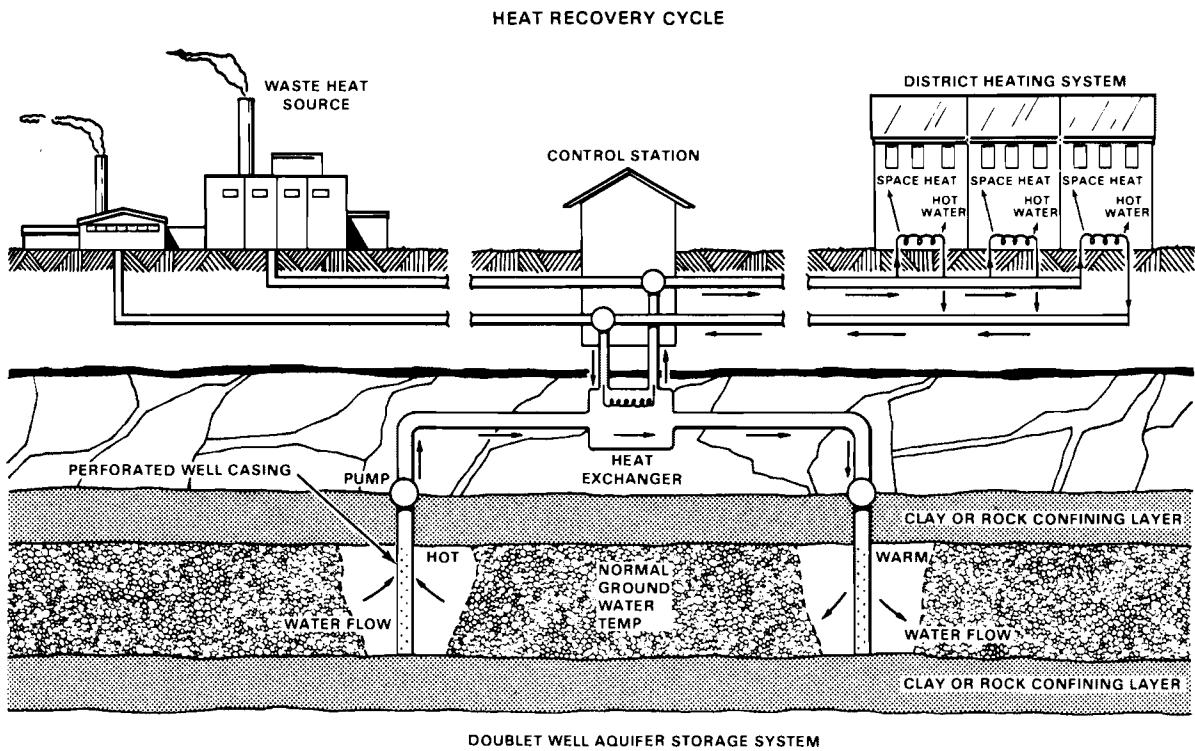
FIGURE 2.2. Aquifer Thermal Energy Storage System Based on the Doublet Supply-Injection Well Configuration

disadvantages can be identified clearly before major amounts of money are invested. Reporting such a study is a major objective of this document.

There are obvious advantages to storing water at higher temperatures. However, potential problems arise also. Detrimental chemical reactions, if any, will accelerate with temperature. In addition, the density of water decreases with temperature, and buoyancy-induced flow (free thermal convection) could become important. Convection could have a marked negative effect on energy recovery because the relatively light hotter water would float to the top of the aquifer and spread laterally. Recovery pumping would then mix hot water from the top of the aquifer with cold water from the bottom. A second major objective of this report is to document aquifer storage problems at the Mobile site with injection temperatures in the 80°C range.

Determination of the suitability of the specific confined aquifer requires performing a variety of hydraulic, thermodynamic and chemical tests. Important parameters include the regional hydraulic gradient, vertical and horizontal permeability of the storage aquifer, horizontal dispersivity, vertical permeability of the upper and lower aquitards, thermal conductivities, heat capacities and chemical characteristics of the aquifer matrix and native ground water.

Most chemical and thermodynamic tests can be performed in the laboratory using core samples and ground-water samples. Permeability and dispersivity measurements, however, are best performed in the field using a variety of available pumping tests and data reduction procedures. The resulting data can serve as a basis for developing a conceptual design of a proposed aquifer storage system and estimating its thermal efficiency. Also, attempts can be made to anticipate any geochemical problems (e.g., corrosion, precipitation, solution, clay swelling) that may occur.

A third objective of this report is to describe the hydraulic, thermodynamic and chemical tests performed at the Mobile site. These procedures constitute a fairly complete program for obtaining the data necessary for determining the potential of a confined aquifer for thermal energy storage.

3.0 PRE-INJECTION AQUIFER TESTING

The project site is located in a soil borrow area at the Barry Steam Plant of the Alabama Power Company, about 32 km north of Mobile, Alabama [see Molz, Warman and Jones (1978) for details]. The surface zone comprises of a low-terrace deposit of Quaternary age consisting of interbedded sands and clays that have, in geologic time, been recently deposited along the western edge of the Mobile River. These sand and clay deposits extend to a depth of approximately 61 m where the contact between the Tertiary and Quaternary geologic eras is located. Below the contact, deposits of the Miocene series are found that consist of undifferentiated sands, silty clays, and thin-bedded limestones extending to an approximate depth of 305 m.

The well field was established in the Quaternary deposits. Based on drilling logs, the fence diagram shown in Figure 3.1 was constructed. Each vertical line on the diagram represents a well of some type. These wells were screened in the sand formation, which extends from approximately 30 to 61 m below the land surface. This formation constitutes the confined aquifer used for thermal energy storage. Details of aquifer and observation well geometry are given in the Appendix.

At the beginning of a serious site evaluation, one usually has a rough idea of the potential storage aquifer geometry. The objective is to determine if the various parameter values at the site are such that the aquifer and confining layers are compatible with the requirements of thermal energy storage.

3.1 AQUIFER HYDRAULIC TESTING

The initial hydraulic tests performed at a potential site should include a short-duration standard pumping test using a single observation well followed by a precise set of measurements of piezometric head for at least three observation wells. Such tests will provide the data needed to determine hydraulic conductivity and the hydraulic gradient by the well

Scale in meters

SAND & CLAY
SAND
SAND & GRAVEL
CLAY
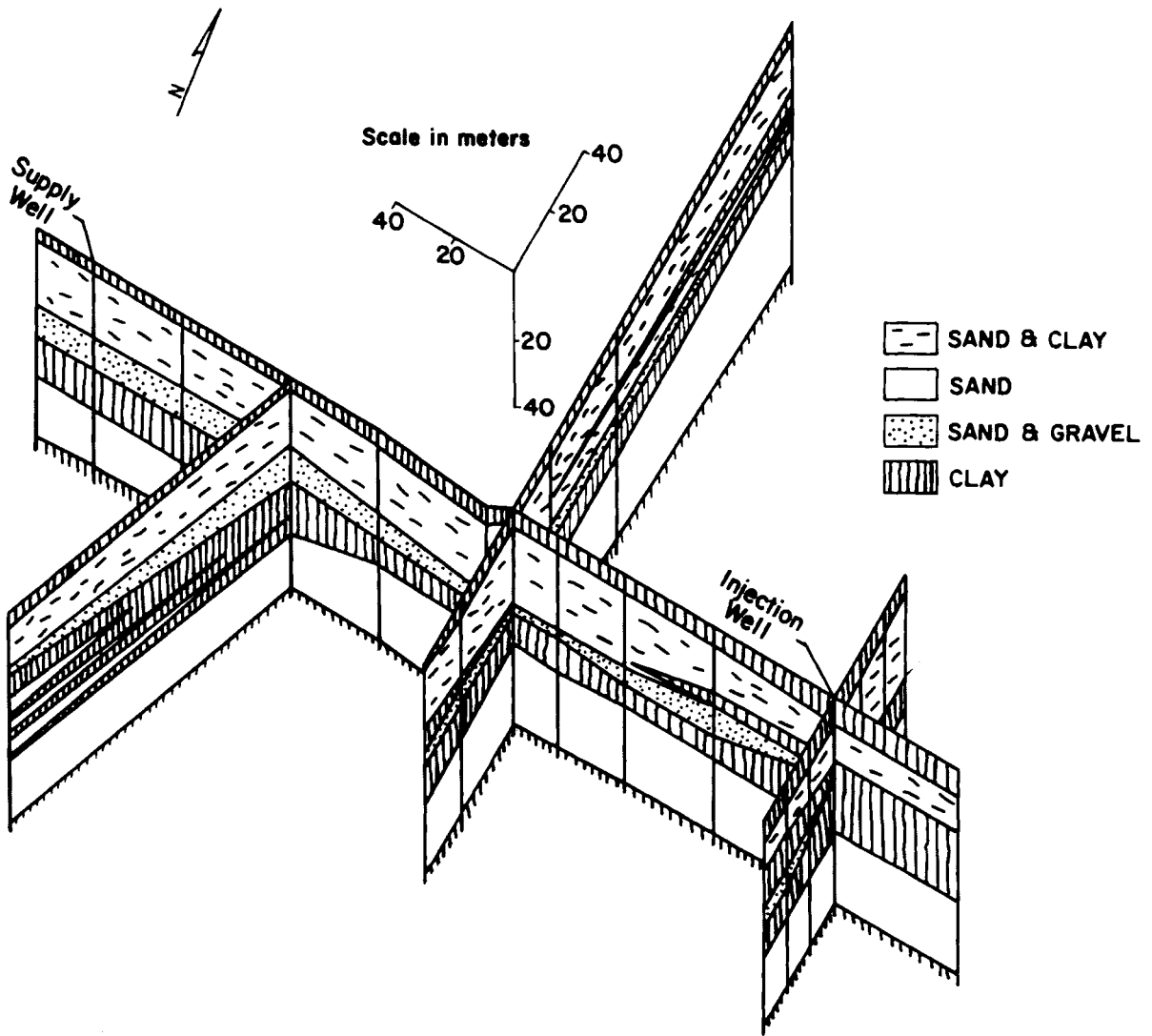
FIGURE 3.1. Fence Diagram Constructed from Well Logs at Mobile Site

triangulation method (Todd 1980). These parameters, together with the porosity, can be used to calculate the natural pore velocity and storage zone drift. Acceptable spacings for the observation wells used in defining the piezometric surface are dependent on both the precision of the leveling instruments and on the magnitude of the hydraulic gradient at the site. The following procedure can minimize the possibility of having to construct extra observation wells because the initial wells were not spaced properly.

Storage zone drift during a time interval Δt is equal to $\bar{v}\Delta t\, n\, C_w/C_{va}$ where $\bar{v}$ = the pore velocity, n = aquifer porosity, C_w = volumetric heat capacity of water and C_{va} = the volumetric heat capacity of the entire aquifer, which includes solid and liquid. For a given injection-storage-recovery time sequence, one can decide on a maximum acceptable storage zone drift. Knowing the hydraulic conductivity and porosity, one can calculate the maximum tolerable gradient. Then two additional observation wells can be located so that a gradient equal to or greater than the maximum tolerable can be measured with available instrumentation. A more careful procedure would assure the ability to measure some fraction of the maximum tolerable gradient. The main consideration is to avoid placing the observation wells so close together that the maximum tolerable gradient cannot be measured due to exceedingly small differences in water levels.

At the Mobile site, the latest measurement indicated a regional gradient of 3.3×10^{-4} m/m. This value, along with a porosity of 0.33, a hydraulic conductivity of 53.6 m/day, a volumetric aquifer heat capacity of 661 kcal/m^3°C, and a volumetric water heat capacity of 1000 kcal/m^3°C, yields a storage zone drift of approximately 0.8 m/month. This drift is small compared with a planned storage zone radius in excess of 50 m and a six-month injection-storage-recovery cycle.

After the regional gradient was determined, several types of pumping and dispersivity tests were performed and analyzed using a variety of classical and modern methods. Classical pumping test procedures (Ferris et al. 1962) are still very applicable and several were performed. However,

more recently-developed procedures were required to determine parameters such as vertical to horizontal permeability ratio and aquitard vertical permeability. The pumping tests performed and their objectives are outlined in Table 3.1 and described fully in the next three subsections. Dispersivity tests are detailed in Section 3.1.4.

TABLE 3.1. Parameters Obtainable from Pumping Tests Performed at the Mobile Site

Test Type	Measurements Obtained
Anisotropy Pumping Test	Horizontal permeability of aquifer Storage coefficient of aquifer Vertical permeability of aquifer
Standard Pumping Test	Horizontal permeability of aquifer Storage coefficient of aquifer Location of lateral boundaries
Leaky Aquifer Pumping Test	Horizontal permeability of aquifer Storage coefficient of aquifer Vertical hydraulic diffusivity of aquitards

It should be noted that the analyses of all tests assumed a homogeneous, anisotropic aquifer with principal axes in the horizontal and vertical directions. To a significant but unknown degree, the assumption of homogeneity is violated at the Mobile site. The analyses of most pumping tests are subject to such violations.

3.1.1 Anisotropy Test

The ratio of horizontal to vertical permeability is a parameter that strongly affects the degree of tilting of the thermal front for a mass of hot water injected into a confined aquifer. Substantial tilting of the thermal front provides a larger surface area for conductive heat loss to the upper confining layer and admits cold water near the bottom of the aquifer during recovery pumping. Both phenomena contribute to poor energy

3.4

recovery. First, a method for analyzing anisotropy pumping tests will be discussed; then the method will be applied to the Mobile field data.

Weeks (1969) presented three methods whereby drawdown data in partially-penetrating observation wells or piezometers near a partially-penetrating well pumped at constant rate can be analyzed to determine the permeability ratio. This report will consider Weeks' Method 2 for piezometers or observation wells screened over no more than about 20% of the aquifer thickness. The method is based on Hantush's drawdown equation (Hantush 1961, p. 90).

$$s = \frac{Q}{4\pi T} [W(u) + f]$$

$$= \frac{Q}{4\pi T} \left(W(u) + \frac{4b}{\pi(z_w - d)} \sum_{n=1}^{\infty} \frac{1}{n} K_0 \left[\frac{n\pi r}{b} \left(\frac{K_z}{K_r} \right)^{1/2} \right] \right.$$

$$\left. (\sin \frac{n\pi z_w}{b} - \sin \frac{n\pi d}{b}) \cos \frac{n\pi z}{b} \right) \qquad (3.1)$$

in which s = drawdown, m

Q = pumping rate, m^3/day

T = transmissivity, m^2/day

W(u) = well function

where $u = \frac{r^2 S}{4Tt}$

r = distance from pumped well to piezometer, m

S = storage coefficient

t = time, days

K_0 = modified Bessel function of the second kind and zero order

3.5

K_z = vertical permeability, m/day

K_r = horizontal permeability, m/day

and the rest of the terms are defined in Figure 3.2. The dimension z is measured from the middle of the screen for observation wells. Equation (3.1) applies for $t > bS/2K_z$.
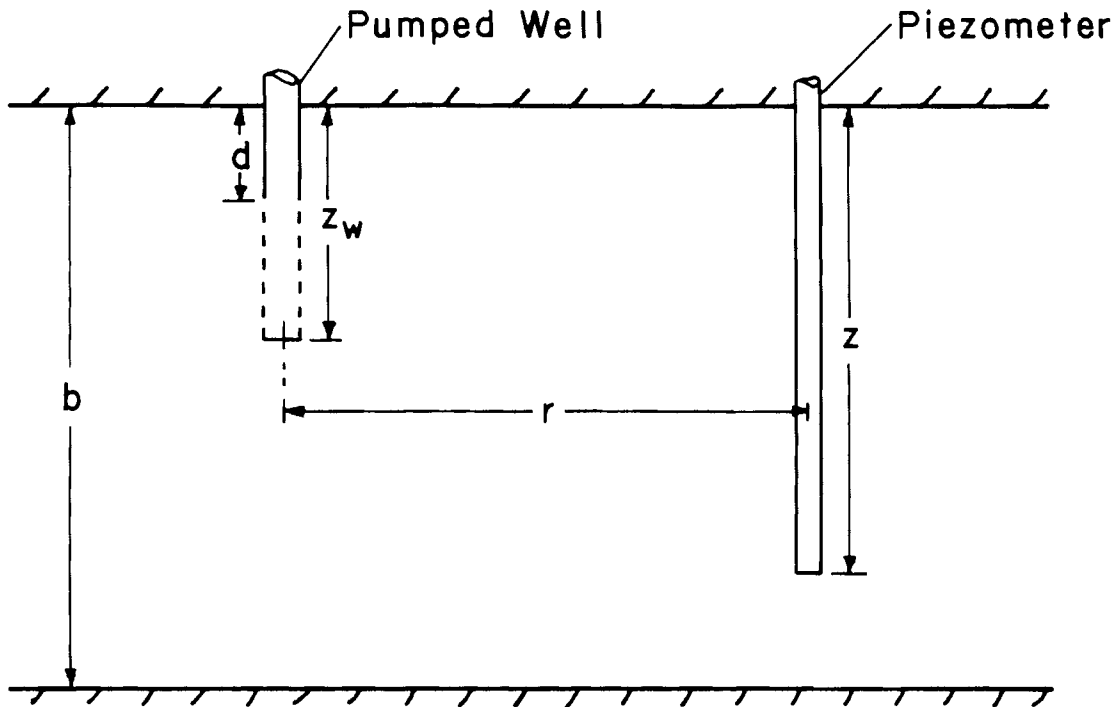
FIGURE 3.2. Definition Sketch for Equation (3.1)

The term f in Equation (3.1) accounts for the deviation in drawdown observed in a partially-penetrating piezometer in an anisotropic aquifer from that predicted for a fully penetrating observation well at the same location. The deviation is, therefore, given by

$$\delta s = \frac{Q}{4\pi T} f \qquad (3.2)$$

where δs is in meters.

Two or more partially screened piezometers are required to perform Method 2. The procedure, as given by Weeks, is paraphrased as follows:

Step 1. Determine values of T for each piezometer from the time-drawdown plots using the modified nonequilibrium method.

Step 2. For a selected time, plot drawdown versus r for each of the wells on semilog paper with r on the logarithmic scale. Also draw a line of slopes $\delta s = \frac{2.3Q}{2\pi T}$ beneath the data points if δs is negative (or above if δs is positive).

Step 3. Determine trial values of δs for each well by subtracting observed drawdown from the corresponding straight-line drawdown.

Step 4. Determine f for each well from Equation (3.2) using the trial δs values obtained in Step 3 and make a semilog plot of f versus r/b with f on the arithmetic scale.

Step 5. Prepare a type-curve on semilog paper of f from Equation (3.1) versus $\left(\frac{r}{b}\right)\sqrt{\frac{K_z}{K_r}} = r_c/b$ with f on the arithmetic scale.

Step 6. Match the data plot with the type-curve and select a match point.

Step 7. Determine the r/b and r_c/b coordinates for the match point; then calculate the permeability ratio from

$$\frac{K_r}{K_z} = \left(\frac{r/b}{r_c/b}\right)^2 \tag{3.3}$$

Step 8. Correct the trial f values computed in Step 4 by adding algebraically the value obtained by subtracting the data-curve value of f from the type-curve value of f for the match point. (NOTE: This step seems to be misworded in Weeks' paper).

Step 9.   Determine a calculated storage coefficient, S_c, for each well from the time-drawdown plots assuming the wells are fully penetrating.

Step 10.   Determine the true storage coefficient for each well by using the corrected f values from Step 8 and the calculated storage coefficients from Step 9 in the equation

$$S = S_c \exp{(f)} \qquad (3.4)$$

Figure 3.3 shows the well configuration used for the anisotropy pumping test at the Mobile site. Observation wells screened over 3.05 m were located 7.62, 15.2, and 22.9 m north of the partially screened pumped well. Throughout the pumping test, water was pumped from the confined aquifer at a constant rate of 818 m^3/day. Drawdowns, measured by pulley-float systems, are shown in Figure 3.4 for each of the observation wells. The effect of a boundary is noted about 20 min after startup. Regres-sion analysis was used on the data for which u <0.01 and t < 20 min to determine the following relationships:

$$s_1 = 8.55 + 12.9 \log t \qquad (3.5)$$

$$s_2 = 6.83 + 13.4 \log t \qquad (3.6)$$

$$s_3 = 6.10 + 13.1 \log t \qquad (3.7)$$

where s_1, s_2 and s_3 are drawdowns (in cm) of observation wells located at r = 7.62, 15.2, and 22.9 m, respectively, and t is in min. These equations are shown as straight lines passing through the appropriate early data in Figure 3.4. The data analysis by the procedure given above was performed as follows:

Step 1.   The transmissibility, T, was determined for each well accord-ding to the modified nonequilibrium method (Jacob 1950) by the equation

$$T = \frac{2.30}{4\pi(\Delta s/\Delta(\log t))} \qquad (3.8)$$
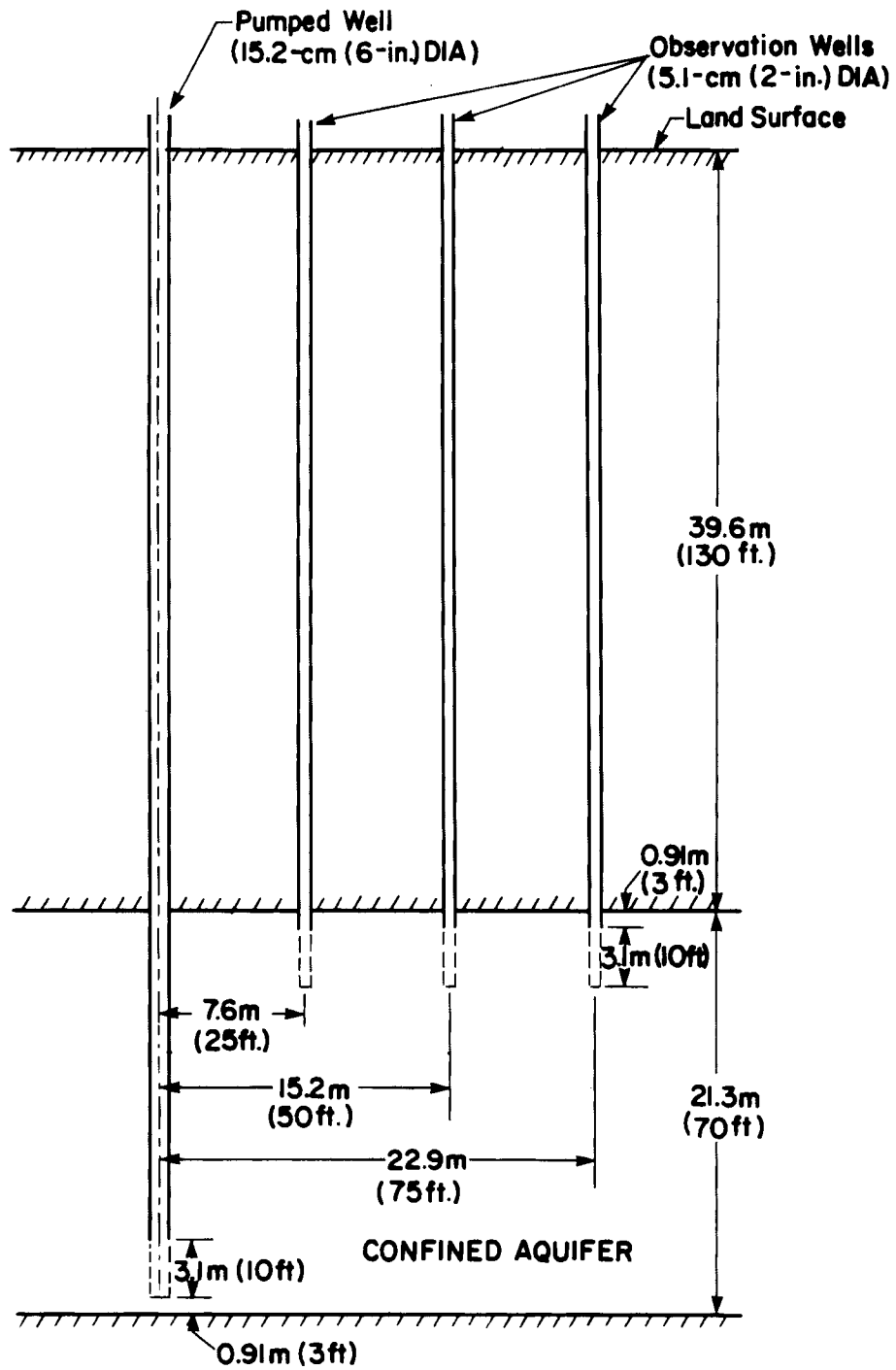
FIGURE 3.3. Well Configuration for Anisotropy Pumping Test
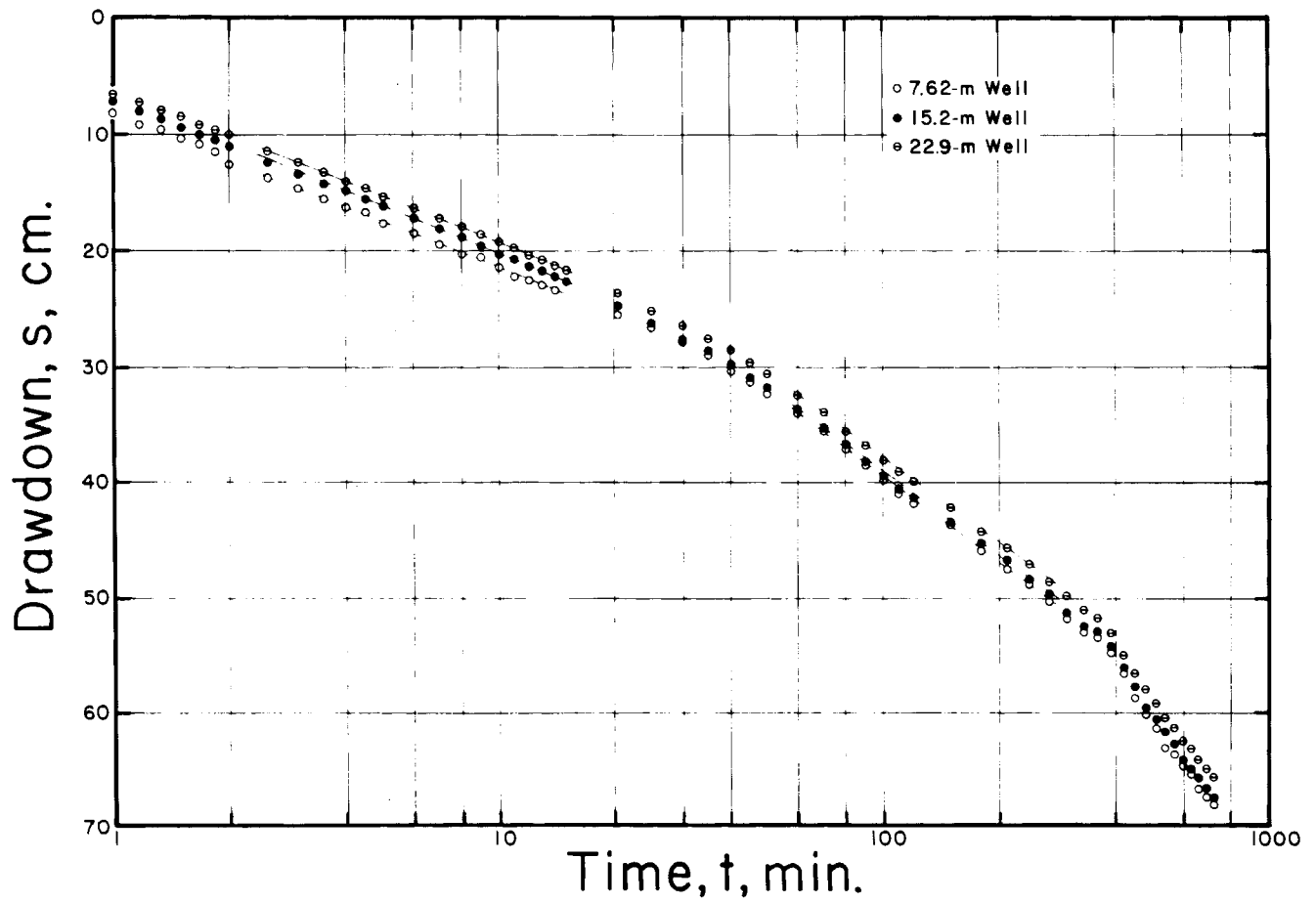
FIGURE 3.4. Drawdown Versus Time for Anisotropy Pumping Test

where $\Delta s / \Delta(\log t)$ is the slope of the s versus log t curve for u <0.01 and must be expressed in units consistent with Q and T. The values of T for each well determined by this method using Equations (3.5) through (3.7) are shown in Column 4 of Table 3.2.

Step 2. The drawdowns at t = 10 min as determined from Equations (3.5) through (3.7) are plotted in Figure 3.5, together with a straight line with a slope of $\frac{2.3Q}{2\pi T_{ave}}$ = 0.263 m, where T_{ave} = 1140 m^2/day = average transmissibility for the three observation wells.

Step 3. The trial drawdown deviations, δs, shown on Figure 3.5, are given in Column 5 of Table 3.2.

Step 4. Values of f determined from Equation (3.2) are shown in Column 6 of Table 3.2.

Step 5. The data- and type-curves are shown, overlain, in Figure 3.6. Note that the coordinate axes of the graphs must be parallel.

Step 6. The match-point is shown on Figure 3.6.

Step 7. The match-point coordinates for the abcissas are r/b = 2.59 and r_c/b = 1. Equation (3.3) yields

$$\frac{K_r}{K_z} = \left[\frac{(r/b)}{(r_c/b)}\right]^2 = \left[\frac{2.59}{1}\right]^2 = 6.71$$

Step 8. The correction factor is
$\Delta f = f_{tc} - f_{dc}$ = -2 m - (-2.60 m) = +0.60 m
where f_{tc} = f match-point value for type curve, and f_{dc} = f match-point for data curve. The corrected values of f, obtained by adding 0.60 m to the initial f values in Column 6, are shown in Column 7 of Table 3.2.

TABLE 3.2. Parameters for Analysis of Anisotropy Pumping Test

Observation Well Number	Distance from Pumped Well, r (m)	r/b	Transmissibility, T (m^2/day)	δs (m)	f(s)	f(s)	S_c	S
1	2	3	4	5	6	7	8	9
1	7.62	0.357	1,160	0.187	-3.28	-2.68	0.00679	0.00047
2	15.2	0.714	1,120	0.120	-2.10	-1.50	0.00234	0.00052
3	22.9	1.07	1,140	0.084	-1.47	-0.87	0.00116	0.00049
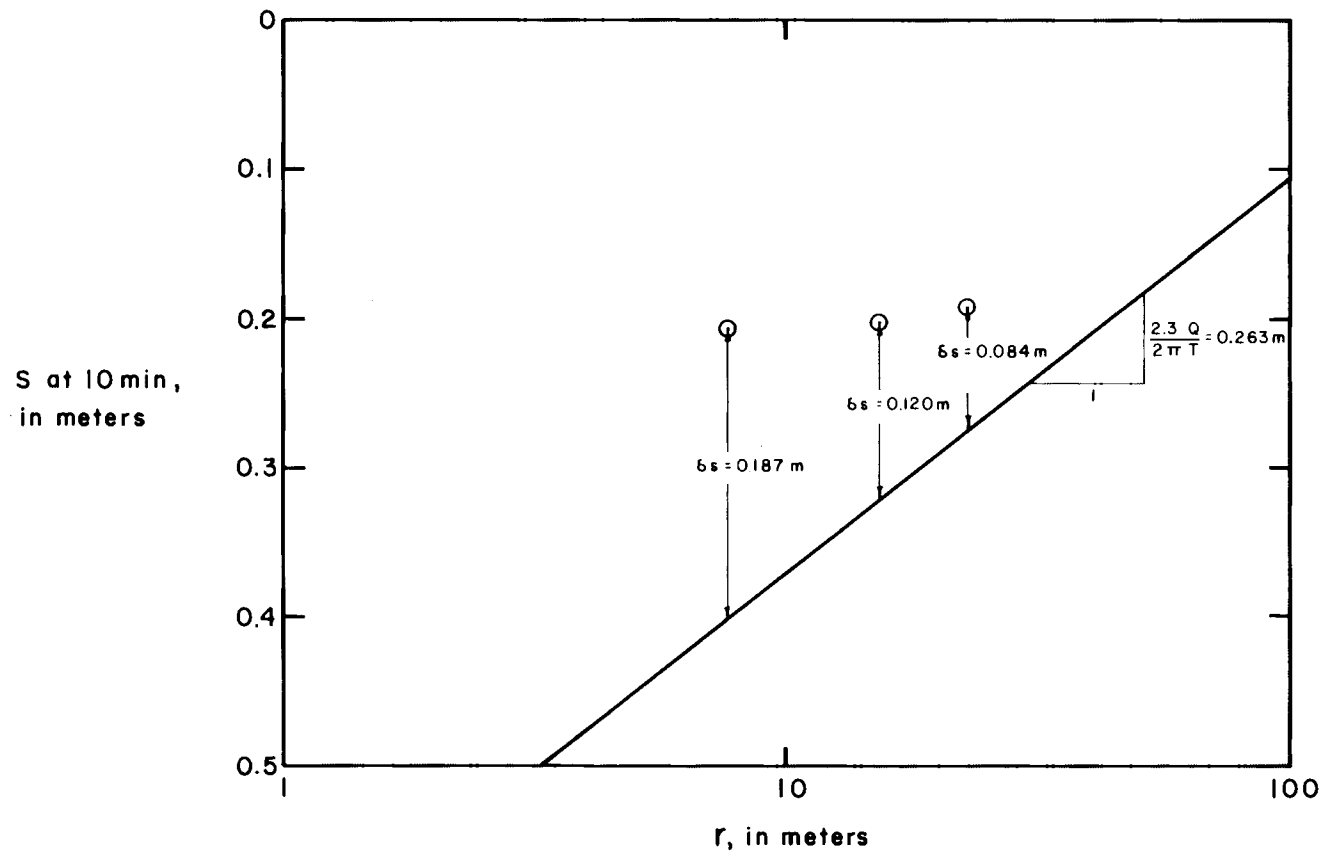
FIGURE 3.5. Distance-Drawdown Plot at t = 10 min for Observation Wells
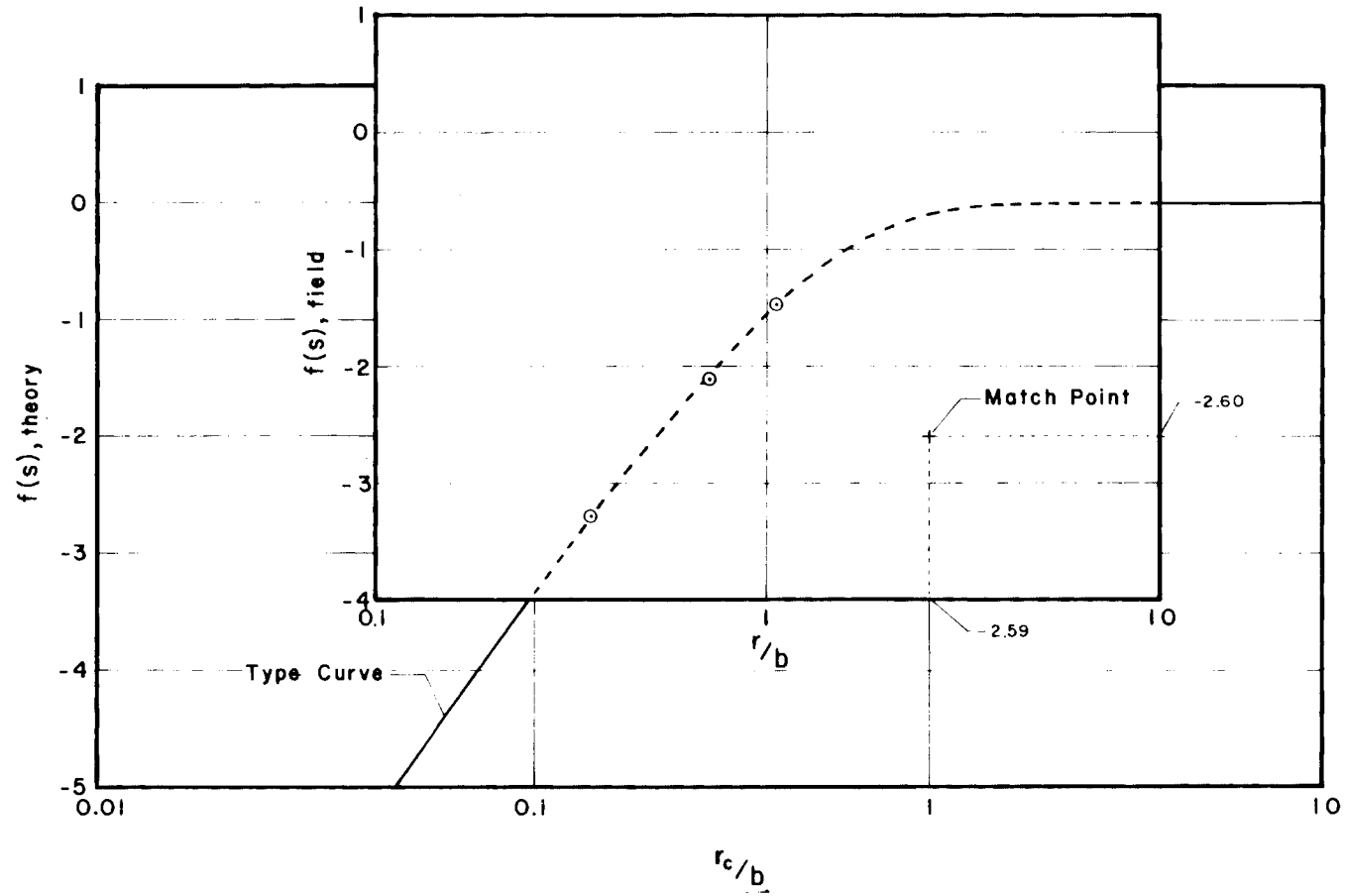
FIGURE 3.6.   Superposition of f(s) versus r/b Data Curve and f(s) versus r_c/b Type Curve

Step 9. The calculated storage coefficients, S_c, can be obtained for each of the wells from the equation (Jacob 1950)

$$S_c = \frac{2.25T \, t_o}{r^2} \qquad (3.9)$$

where t_o is determined by setting s = 0 and solving for t in Equations (3.5) through (3.7). The values of S_c are given in Column 8 of Table 3.2.

Step 10. The true value of the storage coefficient as determined by Equation (3.4) is shown in Column 9 of Table 3.2.

Where the storage coefficient is known from previous pumping tests, the permeability ratio can be determined with only one partially-penetrating observation well and one partially-penetrating pumping well. This method entails calculating the transmissibility for the observation well by the modified nonequilibrium method, as discussed above, then determining K_r/K_z by trial and error from Equation (3.1) for a measured drawdown at a specified time (where u <0.01). Values of K_r/K_z obtained in this manner for the data shown in Figure 3.4 and for S = 0.0005 are 5.98, 7.20, and 6.74 for observation wells 1, 2, and 3, respectively. Weeks' Method 3 can also be used to determine the permeability ratio with one observation well. It does involve plotting a type-curve, however.

3.1.2 Standard Pumping Test and Boundary Location

After the anisotropy test was completed, the temporary partially-screened observation wells were removed and a permanent fully-penetrating screen was installed in the injection well. A standard well test was then performed in which water was pumped at a constant rate of 600 m^3/day from the confined aquifer. The drawdown in a fully-screened observation well located 15 m north of the pumped well is shown in Figure 3.7. A boundary effect was again noticed about 20 minutes after startup. Regression analysis was used to determine the following relationship for u <0.01 and for t < 20 minutes:
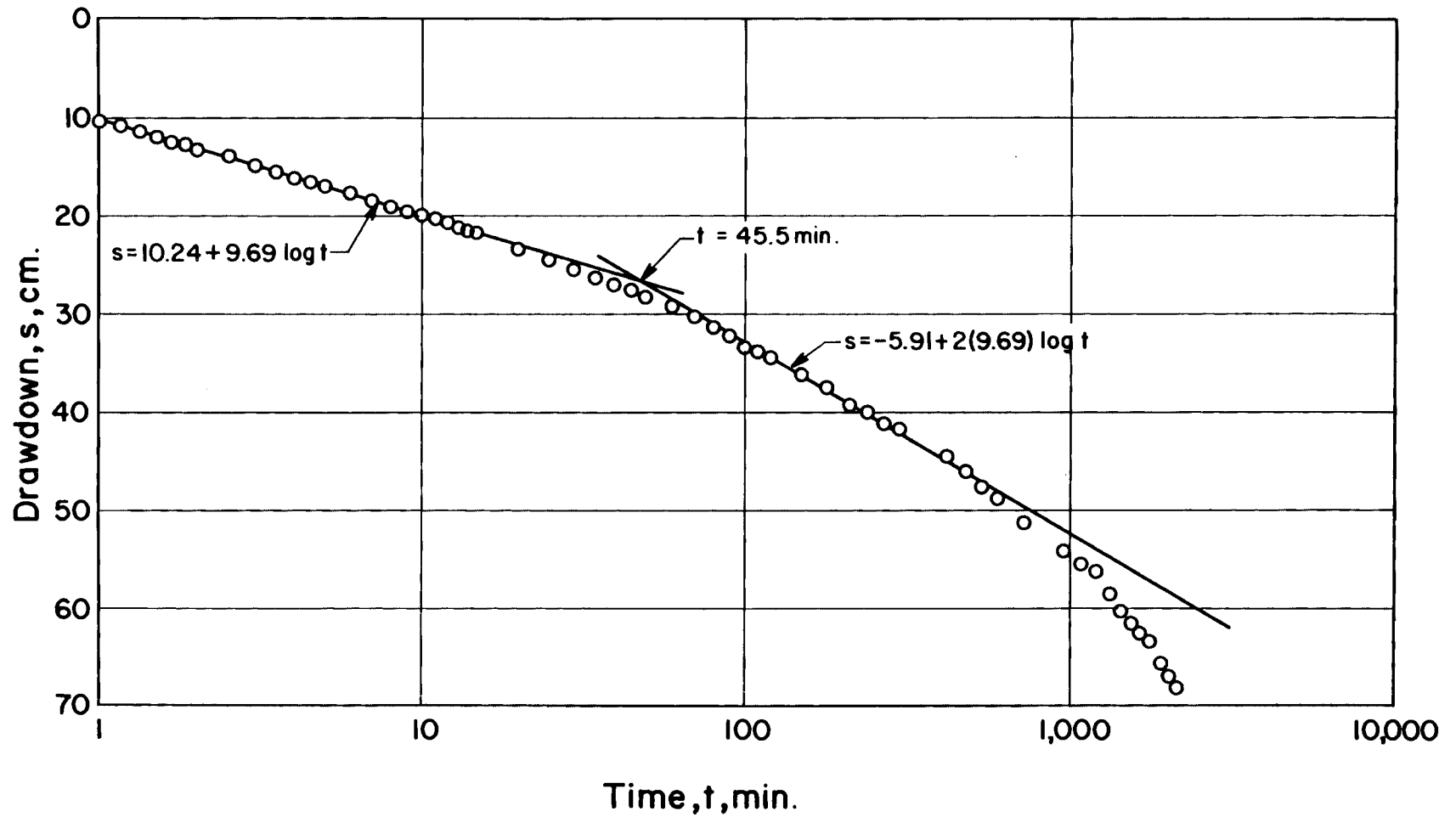
FIGURE 3.7. Drawdown versus Time for Standard Pumping Test

3.16

$$s = 10.24 + 9.69 \log t \qquad (3.10)$$

where s is in cm and t is in min. Equation (3.10) is shown as a solid line passing through the early drawdown data in Figure 3.7. The slope of Equation (3.10) can be used to determine T from Equation (3.8) of the modified nonequilibrium method as follows:

$$T = \frac{2.3Q}{4\pi[\Delta s/\Delta(\log t)]} = \frac{2.3(600 \text{ m}^3/\text{day})}{4\pi(9.69 \text{ cm})(0.01 \text{ cm/m})} = 1{,}130 \text{ m}^2/\text{day} \qquad (3.11)$$

The storage coefficient can then be determined by the equation

$$S = \frac{2.25Tt_0}{r^2} = \frac{2.25(1{,}130 \text{ m}^2/\text{day})10^{-\frac{10.14}{9.69}}\text{min}}{(15^2 \text{m}^2)(1440 \text{ min/day})} = 0.00069 \qquad (3.12)$$

The same experimental setup and data analysis procedure were also used to determine T = 1,140 m^2/day and S = 0.00066 for a constant pumping rate of 2,125 m^3/day.

The straight line passing through the latter drawdown data on Figure 3.7 is given by the equation

$$s = 5.91 + 2(9.69) \log t \qquad (3.13)$$

where s is in cm and t is in min. This expression is the "best fit" line, with a slope that is two times the slope of the first limb [Equation (3.10)], that passes through the drawdown affected by the first boundary. A method for locating the boundary is given by Bear (1979, pp. 479-481). The effect on drawdown of a boundary can be simulated by an imaginary well with the same pumping rate located beyond the boundary, with the boundary face perpendicularly bisecting the line between the real and imaginary wells. The distance from the observation well to the imaginary well is

$$r_1 = \left[\frac{r_0^2}{t_0} t_1 \right]^{1/2} \qquad (3.14)$$

3.17

where r_1 = distance from observation well to imaginary well; r_0 = distance from observation well to pumped well; t_0 = time corresponding to $s = 0$ on first straight-line plot, or limb; and t_1 = time at the intersection of the first and second limb. Therefore, for Figure 3.7, the distance from the observation well to the imaginary well is

$$r_1 = \left[\left(\frac{15^2 m^2}{0.113 \text{ min}}\right) 45.5 \text{ min}\right]^{1/2} = 301 \text{ m}$$

Because the observation well is very near the pumped well, the distance from the pumped well to the image well is roughly 300 m; the distance from the pumped well to the boundary is approximately 150 m. Similar analyses for at least two or more wells are required, however, to determine the location of the boundary (Todd 1980, pp. 147-149).

The effect of another boundary is apparent from Figure 3.7 as the data points fall below the second limb. If the aquifer were homogeneous, a line with three times the slope of the first limb could be passed through the data and the distance from the observation well to a second image well could be determined. This was not done for the drawdown data of Figure 3.7, however, because the steep slope of the data affected by the second boundary indicated nonhomogeneity.

3.1.3 Leaky Aquifer Pumping Test

One of the principal sources of energy loss in aquifer thermal energy storage systems is transport of heat by conduction and convection to the confining layers and, ultimately, to overlying or underlying aquifers. To estimate the extent of this process, a leaky aquifer pumping test should be performed to determine the vertical permeability of the confining layers.

The ratio method proposed by Neuman and Witherspoon (1972) provided the basis for the design and analysis of the leaky aquifer test performed

3.18

at the Mobile site. Figure 3.8 shows the well configuration used to per-
form the test, which was conducted concurrently with the 600 m^3/day stan-
dard well test discussed previously. The partially-screened aquitard
observation wells, well No. 13 and well No. 14 in the appendix, were 15 m
from the pumped well. The drawdown for the aquitard and aquifer wells is
shown in Figure 3.9.
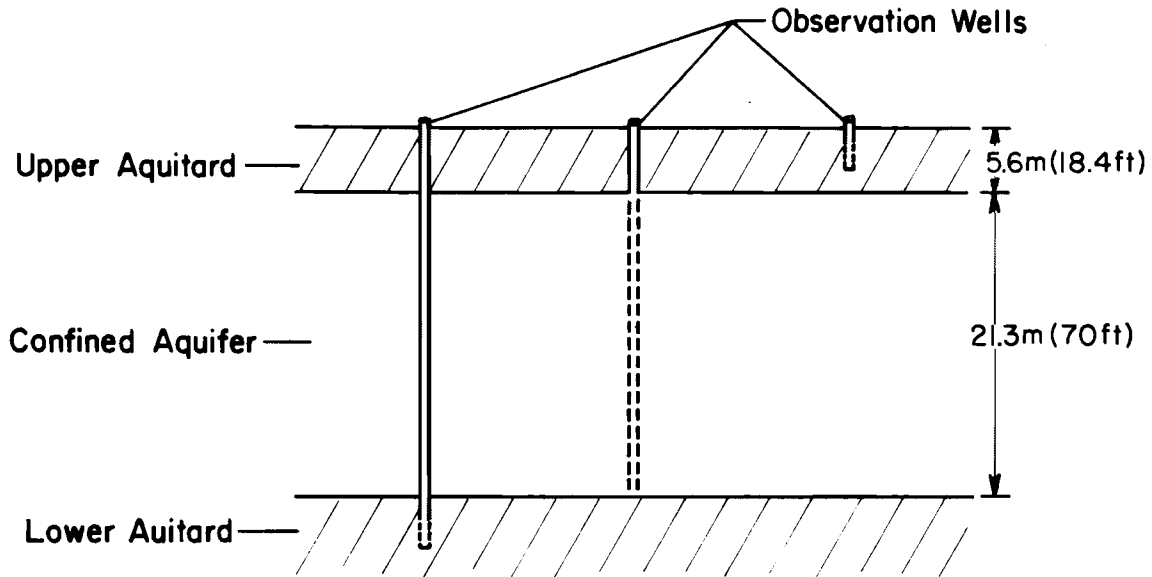
FIGURE 3.8. Well Configuration for Leaky Aquifer Pumping Test

Neuman and Witherspoon state that the values of T and S for a leaky
aquifer can be determined by standard procedures for a close well at early
times. Because previous tests of the Mobile site have shown that the con-
fining layers are classified as slightly leaky, the values of T = 1,130
m^2/day and S = 0.00069 obtained by the modified nonequilibrium test dis-
cussed previously are appropriate.
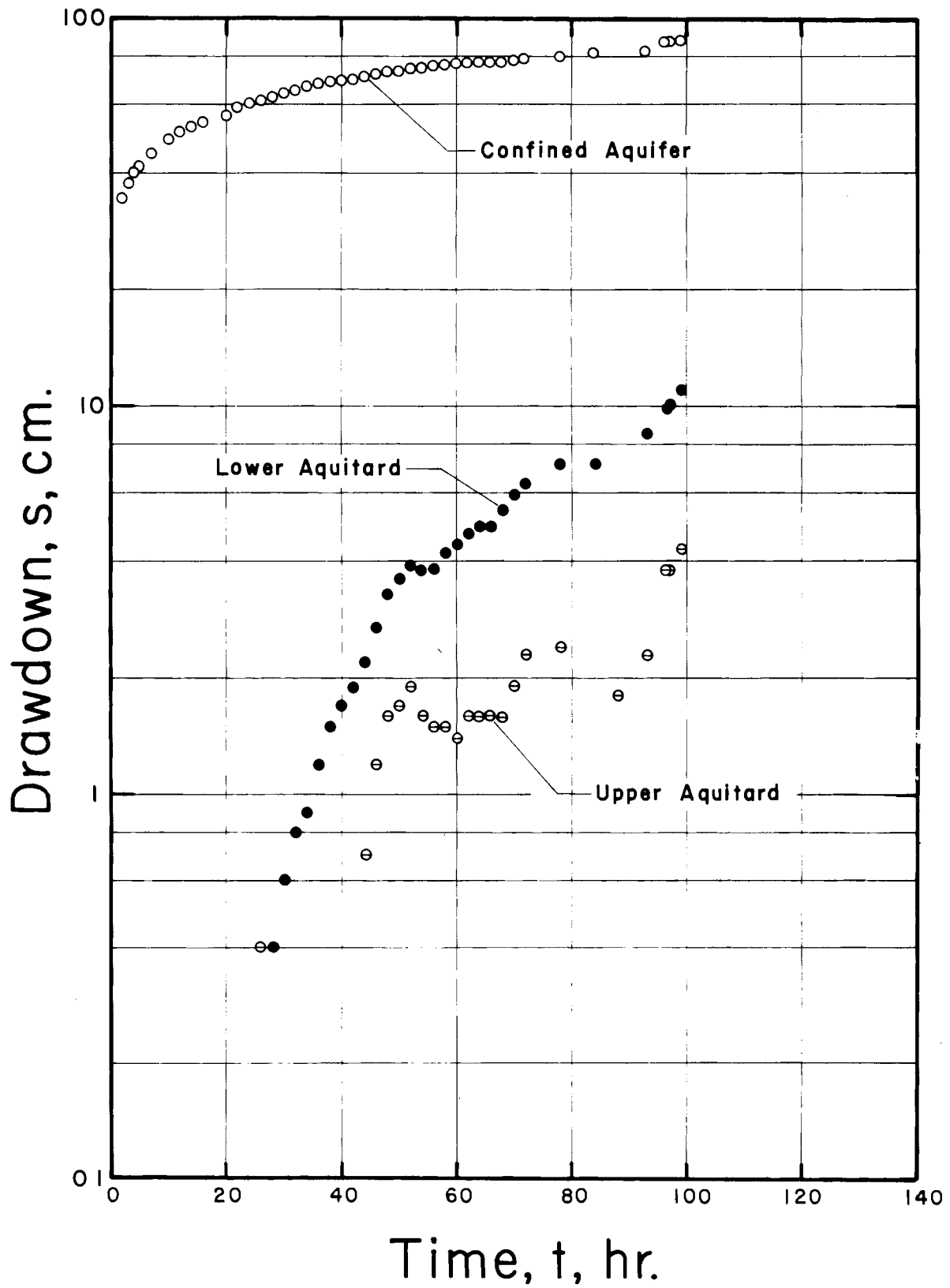
FIGURE 3.9. Drawdown versus Time for Leaky Aquifer Pumping Test

The ratio method is straightforward and does not require curve match-
ing. When

$$t < 0.1S_s' b'^2/K'$$ \hfill (3.15)

where t = time in days, S_s' = aquitard specific storage in m^{-1}; b' = aqui-
tard thickness in m; and K' = vertical aquitard permeability in m/day. The
following procedure can be used to determine K' when S_s is known.

Step 1. Calculate s'/s at a given radial distance r at a specific
time t, where s and s' are the observation well drawdowns in
the aquifer and aquitard, respectively.

Step 2. Calculate $t_D = Tt/Sr^2$ for the time used in determining s'/s
in Step 1.

Step 3. Read a value of $t_D' = \dfrac{K't}{S_s'z^2}$ corresponding to the s'/s and t_D

values from Figure 3.10, where z is the distance from the
middle of the aquitard observation well screen to the
aquifer-aquitard interface.

Step 4. Calculate the aquitard hydraulic diffusivity (or coefficient
of consolidation) from the equation

$$\alpha' = (\frac{z^2}{t}) \ t_D'$$ \hfill (3.16)

Step 5. Determine the vertical permeability of the aquitard from the
formula

$$K' = \alpha'S_s'$$ \hfill (3.17)

This procedure is simple to apply. It is suggested, however, that the
detailed discussion of Neuman and Witherspoon (1972) be read to fully
appreciate the applicability of the ratio method.
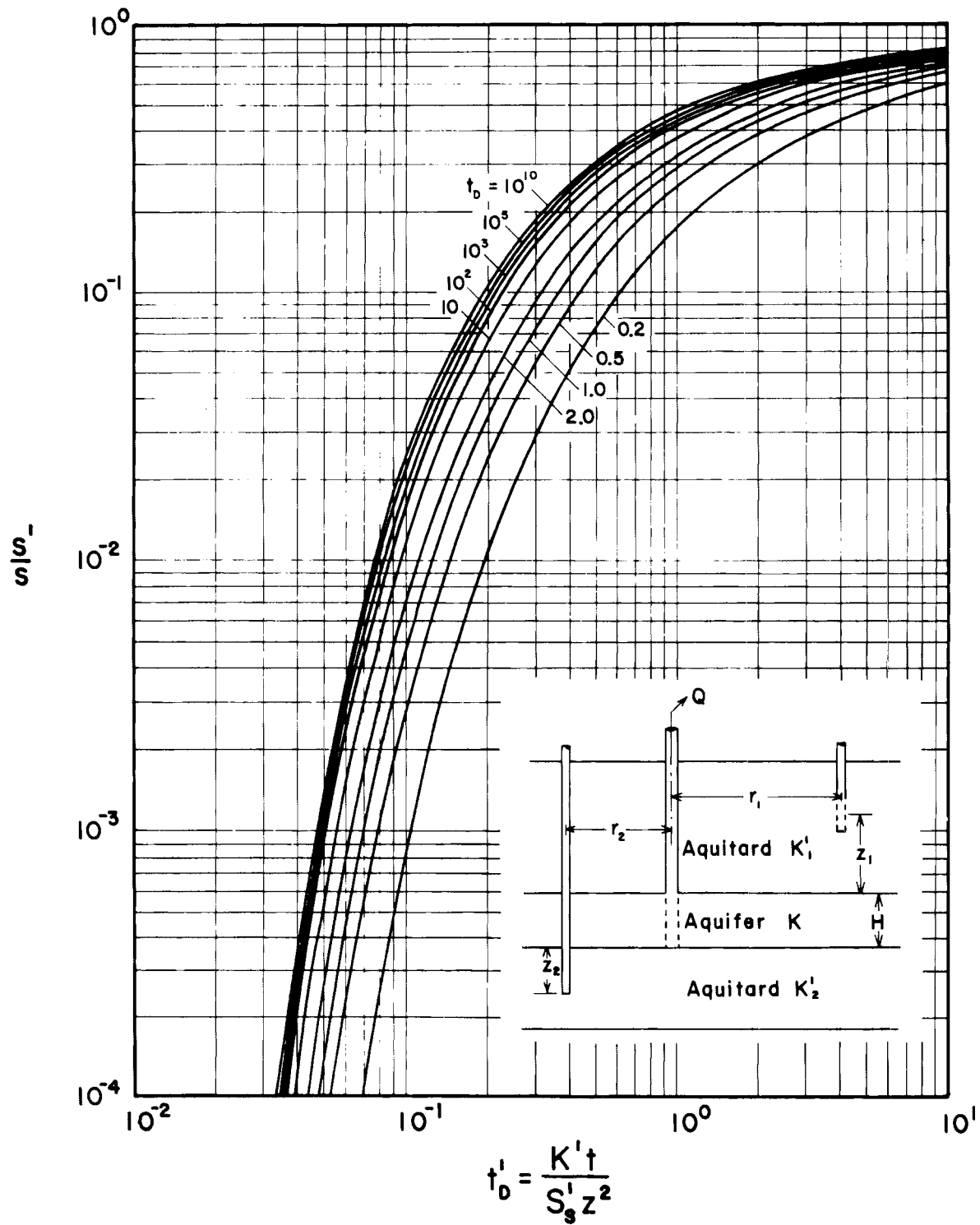
FIGURE 3.10. Dimensionless Graph of s'/s versus t_d' for Semi-Infinite Aquitard (from Newman and Witherspoon 1972)

3.22

The Mobile drawdown data at t = 50 hr will be considered to provide an example of the application of the ratio method. The results of the procedure given above are presented in Table 3.3.

TABLE 3.3. Results of Ratio Method Analysis for Drawdowns at t = 50 Hours

	z (m)	s' or s (m)	s'/s	t_D	t_D'	K'/S_S' (m^2/day)
Lower Aquitard	3.58	0.017	0.0231	15,200	0.220	0.68
Upper Aquitard	4.11	0.036	0.0489	15,200	0.150	1.22
Aquifer		0.736				

Step 5 of the ratio method has not been performed because the consolidation tests to determine S_S' for the upper and lower aquitards are incomplete.

The drawdown data for the lower aquitard followed the shape of Neuman and Witherspoon's theoretical curves. This was because the lower aquitard is quite thick, and it is relatively easy to place an isolated observation well (well logging to depths about 50 m below the storage formation have not identified an underlying aquifer). The average value of the lower aquitard hydraulic diffusivity, $\alpha' = K'/S_S'$ for all of the data points is 1.10 m^2/day.

The upper aquitard is only about 5.6 m thick, and communication with the overlying aquifer near the top of the observation well screen may have affected the drawdown approximately 54 hr after pumping began. The average value of the upper aquitard hydraulic diffusivity for the first six draw-down values is 0.71 m^2/day.

3.23

3.1.4 Dispersivity Testing

The hydrodynamic dispersion coefficient is an ill-defined but important parameter that can affect the efficiency of a thermal energy storage system. In general, the smaller the dispersivity, the sharper the interface between hot and cold water. Minimal mixing of injected and native waters maximizes the recovery temperature.

In an attempt to provide a useful measure of the dispersion coefficient at the Mobile site, a conservative tracer test was performed during first cycle injection. Sodium bromide was combined with the hot injection water at a concentration of approximately 11 mg/l (Davis et al. 1980). The resulting concentration in the storage aquifer was recorded in a tracer observation well (well #15) located 15.2 m from the injection well. This well was screened over a length of 1.52 m with the screened section located in the middle of the confined aquifer.

The sampling apparatus was a section of 2.54-cm ID fiberglass pipe. Holes were drilled in the pipe to coincide with the screened section of the well. Flexible tubing (0.95-cm ID) was used to transport the samples to the ground surface. Vacuum tubing was required to eliminate collapse in the event of some clogging of the line. Plugs of silicon were injected into the fiberglass pipe to isolate the sampling section and to secure the flexible tubing. The entire fiberglass pipe and flexible tubing apparatus was lowered, by hand, into the wells with a nylon rope. A coarse sand was backfilled into the space between the fiberglass pipe and the well casing. Continuous or intermittent sampling was accomplished with variable speed peristaltic pumps. For intermittent sampling, the pumps were run at 1 l/min for 1 hr before taking a sample.

A 22.7-m^3 tank containing NaBr at 40,000 mg/l was prepared, and a diaphragm pump was used to control flow of the tracer into the injection line. Because of possible clogging in the aquifer, constant tracer flow against a variable head was a desired capability of the system. However, no significant pressure increase occurred and the diaphragm pump, designed to operate against higher heads, did not operate consistently. Changes in

field temperatures also contributed to inconsistent pump behavior. A variable speed peristaltic pump has been used successfully in later experiments.

Variation in the injected water tracer concentration over the duration of the experiment (756 hr) was between 19.5 and 11.0 mg/l. This variation was due to inconsistent diaphragm pump behavior and also to several down periods necessary for boiler repairs.

Experimental results are summarized in the breakthrough curve shown in Figure 3.11. During the first 100 hr of the experiment, the injection concentration, C_0, was relatively constant and averaged 11.0 mg/l. As an initial estimate of longitudinal dispersivity, α, the method described by Gupta, Batta and Pandey (1980) was applied to the four data points shown on the breakthrough curve.
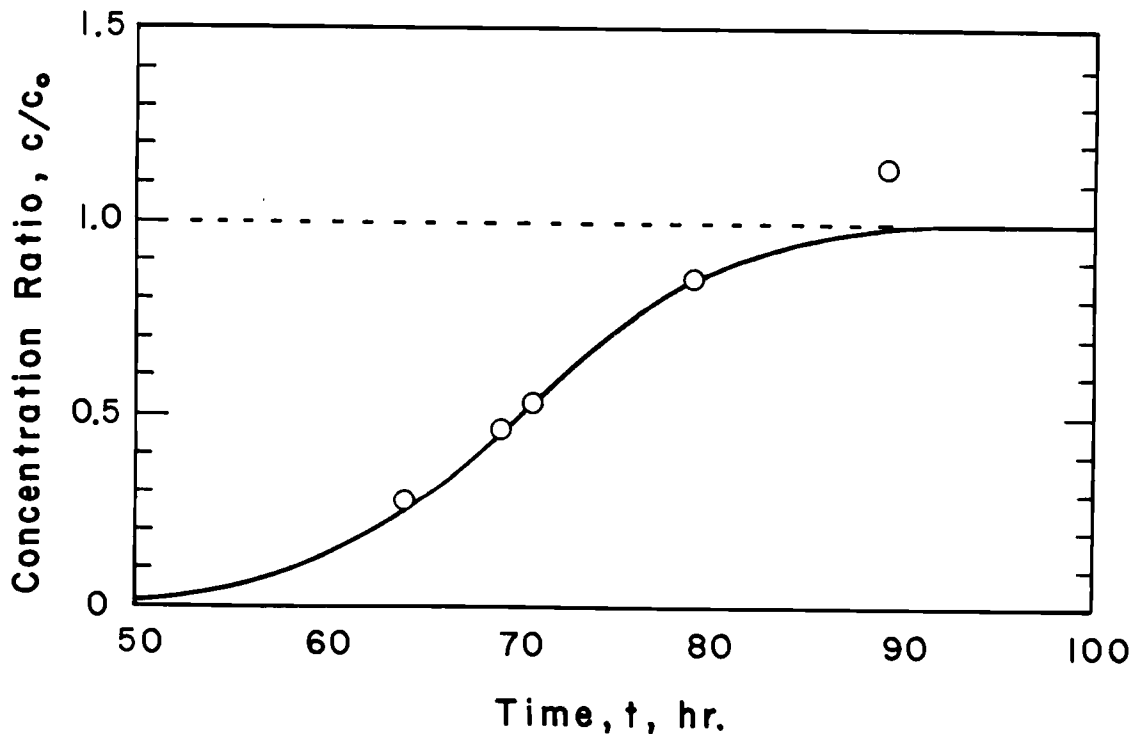
FIGURE 3.11. Concentration Ratio at Tracer Well #15 Located at r = 15 m
Note: (C_0 = 11.0 ppm for first 100 hours of experiment).

3.25

This procedure is based on an approximate solution to the radial flow dispersion equation given by (Hoopes and Harleman 1967)

$$c/c_0 = 0.5 \text{ erf}_c (u) \tag{3.18}$$

where erf_c = complementary error function, $u = (r^2/2 - At)/(4\alpha r^3/3)^{1/2}$, r = radius from injection well, α = dispersivity, t = time, and $A = Q/2\pi bn$, Q = injection rate, b = aquifer thickness, and n = porosity. Through manipulation of Equation (3.18), $\text{erf}(u) = 1-2c/c_0$ or

$$\text{inverf } (1-2c/c_0) = u \tag{3.19}$$

Hence,

$$\sqrt{\alpha} \text{ inverf } (1-2c/c_0) = (r^2/2-At)/(4r^3/3)^{1/2} \tag{3.20}$$

Thus, a plot of $\text{inverf } (1-2c/c_0)$ versus $(r^2/2-At)/(4r^3/3)^{1/2}$ is a straight line with a slope equal to $\sqrt{\alpha}$. Such a plot for the Mobile tracer data, shown in Figure 3.12, yielded a dispersivity of 9.1 cm. The continuous curve in Figure 3.11 is based on $\alpha = 9.1$ cm.

If a homogeneous aquifer is assumed at the Mobile site, the arrival time of a nondispersed front of injected fluid is given by $t = \pi r^2 nb/Q = 112$ hours, where $r = 15.2$ m, $n = 0.33$, $b = 21.3$ m, and $Q = 45.4$ m^3/hr. The corresponding time on the dispersed front of the approximate solution is the time when $c/c_0 = 0.5$. From the experimental data of Figure 3.11, it is clear that $c/c_0 = 0.5$, $t = 70$ hr. Nonhomogeneous aquifer properties contribute to the difference between theoretical and experimental arrival times. Pumping tests have suggested an increase in aquifer transmissivity in the direction of tracer well #15. More important, temperature data and electric logs indicate that hydraulic conductivity is largest near the center of the confined aquifer and decreases in magnitude near the upper and lower confining layers. Therefore, it is probable at the Mobile site that a measure of the horizontal permeability as a function of depth would be more valuable than some type of global dispersivity in predicting "mixing" effects in ATES.
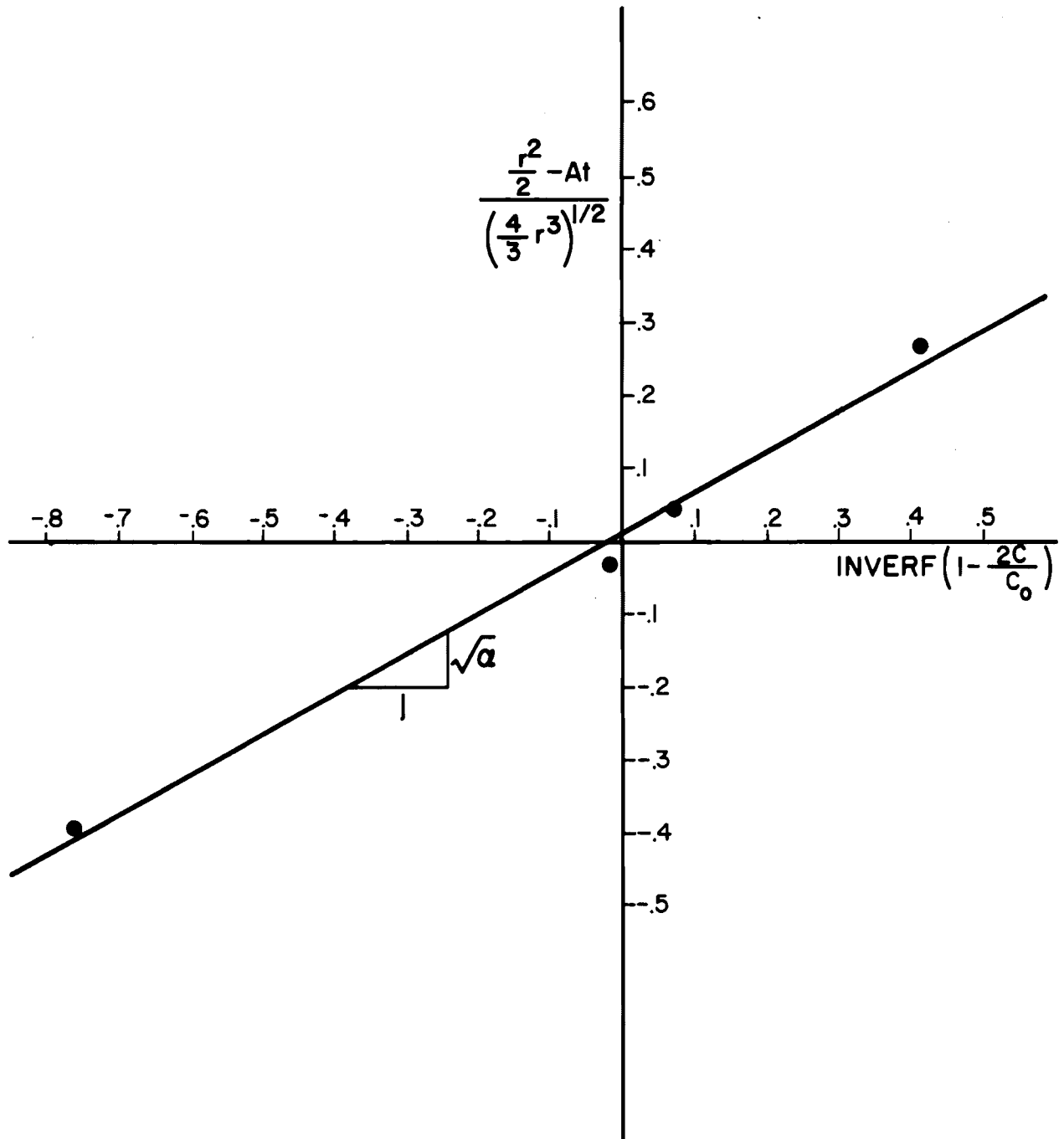
FIGURE 3.12. Slope Plot for Tracer Test Analysis

3.2 GEOCHEMICAL TESTING

Three separate aquifer storage experiments performed in the United States have been plagued by geochemical problems of one type or another. In all cases, the problems led to clogging of a well during injection. Such a situation may be very difficult or impossible to correct once it has occurred. Therefore, the goal of geochemical testing should be to anticipate geochemical problems and, if at all possible, prevent their occurrence.

In experiments performed by Texas A & M University, water was cooled by a spray pond prior to injection (Reddell, Davison and Harris 1979). Oxygen that entered the water reacted with iron to produce iron-oxide precipitates capable of plugging the injection well. Clogging was prevented through the use of a rapid sand filter prior to injection. It was necessary to backwash the filter after each injection volume of 950 m^3.

During previous tests at the Mobile site, more serious clogging resulted due to swelling of formation clays (Molz et al. 1979; Molz, Parr and Andersen 1981). Swelling was caused by a moderate water quality difference between ground water native to the storage aquifer and the injected water, which was obtained from a shallow supply aquifer. A particle size distribution analysis indicated that the storage formation is composed of a medium sand containing about 15% silt and clay by weight. Because this fraction contains smectite clays, there is clearly a potential for osmotic swelling and subsequent clay particle dispersion if water from the supply aquifer is injected into the storage aquifer (Van Olphen, 1963). This phenomenon is also called fresh-water sensitivity and occurs when a clay particle containing interlayer water with a relatively high ion concentration comes in contact with water having a relatively low ion concentration. There is then a tendency, similar to osmosis, for the surrounding water to diffuse into the clay particle, causing it to swell. Such swelling has been observed many times in both the laboratory and the field (Brown and Silvey 1977).

As mentioned previously, clay swelling and dispersion caused serious clogging problems at the Mobile site during previous experiments. Regular backwashing of the injection well was required to maintain even minimally acceptable injection rates (Molz et al. 1979; Molz, Parr and Andersen 1981). The problem was solved during the experiments reported herein by obtaining supply water from the storage aquifer itself (doublet supply-injection system) and by increasing the Na ion content of the injected water by approximately 5 mg/l.

A cold storage experiment is currently underway on the Stony Brook Campus of the State University of New York (Stern 1980). Water is being pumped from a supply well, chilled by an air-conditioning system and injected into the same aquifer through a well about 85 m from the supply well. The first injection went smoothly with no apparent problems. However, when water was recovered from the injection well for reinjection through the supply well, serious clogging of the supply well developed. The problem is being studied and appears to be due to sediment in the ground water.

The case histories just presented support the contention that careful geochemical testing must be performed as part of the design of an aquifer thermal energy storage system. Even if potential problems involving changes in oxygen content, biological activity, and water quality differences are eliminated, problems can develop related solely to heating the injection water. Specifically, a temperature increase would affect:

- the chemical equilibrium between the minerals of the aquifer maxtrix and their concentrations in the ground-water solution

- the ion exchange capacity and selectivity of clays

- the distribution of hydrated water

- the rates of chemical and physical reactions.

Heat-induced chemical changes constitute a complex problem that is very site-specific. At the Pacific Northwest Laboratory at Richland, Washington, rigorous field and laboratory test procedures were developed determining the suitability of a confined aquifer for thermal energy storage based on geochemical considerations (Stottlemyre, Cooley and Banik 1980).

3.3 AQUIFER THERMODYNAMIC TESTING

The major thermodynamic quantities that must be measured or at least estimated are the thermal conductivity and heat capacity of the aquifer and confining layers. These quantities are subject to much less natural variation than the hydraulic properties discussed previously. Therefore, they can normally be estimated or measured in the laboratory using core samples obtained during construction of the various exploratory and/or test wells.

The specific heats of many common dry rock materials are in the relatively narrow range of 0.19 to 0.22 kcal/kg/°C (Bear 1972). Using values for pure materials obtainable from standard tables, the effective heat capacity of a water saturated porous medium can be estimated on a volumetric basis using the equation

$$C_{va} = n\rho_w C_w + (1-n)\rho_s C_s \qquad (3.21)$$

where C_{va} = aquifer volumetric heat capacity; ρ_w, ρ_s = densities of water and solid, respectively; C_w, C_s = specific heat of water and solid, respectively; and n = porosity. A porosity in the range of 20% to 60% would yield an effective heat capacity between about 600 and 800 kcal/m^3/°C. Typical porosity ranges for natural materials may be found in Todd (1980). At the Mobile site with an estimated porosity of 0.33, a volumetric heat capacity of 661 kcal/m^3/°C was calculated.

The thermal conductivity of most saturated, porous, sedimentary materials will fall in the range of 0.75 to 3 kcal/(m.hr.°C) depending mainly

on composition and porosity (Mitchell and Tsung 1978). If either or both of these properties are known, the graph reproduced from Mitchell and Tsung (1978, p. 1308) as Figure 3.13, can be used to obtain an estimate that may be adequate for many applications. If a particular value cannot be chosen with an acceptable degree of certainty, an alternative is to base calculations on an upper and lower bound.
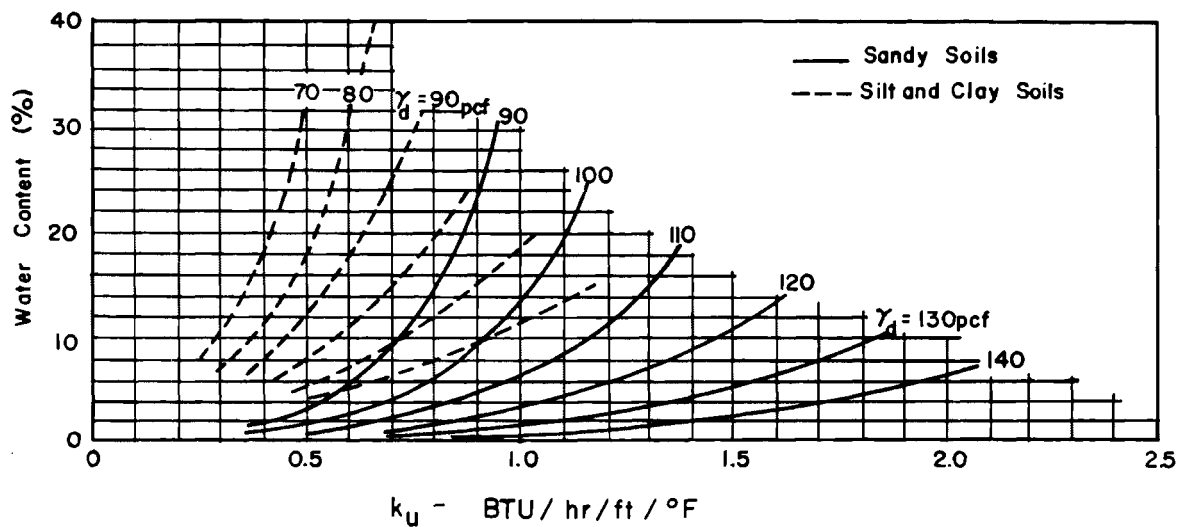
FIGURE 3.13. Thermal Conductivity of Sandy and Silty-Clay Soils as a Function of Water Content and Dry Unit Weight.

Note: For conversion purposes, 1 BTU/hr/ft/°F is equivalent to 1.49 kcal/hr/m/°C. Also, 1 lb/ft^3 is equivalent to 16 kg/m^3.

Source: Mitchell and Tsung (1978, p. 1308)

Several laboratory procedures are available for direct measurement of the thermal conductivity of unconsolidated porous media. Two prominent methods are the thermal needle studied in some detail by Mitchell and Tsung (1978), and the line-source method developed by van der Held and van Drunen (1949) and studied further by Nix et al. (1969).

The line-source method was used to measure the thermal conductivity of the storage aquifer and upper aquitard at the Mobile site. (Dr. John Goodling of the Mechanical Engineering Department at Auburn University supervised the measurements.) Specimens were placed in glass cylinders 20.3 cm long and 5.1 cm in diameter (Figure 3.14). The heater wire, which runs down the center line of the specimen, was composed of constantan and placed across the terminals of a direct current power supply. Heater wire temperature as a function of time was measured with an iron-constantan thermocouple placed as shown in Figure 3.14. This device was calibrated and several runs were made. (Details are available from the authors upon request.) The results indicated an aquifer thermal conductivity of 1.97 ± 0.16 kcal/(m.hr.°C) and an aquitard conductivity of 2.20 ± 0.13 kcal/(m.hr.°C). Using a porosity of 33% and a solids density of 2.6 gm/cm^3, the graph in Figure 3.13 yields a thermal conductivity of about 1.93 kcal/(m.hr.°C), which is in close agreement with the measured aquifer value.

3.4 SUMMARY AND CONCLUSIONS

Extensive testing is required to evaluate the potential of an aquifer for thermal energy storage. Important parameters include the regional gradient, vertical and horizontal permeability of the storage aquifer, horizontal dispersivity, vertical permeability of the upper and lower aquitards, thermal conductivities, heat capacities, and chemical characteristics of the aquifer matrix and native ground water.

At the Mobile site, chemical and thermodynamic tests were performed in the laboratory using core samples and ground-water samples. The chemical analyses indicated a potential for clay particle swelling and loss of permeability in the storage aquifer if relatively high-quality (pure) water was heated and injected. This phenomenon was observed in previous studies when water from a shallow supply aquifer was heated and pumped into the storage aquifer. The problem was eliminated in the current study by obtaining supply water from the storage aquifer itself.
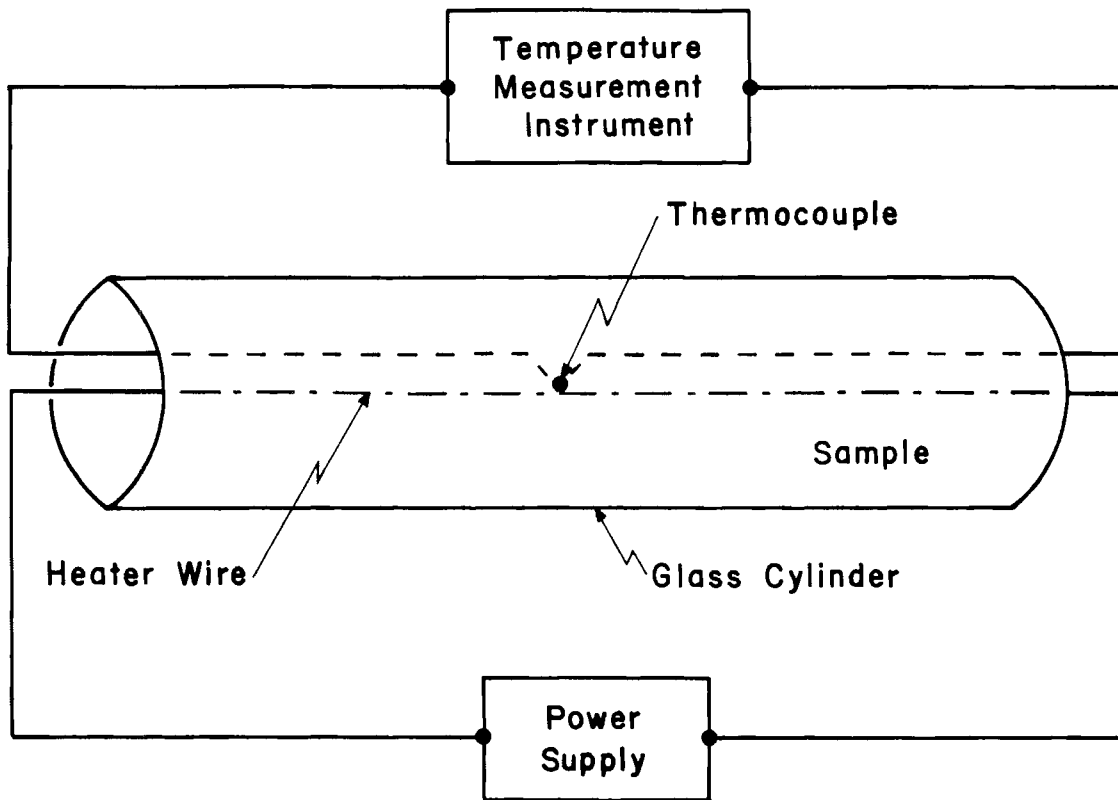
FIGURE 3.14. Line-Source Method for Measuring Thermal Conductivity

It appears that thermodynamic parameters such as heat capacities and thermal conductivities can be estimated without actually performing measurements. The specific heats of many common dry rock materials are in the relatively narrow range of 0.19 to 0.22 kcal/kg/°C. Therefore, effective volumetric heat capacity, which depends on porosity, will usually fall in the range of 600 to 800 kcal/m^3/°C. At the Mobile site, a volumetric heat capacity of 661 kcal/m^3/°C was calculated for the storage aquifer for an estimated porosity of 0.33.

The thermal conductivity of most saturated, porous, sedimentary materials will fall in the range of 0.75 to 3 kcal/(m.hr.°C) depending mainly on composition and porosity. If either or both of these properties are

known, the graph reproduced as Figure 3.13 can be used to obtain an estimate that may be adequate for many applications. Measurements made using the line-source method indicated an aquifer thermal conductivity of 1.97 ± 0.16 kcal/(m.hr.°C). Using a porosity of 33% and a solids density of 2.6 gm/cm^3, the graph in Figure 3.13 yields a thermal conductivity of about 1.93 kcal/(m.hr.°C), which is an excellent estimate of the measured value.

Unlike thermodynamic and chemical properties, the determination of hydraulic parameters requires the performance of extensive field testing. A series of new and existing observation wells was used at the Mobile site to conduct pumping tests in which the storage coefficients and the vertical and horizontal permeabilities of the storage aquifer and the upper and lower confining layers were determined.

Temporary, partially screened observation and pumping wells were installed in the aquifer for the anisotropy test. The pumped well was screened over a 3.1-m section near the bottom of the 21.3-m thick aquifer. The observation wells, located 7.6, 15.2, and 22.9 m, respectively, from the pumped well, were screened over 3.1-m sections near the top of the aquifer. Water was withdrawn at a constant rate of 818 m^3/day for the test. Drawdown in the observation wells was affected by a boundary about 20 min after pumping began. Consequently, the data analysis was based on early data. The average transmissibility and storage coefficient for the test were 1.140 m^2/day and 0.00049, respectively, and the ratio of horizontal to vertical permeability as determined by a method described by Weeks (1969) was 6.71.

Standard pumping tests were performed for pumping rates of 600 and 2,125 m^3/day using fully penetrating pumping and observation wells. Analysis of the drawdown data by the modified nonequilibrium method resulted in values for the transmissibility and the storage coefficient of 1,130 m^3/day and 0.00069, respectively, for the low pumping rate and 1,140 m^2/day and 0.00066, respectively, for the high pumping rate. The drawdown deviation from the Theis curve was analyzed to locate a boundary about 150 m from the pumped well.

Partially-screened observation wells were located 15 m from the fully penetrating pumped well in the upper and lower aquitards for the leaky aquifer test. This pumping test was performed concurrently with the standard pumping test at the withdrawal rate of 600 m^3/day. The drawdown in the aquitard wells and in a fully penetrating aquifer observation well located 15 m from the pumped well were analyzed by the ratio method of Neuman and Witherspoon (1972). Values of the ratio of vertical permeability to specific storage were 0.67 and 1.21 for the upper and lower aquitards, respectively.

This series of pumping tests at the Mobile site emphasized the importance of obtaining good early drawdown data for each of the well tests. Leakage or boundary effects can cause drawdown data to deviate from the Theis curve very soon after pumping begins for confined aquifers. The principal data for evaluating the basic hydraulic parameters at the Mobile site was taken from 2 to 15 min after pumping began.

A dispersivity field test was performed during the first injection cycle at the Mobile test site. Sodium bromide was injected at an average concentration of 11 mg/l into the injection well. The average hot-water injection rate was 45.4 m^3/hr. Water samples withdrawn from a well located 15 m from the pumped well were analyzed throughout the injection. A method outlined by Gupta, Batta and Pandey (1980) was applied to determine an apparent hydrodynamic dispersion coefficient of 9.1 cm at the Mobile site.

4.0 DESCRIPTION AND RESULTS OF THE FIRST TWO
INJECTION-STORAGE-RECOVERY CYCLES

As mentioned in Section 2.0, an important objective of the current experiments (third set) was to ascertain if using storage formation water as supply water for heating would eliminate the clogging problems observed in previous experiments. To eliminate any effects due to earlier experiments, a new storage zone was selected on the eastern side of the original well field (Figures 3.1 and 4.1). A new injection-recovery well (I2) was drilled and surrounded by observation wells designed to measure temperature, hydraulic head or tracer concentration. (The old storage zone was located in the vicinity of the boiler shown in Figure 4.1). Several existing observation wells were incorporated into the new wellfield.
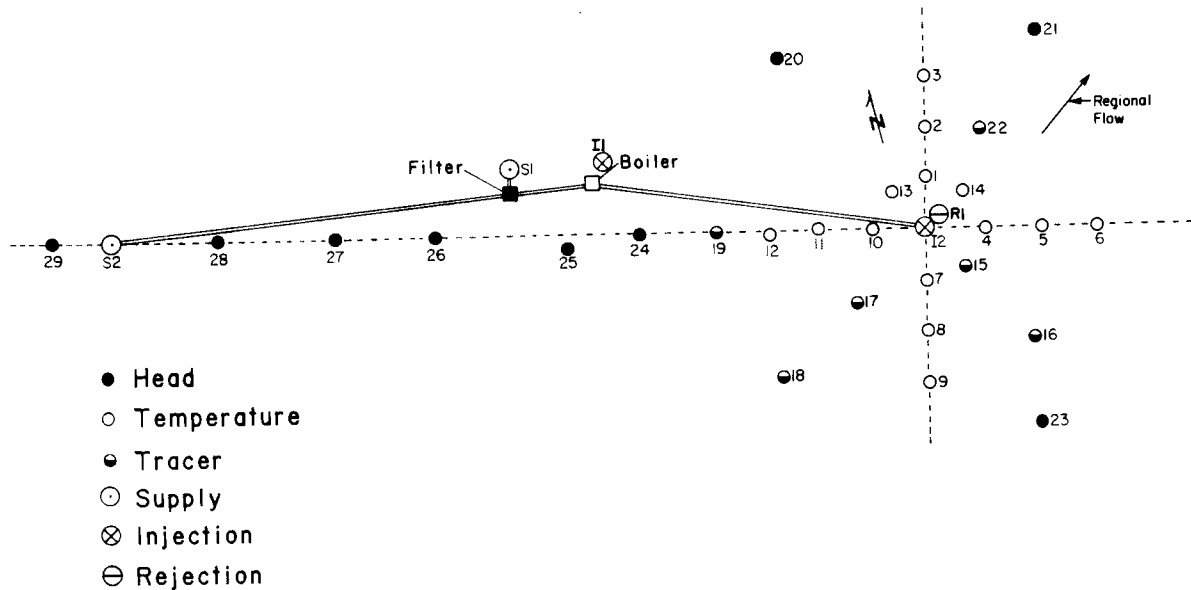
FIGURE 4.1. Top View of Wellfield at the Mobile Site

Because the data collected in the current experiments are serving as the basis for rather extensive mathematical modeling studies, more than the usual attempt was made to determine accurate hydraulic properties of the storage aquifer and aquitards. These properties included both vertical and horizontal permeability of the storage aquifer, storativity, and vertical diffusivity of the upper and lower aquitards. Thermodynamic properties such as thermal conductivity and heat capacity are important also and were measured or estimated in previous studies (Molz, Warman and Jones 1978). Pre-injection aquifer testing at the Mobile site is described in detail in Section 3.0. Relevant properties that were measured or estimated are summarized in Table 4.1.

4.1 DESCRIPTION OF EXPERIMENTS

Observation wells used to measure temperature in the storage formation were constructed as shown in Figure 4.2. Thermistors were employed to measure temperature at six locations in each well. Two thermistors were installed at each location to provide a backup array. The wells were backfilled with sand to minimize unrepresentative thermal convection within the well bores. Temperature was measured also in the upper and lower aquitards. One well is screened in each of the aquitards and temperature was measured at two locations in each well. The observation wells used to measure hydraulic head were constructed similar to the temperature wells but, of course, were not backfilled with sand.

Tracer injection and sampling was performed to compare the movements of solute and heat in the aquifer. A chemical feed system was used to inject sodium bromide into the hot water pipeline throughout cycle 3-1 injection (Figure 4.3). Water samples were obtained from wells I2, 15, 16 and 22 so that tracer concentration could be recorded as a function of time. Rather than continuous tracer injection, two slugs of tracer were added to the supply water during the first week of cycle 3-2 injection.

TABLE 4.1. Summary of Measured and Estimated Aquifer Characteristics

---

Thermal Conductivity

1) Aquifer: 1.98×10^5 J/(m $\cdot$ d $\cdot$ °C); [31.8 BTU/(ft $\cdot$ d $\cdot$ °F)]
2) Aquitards: 2.21×10^5 J/(m $\cdot$ d $\cdot$ °C); [35.5 BTU/ft $\cdot$ d $\cdot$ °F)]

Heat Capacity: 1.81×10^6 J/(m^3 $\cdot$ °C); [27.0 BTU/(ft^3 $\cdot$ °F)]
(The above is an estimate for typical materials)

Hydraulic Conductivity (Horizontal)

1) 1976 Test: 44 m/d; [144 ft/d]
2) 1980 Partially Penetrating Test: 53.6 m/d; [175.8 ft/d]
3) 1980 Fully Penetrating Test: 53.4 m/d; [175.3 ft/d]

Hydraulic Conductivity (Vertical)

1) 1980 Partially Penetrating Test: 7.66 m/d; [25.1 ft/d]

Aquifer Storativity

1) 1976 Test: 5×10^{-4}
2) 1980 Partially Penetrating Test: 4.9×10^{-4}
3) 1980 Fully Penetrating Test: 6.4×10^{-4}

Aquifer Porosity: Estimated at 0.33

Hot water pumped from the injection well (I2) during the recovery phase of each cycle was returned to the confined aquifer through the supply well (S2) to minimize the amount of energy needed to heat water for subsequent injections. It was anticipated that this procedure might create clogging problems, however, because the concentration of clay particles in the pumped water may tend to increase with repeated cycles. To control clogging and to maintain acceptable injection rates, a rapid sand filtering
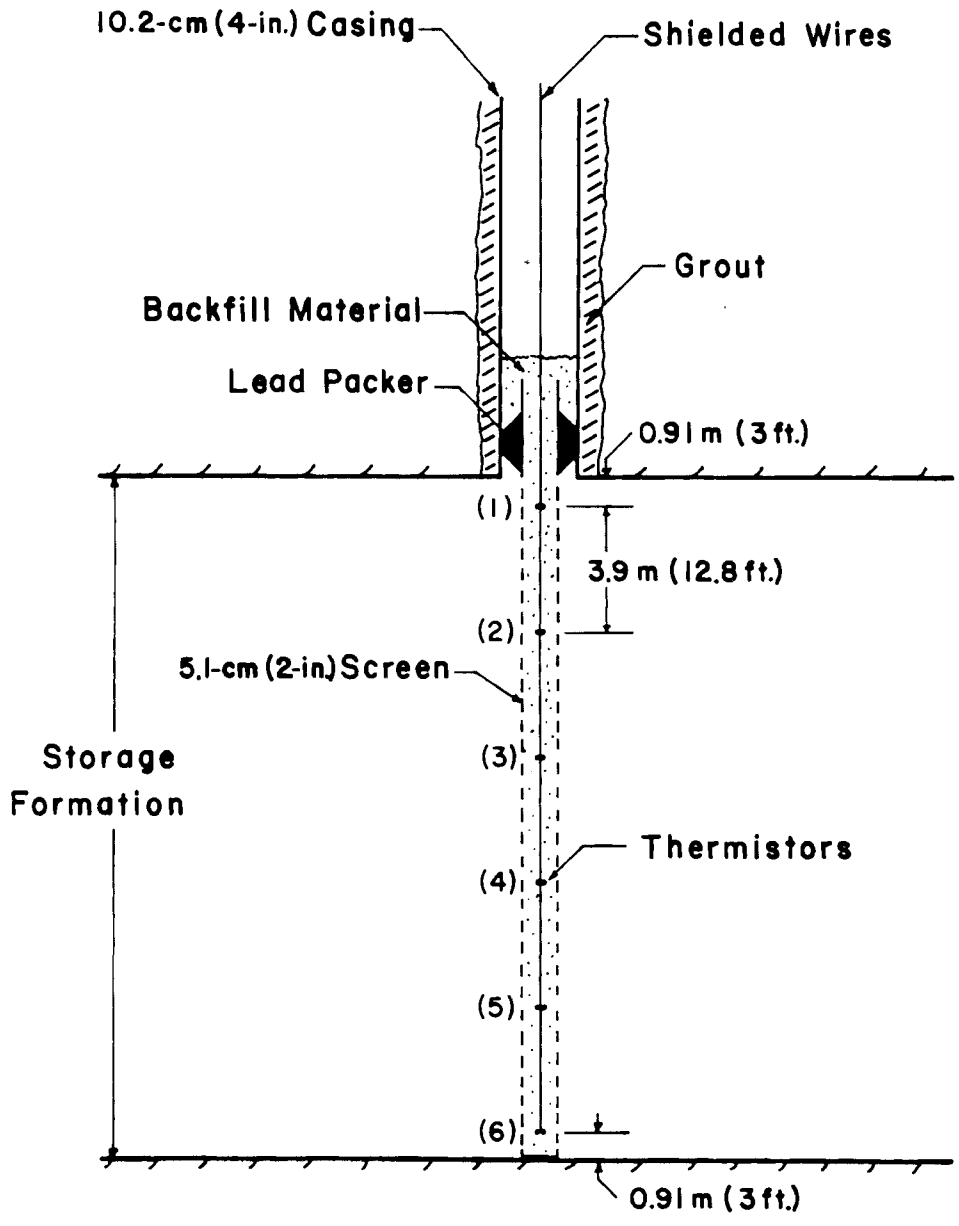
FIGURE 4.2. Typical Temperature Observation Well
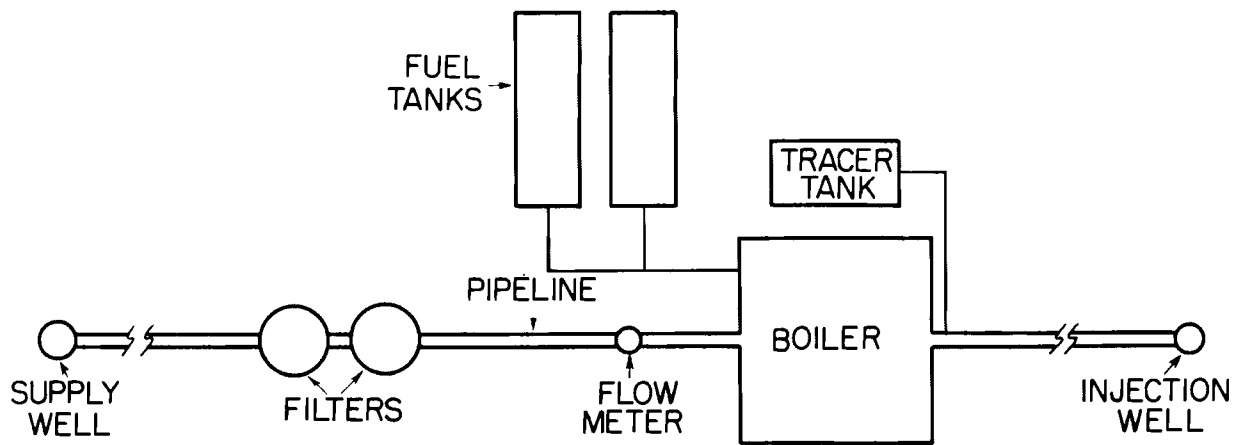
FIGURE 4.3. Schematic Diagram Showing the Tracer Tank, Boiler and Associated Equipment at the Mobile Site.

system was installed. The filtering system can either be used or bypassed during the injection and recovery phases.

At regular intervals during both cycles, careful level measurements were made so that additional data could be obtained on the magnitude of land surface elevation changes caused by ATES at the Mobile site (Molz, Parr and Andersen 1981). The locations of the reference, observation and measurement pads are shown in Figure 4.4. Each pad was constructed of reinforced concrete with a surveying marker embedded in the center. A level was placed on the observation pad; from this location, relative elevations of the markers on pads A and B with respect to those on pads C and D were recorded.

A 3-month injection-storage-recovery cycle (cycle 3-1) followed by a 7.3-month cycle (cycle 3-2) constituted the main experiment. The average injection temperatures were 58.5°C and 81°C for cycle 3-1 and cycle 3-2, respectively. Shown in Figures 4.5 and 4.6 are the cumulative injection volumes for each cycle.
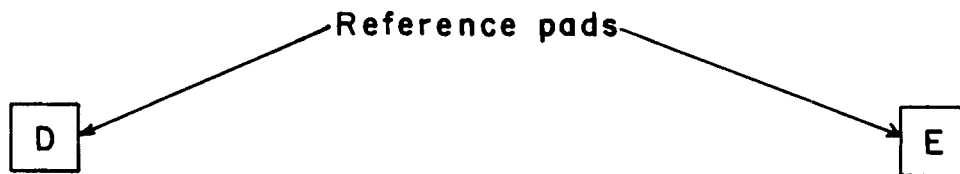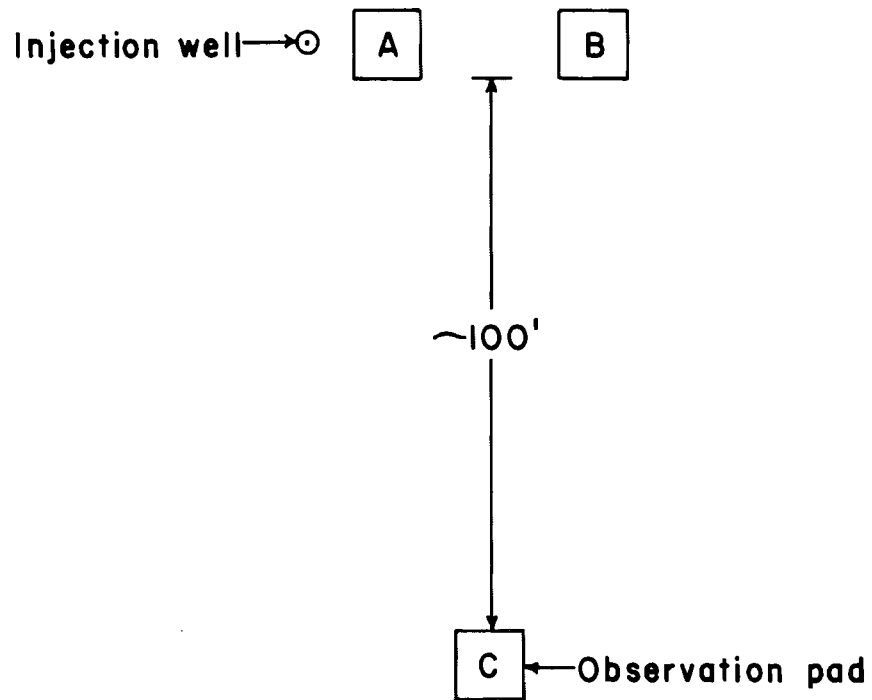
FIGURE 4.4. Relative Locations of the Concrete Pads Used to Monitor
Land Surface Elevation Changes

Cycle 3-1 injection began on 2/17/81 and continued intermittently until 3/21/81 when 25,402 m^3 of water had been injected. Injection temperature versus time is shown in Figure 4.7. Recovery pumping was initiated on 4/21/81 and continued until 5/17/81. Cycle 3-1 recovery rate as a function of time is shown in Figure 4.8. The total volume recovered was 28,924 m^3.
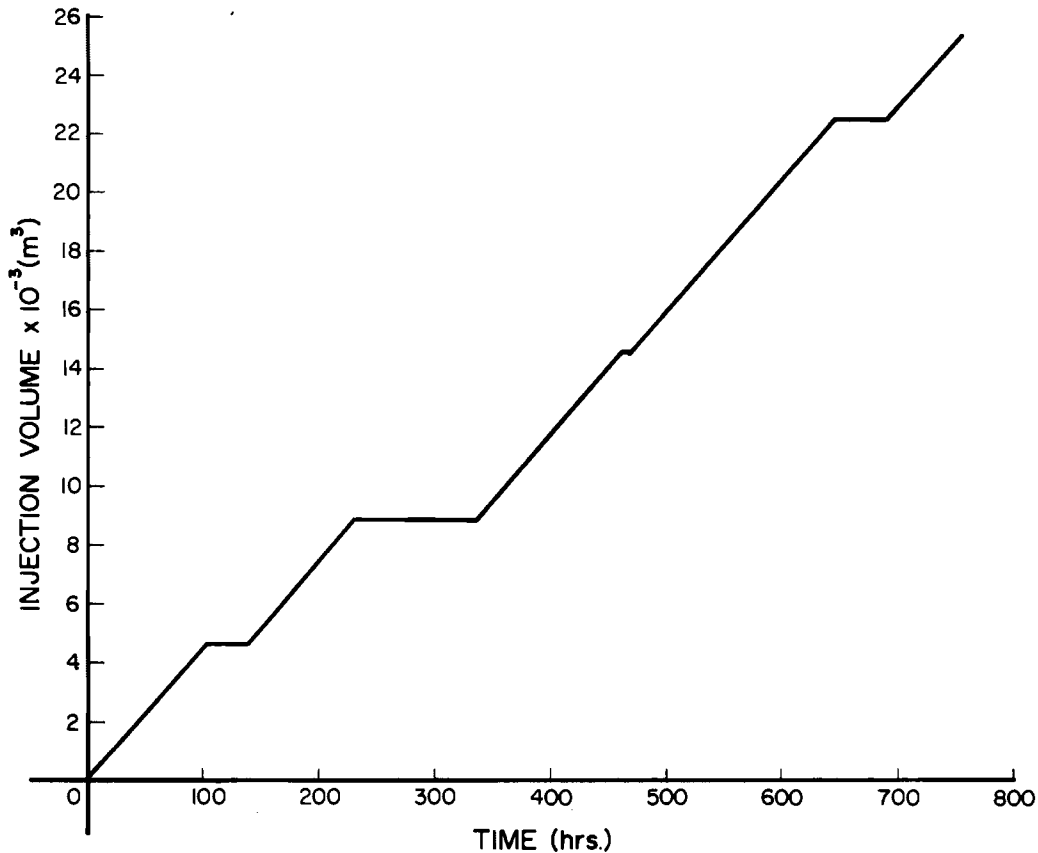
FIGURE 4.5. Cumulative Injection Volume versus Time for Cycle 3-1
Note: The larger horizontal segments were time periods required for unexpected boiler maintenance.

Cycle 3-2 cycle injection of 58,063 m^3 of heated water began on 6/12/81 and continued intermittently until 10/27/81. The injection rate was slower than anticipated because the water heater was operating near its capacity. To maintain a higher injection temperature without firebox
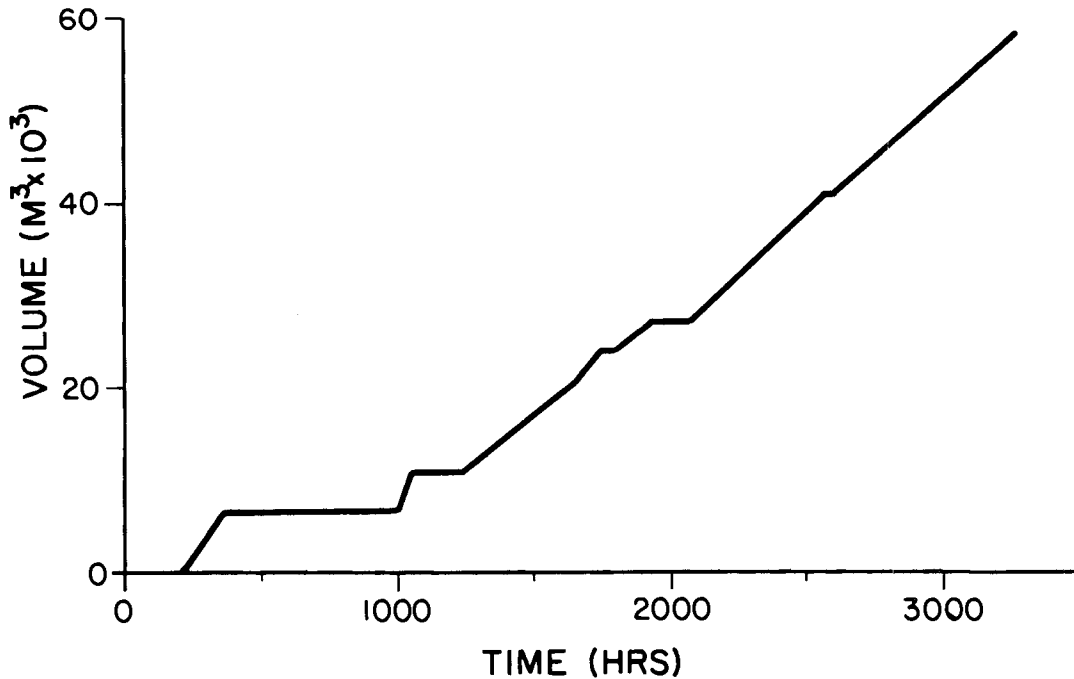
FIGURE 4.6. Cumulative Injection Volume versus Time for Cycle 3-2
Note: During the first 1000 hours of the cycle, boiler
malfunction continued to be a problem.

overheating, the flow rate was reduced to approximately 0.45 $m^3 \cdot min^{-1}$. The resulting injection temperature versus time curve is shown in Figure 4.9. After 34 days of storage, production began on 11/30/81 and continued until 1/23/82, at which time 60,575 m^3 of water had been recovered at an average average rate of 0.8 $m^3 \cdot min^{-1}$ as shown in Figure 4.10.

4.2 RESULTS OF CYCLE 3-1

The temperature history at the recovery well is shown in Figure 4.11. Although the average injection temperature near the end of injection was 52°C and prior to that was 58°C or higher, the initial recovery temperature was less than 48°C. This difference between temperatures at the end of injection and the beginning of recovery was not observed during earlier, comparable experiments at the Mobile site (Molz et al. 1979; Molz, Parr and Andersen 1981) and suggested that a previously unobserved heat loss mechanism was operating. The fundamental differences between this experiment
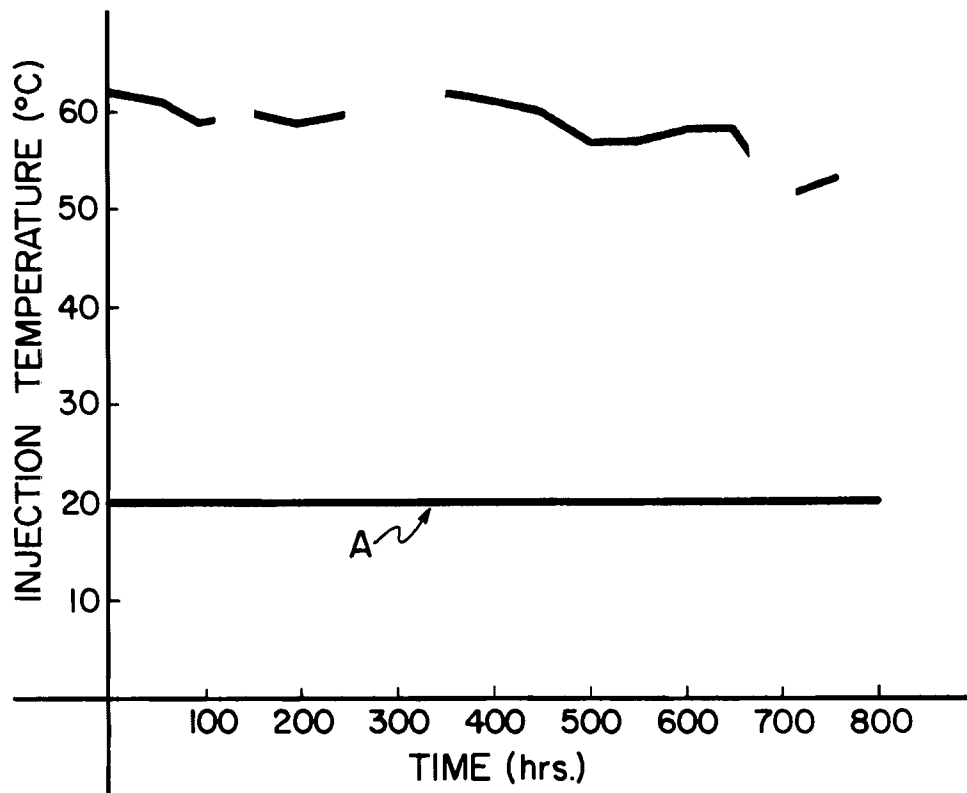
FIGURE 4.7. Injection Temperature versus Time for Cycle 3-1
            Note: The line marked "A" indicates the ambient ground water
                   temperature.

and earlier experiments were that the injection volume (25,402 m^3) was
smaller and the injection-recovery well was fully penetrating. Calcula-
tions indicate that 56% of the injected thermal energy was recovered in a
volume of water equal to the injection volume.

Interpolated temperature contours in the aquifer along two vertical
sections at the beginning and end of storage are shown in Figures 4.12 and
4.13. At the end of the injection period, there was a significantly
greater radial displacement near the middle of the confined aquifer than
near the upper and lower aquitards. Because the injection well, I2, was
fully penetrating, it was concluded that the aquifer has variable

4.9
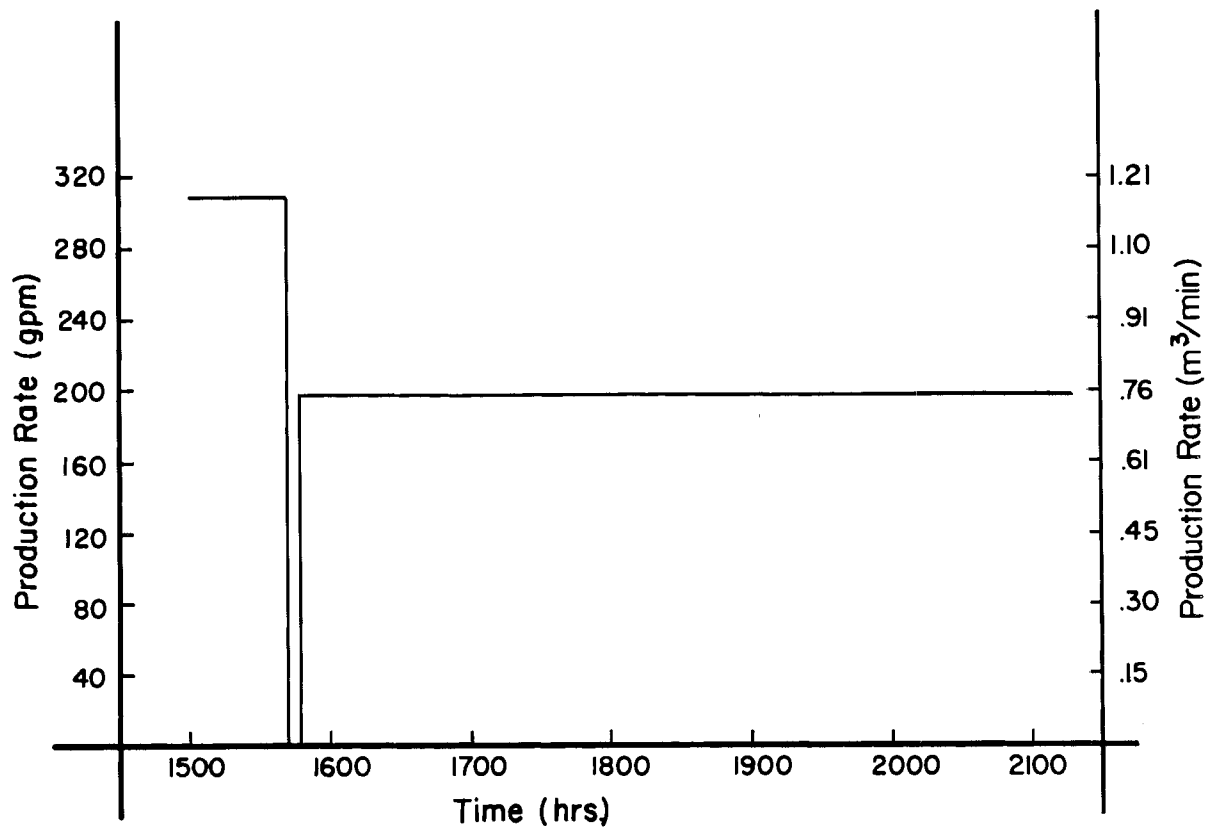
FIGURE 4.8. Cycle 3-1 Recovery Pumping Rate as a Function of Time

horizontal hydraulic conductivity. In the direction of observation wells 10, 11 and 12, the temperature distribution is more uniform vertically. It should also be noted that the thermal radius is not as large in this direction. This asymmetry is probably caused by a variable transmissivity. The regional flow velocity is a relatively small 0.8 m/month in a northeasterly direction.

Because of the relatively low initial recovery temperature, it was suspected that a significant amount of free thermal convection occurred during the storage period. Although significant convection was not observed in previous experiments, we were now in a portion of the aquifer
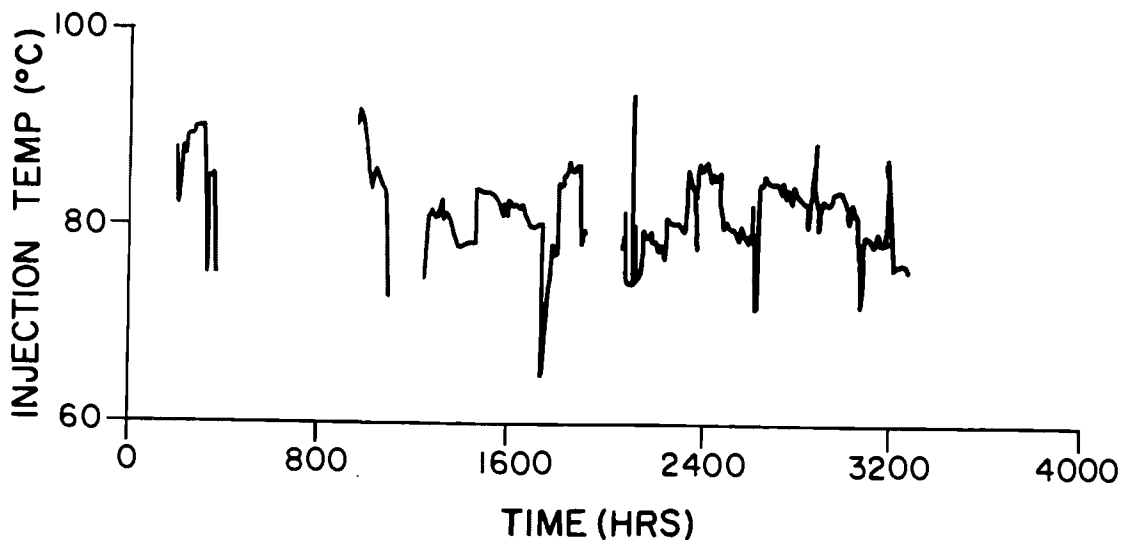
FIGURE 4.9. Cycle 3-2 Injection Temperature as a Function of Time

with slightly higher horizontal permeability and perhaps a significantly higher vertical permeability (Papadopulos and Larson 1978; Sykes et al. 1982). Also, we were working with higher injection temperatures with correspondingly greater buoyant forces to induce convection.

Shown in Figure 4.14 is a plot of ground-water temperature versus time at six elevations in observation well #4, which is approximately 15 m east of the injection well. The thermal front arrived at the central thermistors 100 hr after the start of injection. About 80 hr later it arrived at the thermistors above and below the central thermistors, indicating a significantly higher flow velocity near the center of the aquifer, which, as mentioned previously, is reflected in Figures 4.12 and 4.13.

An indication of the geometry of the high intrinsic permeability zone detected at the present storage location may be obtained by examining Figures 4.15 and 4.16. Shown in these figures are first arrival times of the thermal front recorded in the temperature observation wells during
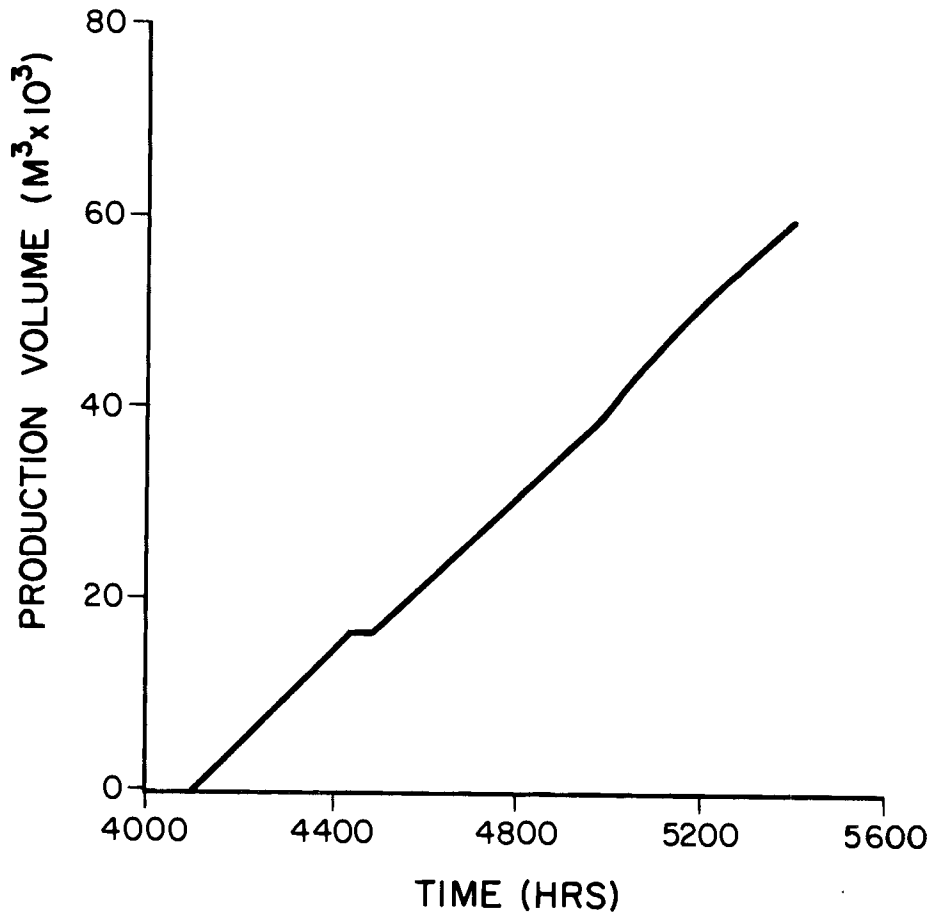
FIGURE 4.10. Cumulative Production Volume versus Time for Cycle 3-2

cycle 3-1. For each aquifer cross section, the locations of the two short-
est arrival times in each observation well are connected to those of neigh-
boring wells by straight lines. The line segments indicate approximate
boundaries of a high permeability zone near the middle of the aquifer.

This approximation correlates well with the temperature distributions
shown in Figures 4.12 and 4.13. It supports also the three-layer aquifer
permeability model used by Buscheck, Doughty and Tsang in their computer
simulations of cycles 3-1 and 3-2.

4.12
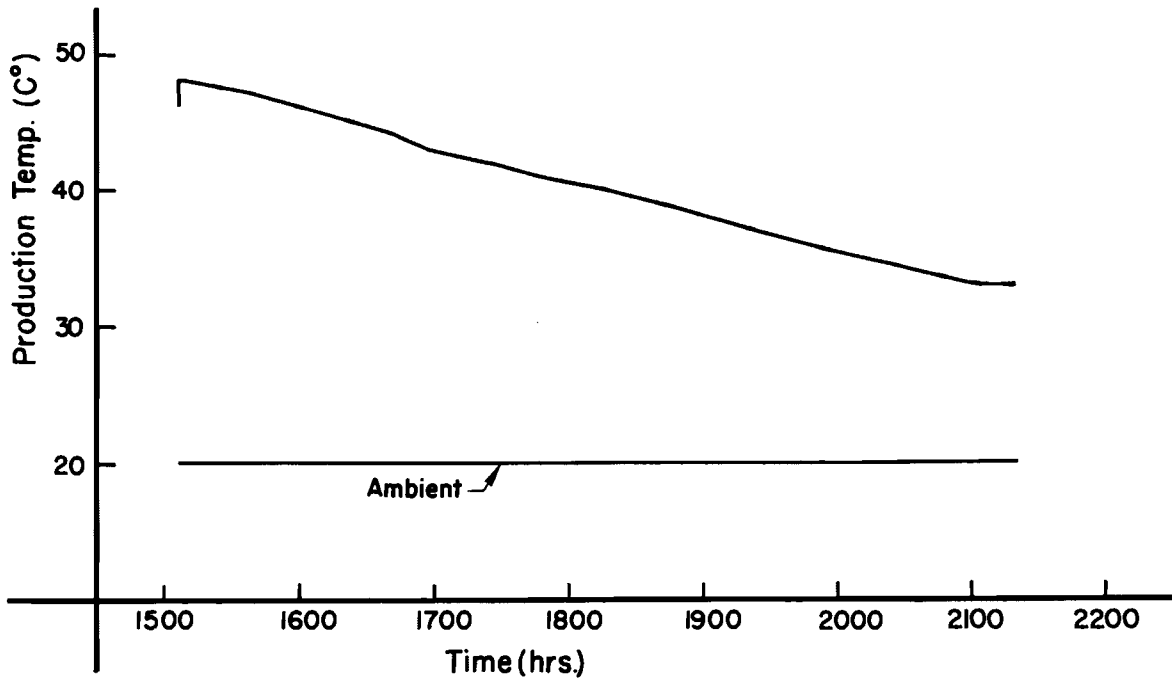
FIGURE 4.11. Production Temperature versus Time for Cycle 3-1

The temperature variation recorded in well #4 shown in Figure 4.14 indicates that the bottom thermistor must be located in a very low permeability zone, which is probably an upward extension of the lower aquitard. Heat is being conducted rather than advected to this position. There is no sharp thermal front and the temperature continues to rise during the storage and part of the production periods. This is to be contrasted with the distinct temperature drop exhibited by thermistors 4 and 5 during the storage period. These thermistors are third and second from the bottom, respectively, and the drop in temperature undoubtedly is due to the occurrence of free thermal convection. Such temperature decreases during storage occurred in one or more thermistors located in the lower zone of the aquifer at all four 15-m temperature observation wells.

4.13
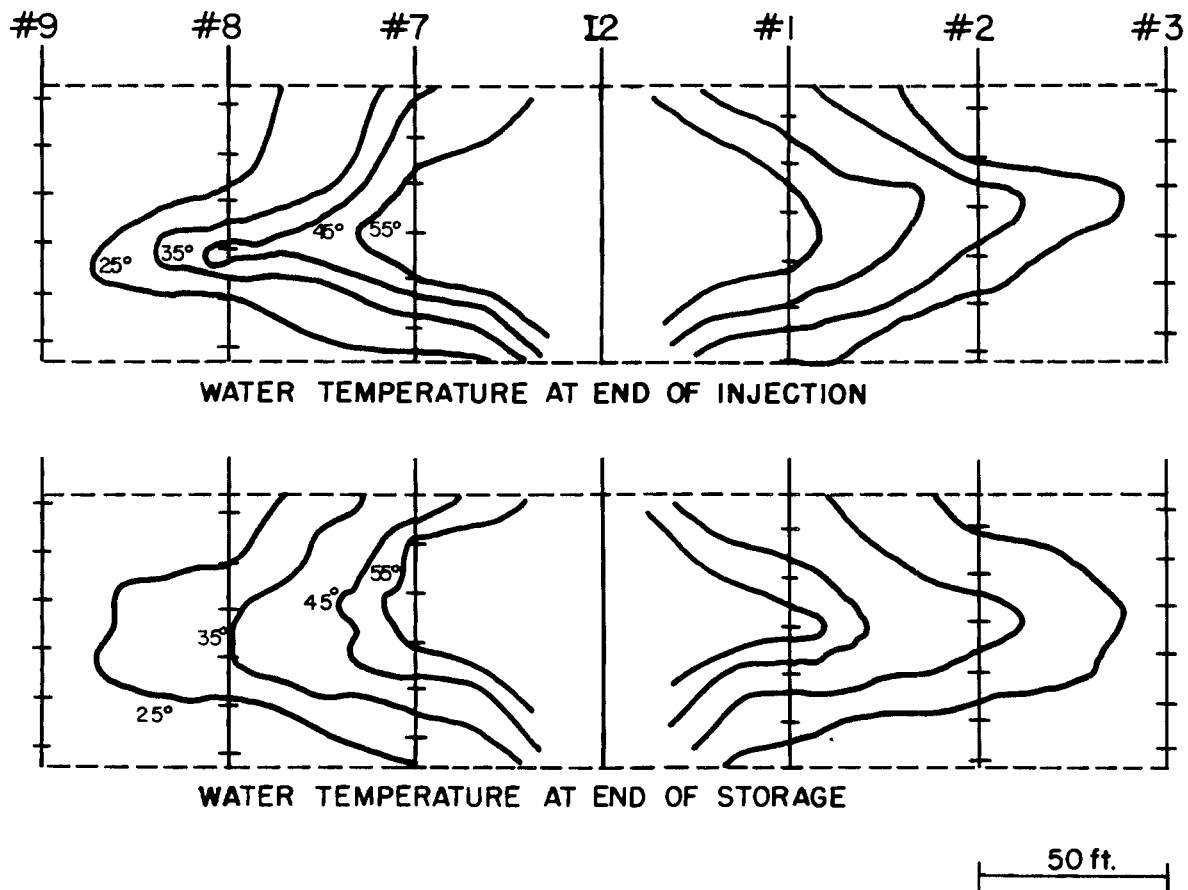
FIGURE 4.12. Interpolated Ground Water Temperature Contours at Selected
Times during Cycle 3-1

Evidence of a more integrated nature, which indicates the occurrence
of a significant amount of free thermal convection, was obtained from the
tracer experiment performed during cycle 3-1. Displayed in Figure 4.17 is
a plot of tracer concentration versus time that was obtained for the injec-
tion-production well. The injection concentration averaged 12.5 mg/l dur-
ing the first 400 hours of injection and 18.8 mg/l during the remaining 350
hours of injection. No samples were taken from I2 during the storage time.

4.14
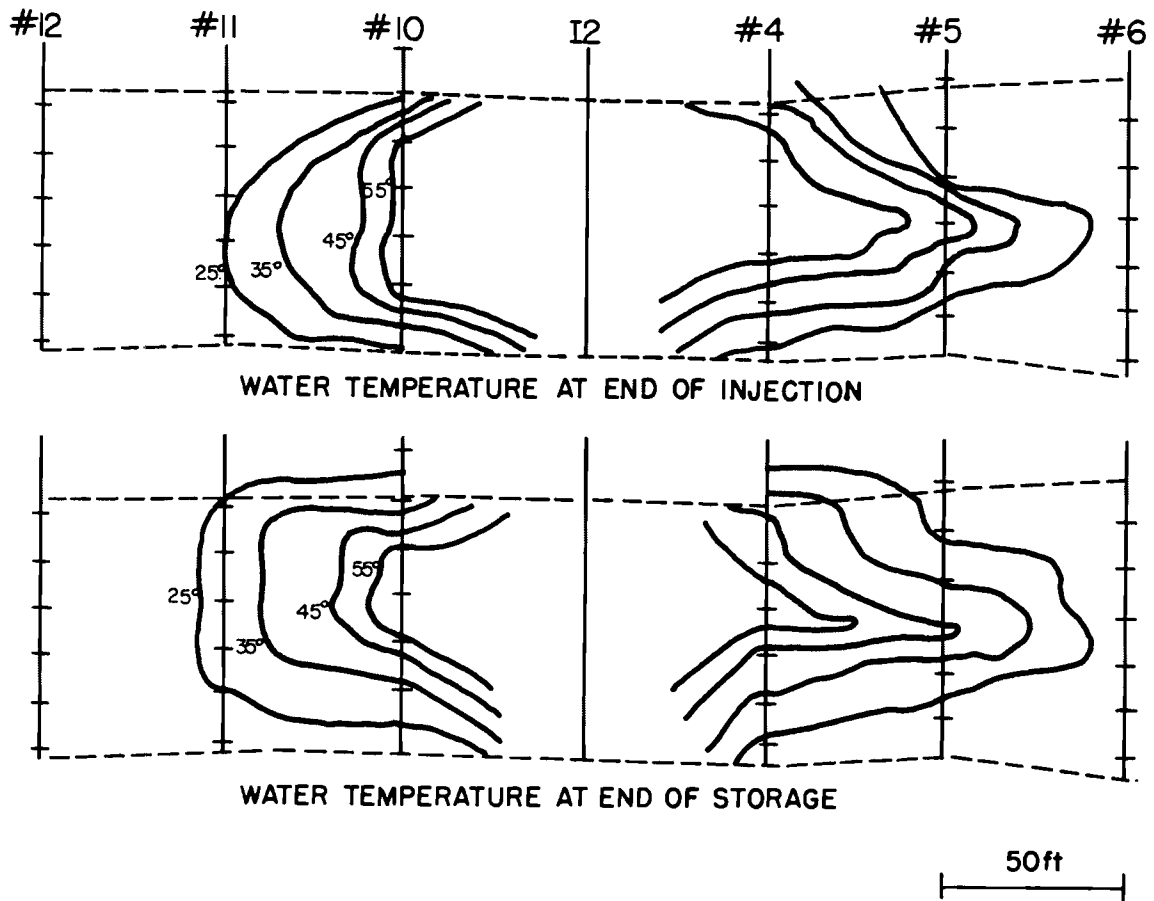
FIGURE 4.13. Interpolated Ground-Water Temperature Contours at Selected Times during Cycle 3-1

Samples taken at recovery initiation show an immediate drop to approximately 15 mg/l from the last injection concentration of 18.8 mg/l. Vertical convection induced by buoyant forces during storage could cause the intrusion of native water at the bottom of the pumping well. This would dilute the recovered water and lead to the observed sudden decline of tracer concentration. The predicted recovery concentration based on a simple radial flow model without convection is shown also in Figure 4.17. The difference between the two curves indicates the possible occurrence of

4.15
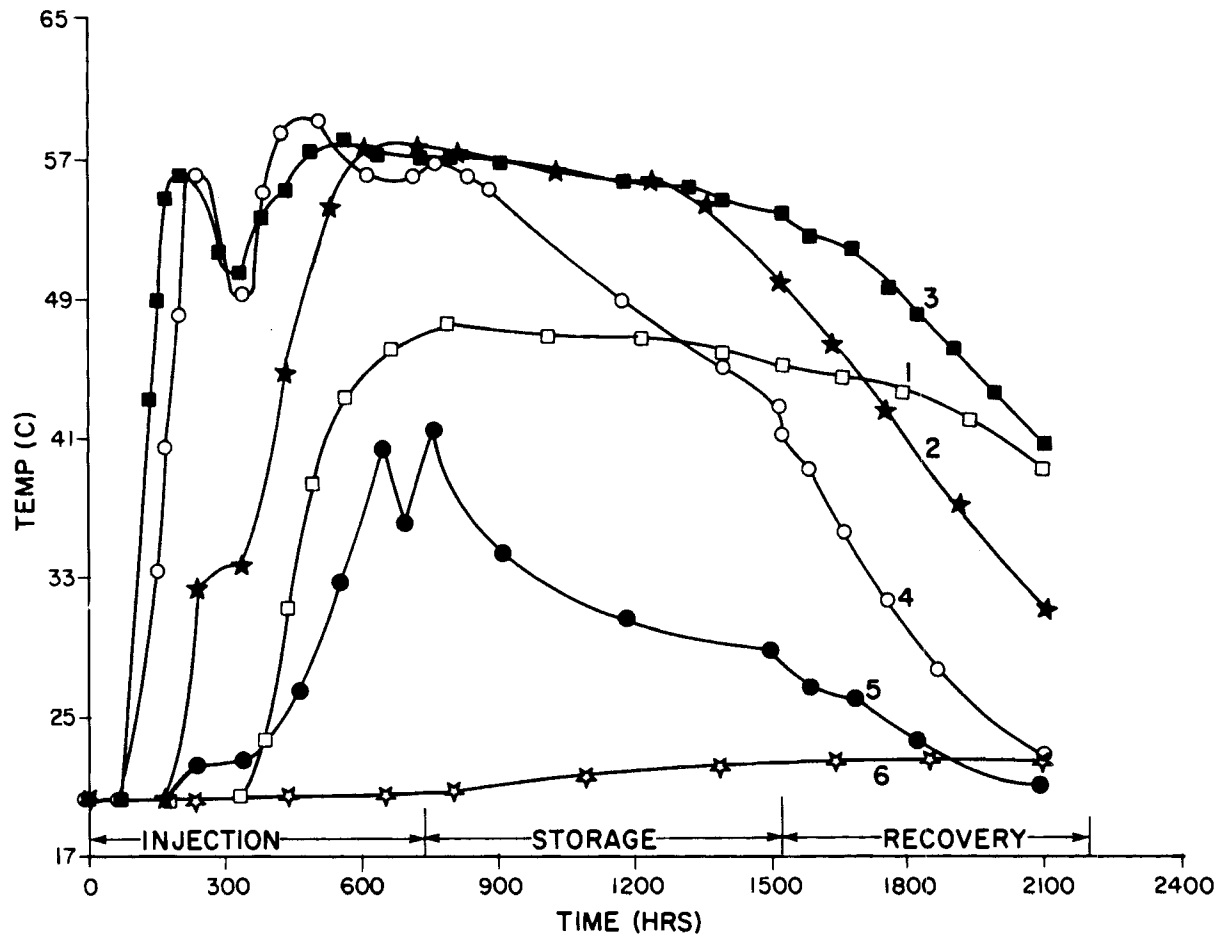
FIGURE 4.14. Ground-Water Temperatures as a Function of Time for Well #4 during Cycle 3-1

Note: The numbers next to the curves correspond to thermistor elevations shown in Figure 4.2

significant thermal convection. The estimated local dispersivity of 0.3 to 3 m is not nearly large enough to account for the low initial production concentration.

A notable result during cycle 3-1 was the absence of injection well clogging due to clay particle swelling, dispersion and migration. During previous experiments, this phenomenon was identified as the major technical

#11   #10   I2   #4   #5

                          110 ft
              NF
                          120 ft
     •   •   •   •NF
     836   328   130   338
                                                           •1174
     703   184   140
                          150   184   745
     703   184   160   151
                                                           500
     703   151   170   151
                          180   500
     703   151   199
                          190
     NF   •   200 •   NF   •NF

     100 80   60   40   20   0   20   40   60   80   100

RADIUS (ft.)
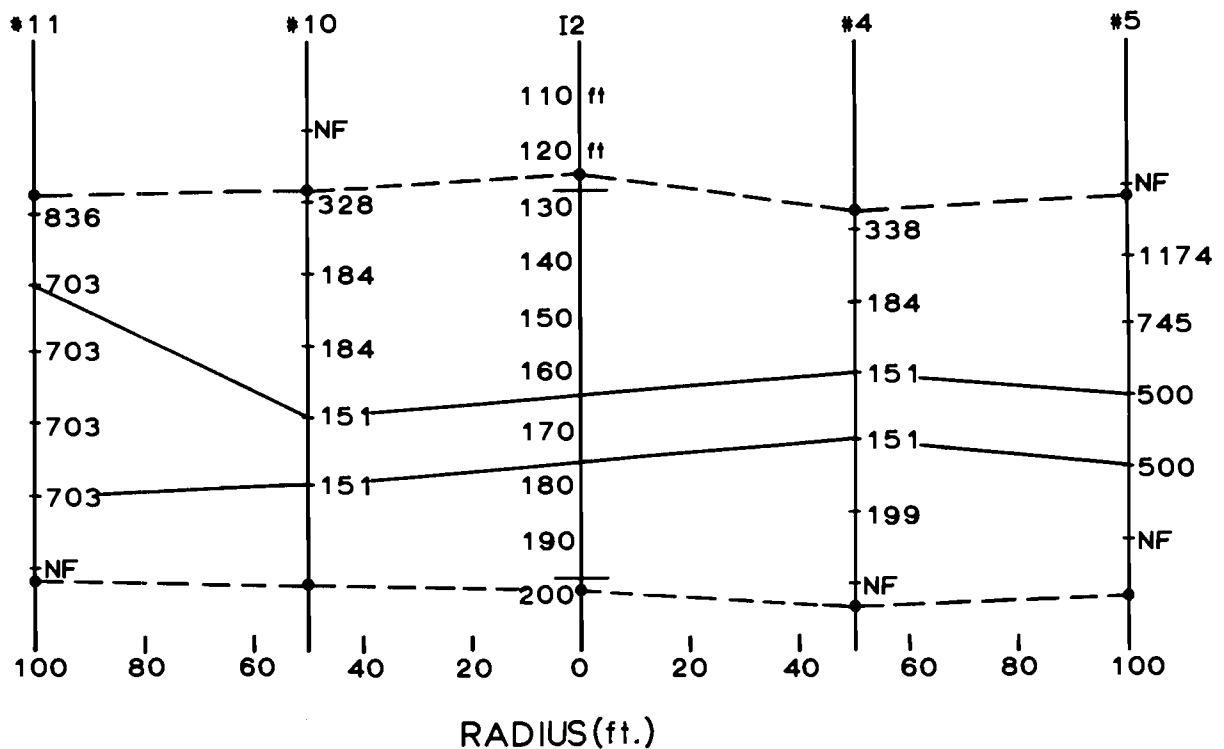
FIGURE 4.15. West to East Vertical Aquifer Profile Showing First Thermal
              Arrival Times (hr) at the Various Thermistors During Cycle
              3-1 Injection

              Note: NF indicates that a definite thermal front did not
                     arrive.

problem (Molz et al. 1979; Molz, Parr and Andersen 1981). As mentioned
in Section 2.0, osmotic swelling occurs when clay platelets in
equilibrium with ground water having a relatively high ion concentration
come in contact with water having a relatively low ion concentration.
Such a situation occurred in previous experiments at the Mobile
site when relatively pure supply water from a shallow aquifer was
heated and injected into a deeper storage aquifer. In the current
experiments supply water was obtained directly from the storage
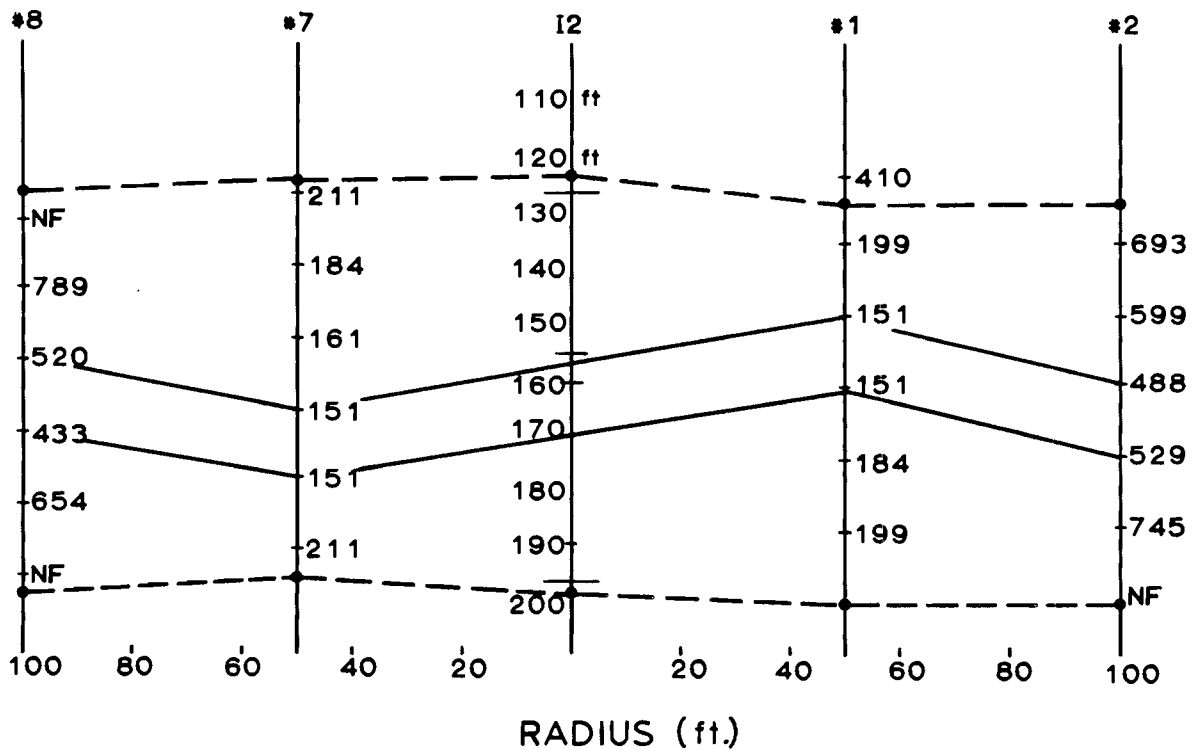
FIGURE 4.16. South to North Vertical Aquifer Profile Showing First Thermal Arrival Times (hr) at the Various Thermistors During Cycle 3-1 injection

Note: NF indicates that a definite thermal front did not arrive.

aquifer and NaBr was added, which increased the Na concentration by about 5 mg/l. Thus, the water injected had a slightly higher cation concentration than the native ground water, which would further retard osmotic swelling.

Shown in Figure 4.18 is the best specific capacity history obtained in previous experiments (Molz, Parr and Andersen 1981) along with that obtained in cycle 3-1. In the previous experiment, regular backwashing was
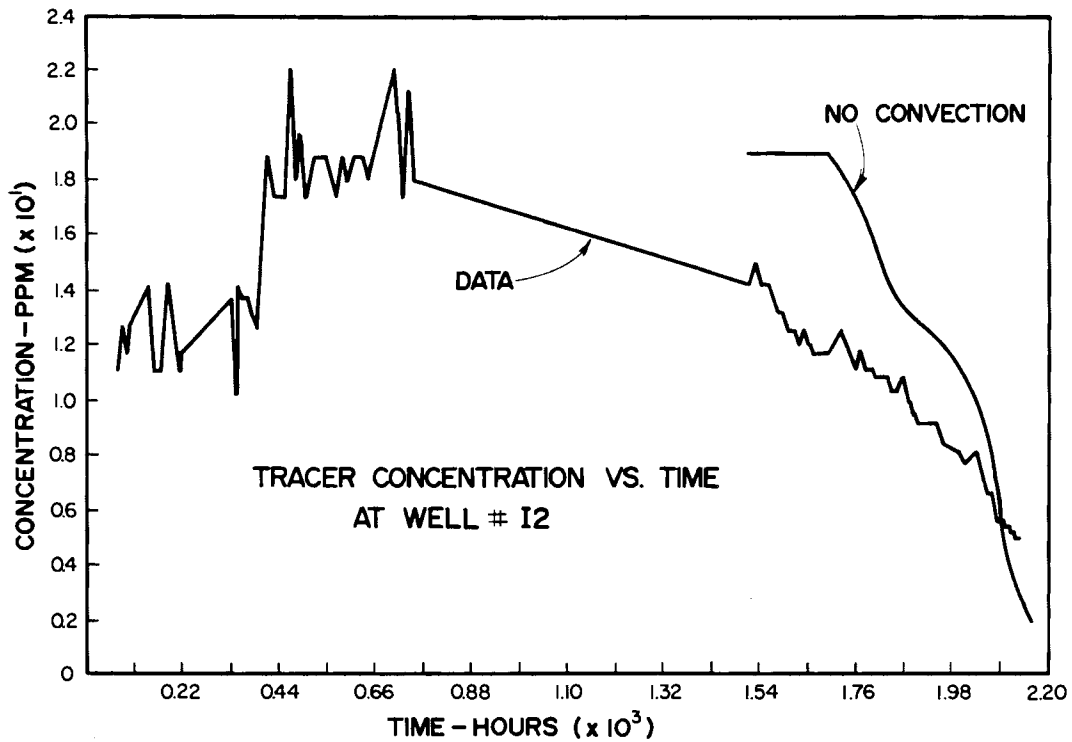
FIGURE 4.17. Tracer Concentration versus Time at the Injection-Production Well

Note: The curve labeled "No Convection" is a theoretical prediction of the concentrations that should have resulted in the absence of free thermal convection.

required to maintain an acceptable injection rate. Backwashing was initiated whenever the injection pressure reached 0.145 MPa (21 psi). This is to be contrasted with the current cycle 3-1 where the injection pressure remained stable over relatively long periods of time and the specific capacity was 5 to 15 times larger than that obtained previously.

Lack of clay particle dispersion was indicated also by the relatively low suspended solids concentration in the water recovered from the storage zone and reinjected to the supply zone. During cycle 3-1 the average value was 2.7 mg/l^{-1}. In previous comparable experiments, suspended solids averaged 35 mg/l^{-1} (Molz, Parr and Andersen 1981).
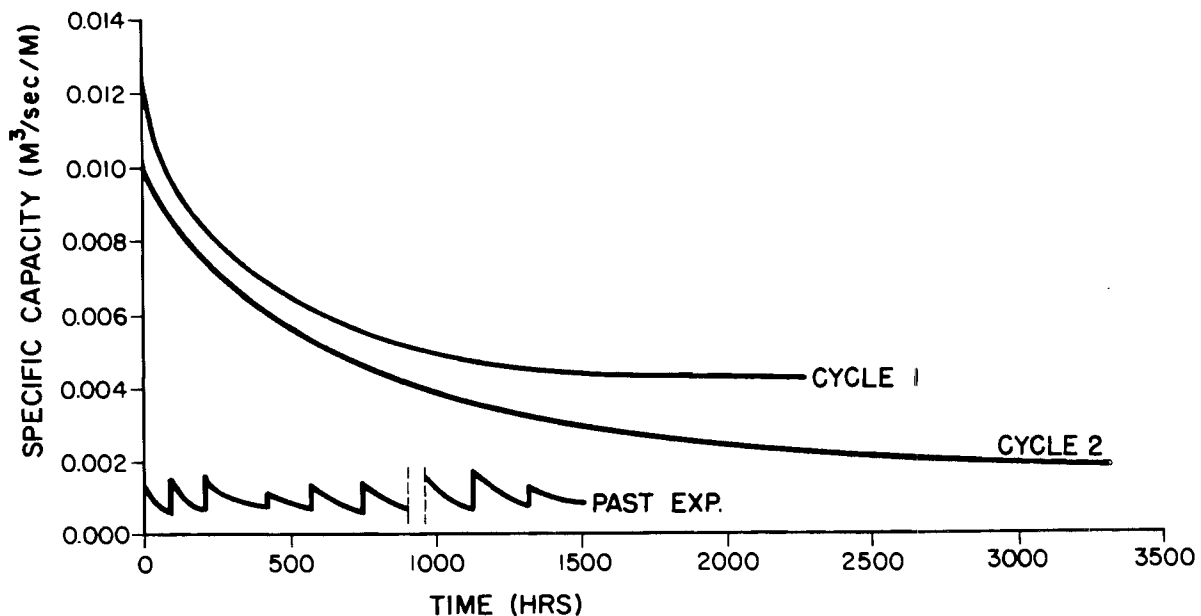
FIGURE 4.18. Specific Capacity of the Injection-Production Well During
Cycle 3-1, Cycle 3-2 and a Previous Experiment When Clogging
Occurred Due to Clay Dispersion

4.3 RESULTS OF CYCLE 3-2

Based on the results of cycle 3-1, there was concern that free thermal
convection would be an even more severe problem at the higher injection
temperature planned for cycle 3-2, which averaged 81°C. As shown in Figure
4.19, the concern was well founded. Shortly after production pumping was
initiated, the recovery temperature peaked at 55.1°C and began to decline.
Within 2 weeks the recovery temperature dropped into the upper forties, and
an energy recovery of less than 45% was projected in a recovery volume
equal to the injection volume.

Examination of ground-water temperature data clearly indicated
significant free thermal convection. Shown in Figure 4.20 are average
temperature contours on a radial section of the storage aquifer at three

4.20
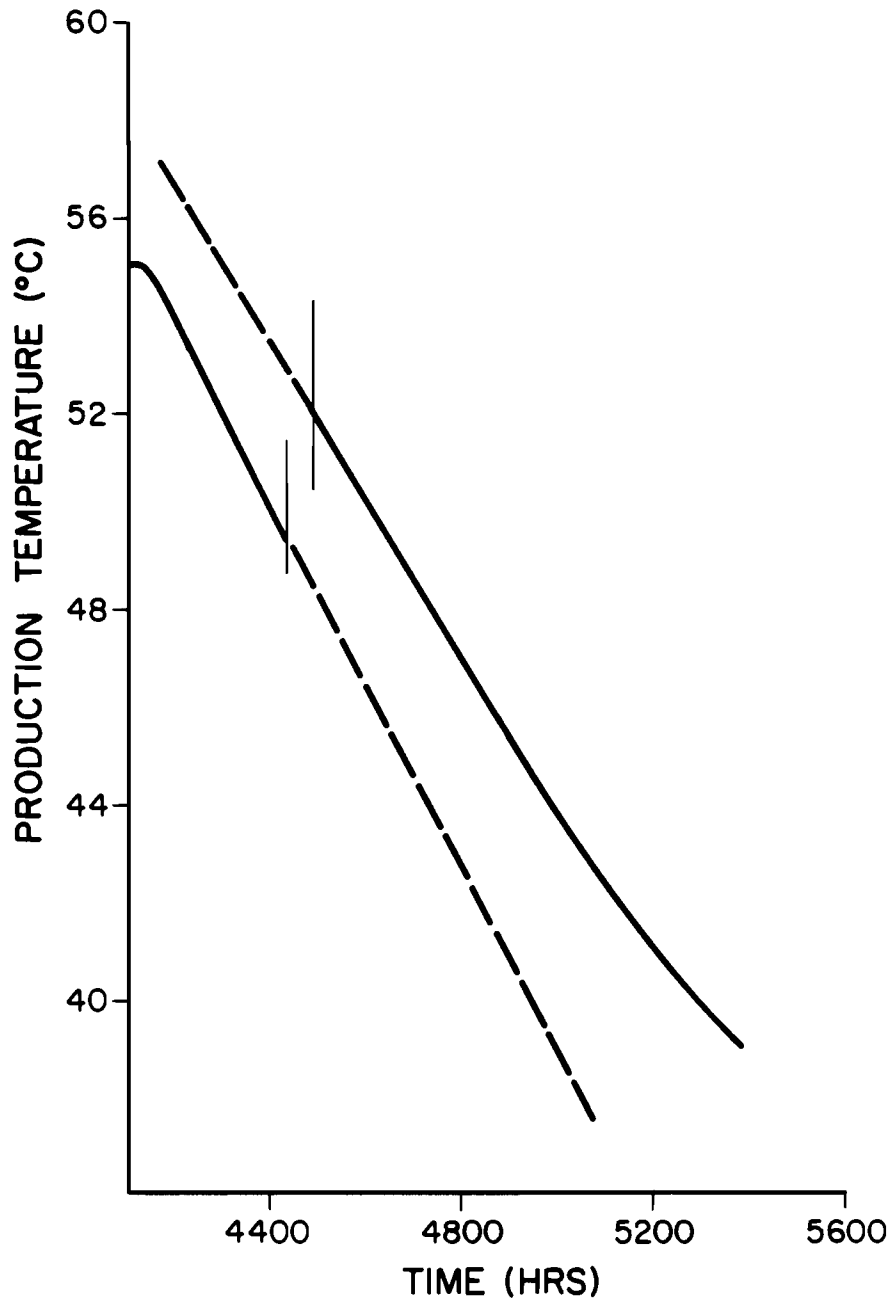
FIGURE 4.19. Production Temperature versus Time for Cycle 3-2
Note: The dashed lines are linear extrapolations
of the date segments.

4.21

different times. Plots were obtained by averaging data from observation wells at equal radial distances from the injection-production well. The shape of curves outside the zones where data were collected were inferred from computer simulations provided by Lawrence Berkeley Laboratory. Of particular interest are the positions of the 25°C and 35°C isotherms at the end of injection (Figure 4.20a) and 2 weeks after the beginning of recovery (Figure 4.20b). An upward migration of heat during and after the storage period was apparent. Due to the segregation of hot and cold water, a relatively large fraction of the injected heat remained in the aquifer after recovery was terminated. This is discussed further in Section 5.0.

In an attempt to improve energy recovery, production pumping was halted on December 14, 1981 so that the recovery well (I2) could be modified. The bottom half of the well was filled with sand and a figure-k packer was placed above the sand. It was reasoned that pumping only from the upper half of the production well would pull relatively more water from the upper and hotter portion of the storage aquifer. On December 16, recovery was resumed.

The result of recovery well modification can be seen clearly in Figure 4.19. Upon resumption of pumping the recovery temperature jumped from 49.5°C to 52.5°C, which is reflected by the discontinuity in the temperature versus time curve at 4430 hr. Ultimately, the energy recovered in the volume of water equal to the injection volume was 45.2%. Based on linear extrapolations of the two temperature curve segments, it was estimated that the energy recovery would have been 40% if modifications had not been made and 46 to 47% if modifications had been made prior to initiation of the production period. Thus, an energy recovery increase of approximately 7% would have been obtainable with the modifications that were made. It would have been possible to recover additional energy if the effective penetration of the recovery well had been reduced significantly below 50%. Computer simulations, using a model validated with previous data from the Mobile site (Tsang, Buscheck and Doughty 1981), have been run to estimate

35°

25°

A

END OF INJECTION

Injection
Well
15 m Well
30 m Well
46 m Well
Top of
formation

65°

55°

45°

35°

25°

B

AT WELL MODIFICATION

bottom of
formation
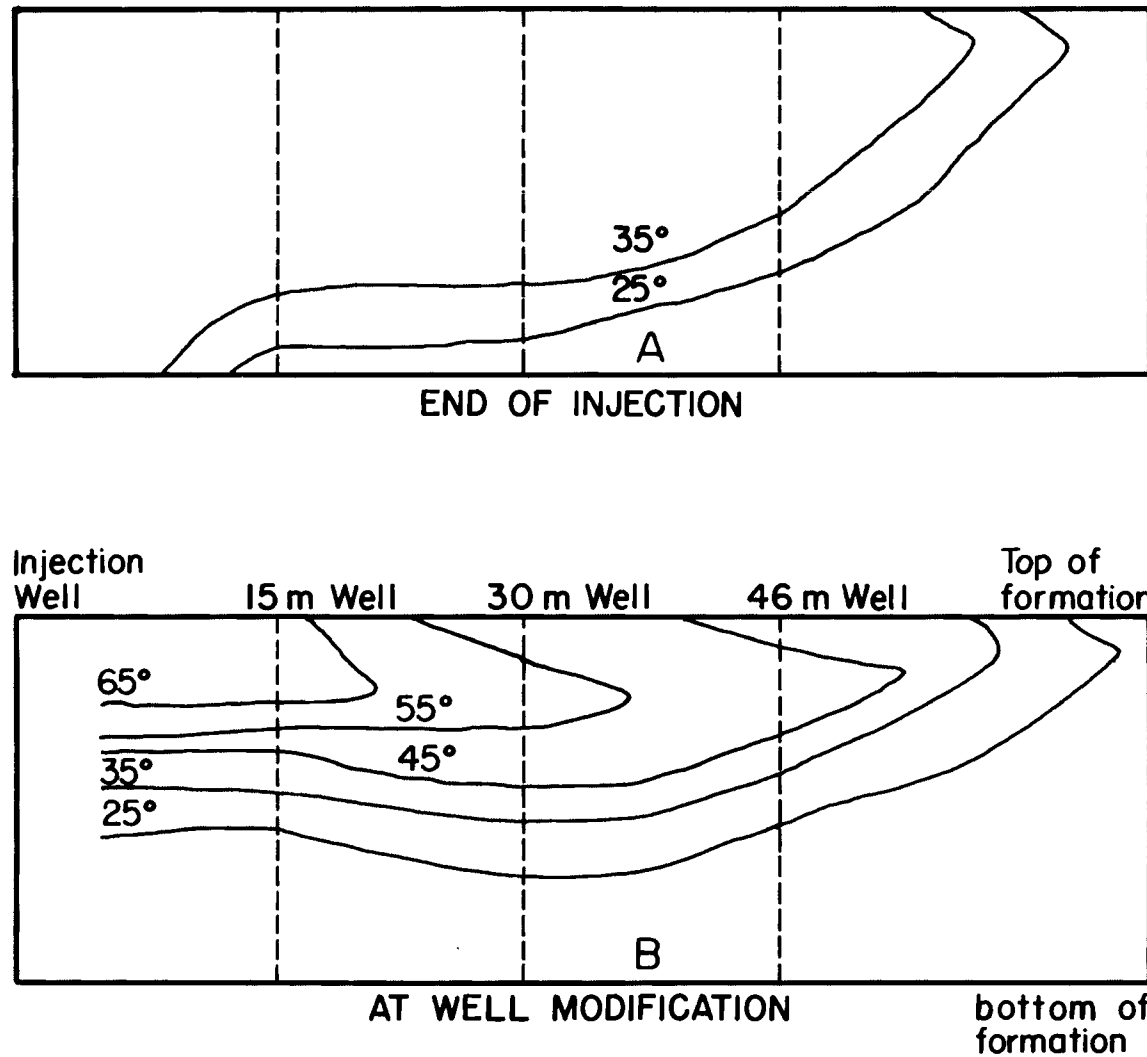
FIGURE 4.20.   Average Radial Temperature Profiles in a Vertical Section at Selected
Times During Cycle 3-2

4.23

the influence of partial penetration on recovery efficiency. In all cases, however, recovery factors of less than 51% were projected, according to information provided by Lawrence Berkeley Laboratory. Therefore, it must be concluded that partially penetrating recovery wells alone are significantly incable of overcoming the negative effects of free thermal convection in ATES.

Cycle 3-2 was similar to cycle 3-1 in that no clogging of the injection well was observed during injection. The specific capacity history is shown in Figure 4.18. During production the average suspended solids concentration was 1.8 mg/l.

At the higher injection temperature utilized in cycle 3-2, relatively large volumes of gas (mostly CO_2) were driven out of solution, requiring the addition of a gas release mechanism. This was accomplished readily through the use of an open standpipe near the injection well. The 5-cm diameter pipe was about 3.5 m tall, so that the injection pressure did not cause overflow but gas could bubble out freely.

Throughout the first and second cycle, relative land elevation changes were recorded between two points near the injection-production well (I2) and two benchmarks located beyond the thermal radius of influence (Figure 4.4). The results of these measurements are shown in Figure 4.21. By the end of cycle 3-1 injection, the land surface 4.6 m from the injection well had risen 0.43 cm. The maximum elevation increase of 1.24 cm was recorded near the end of cycle 3-2 injection. This magnitude of surface elevation change is not negligible and would have to be considered, especially if an ATES system were being designed in an urban environment. Depending on local stratigraphy, injection temperature and injection volume, elevation changes of 2 or 3 cm or more would seem possible.

In a previous publication, it was concluded that surface elevation changes observed at the Mobile ATES test site were due to thermal expansion of low permeability, water-saturated clays (Molz, Parr and Andersen 1981). Heat causing such expansion could flow upward and downward from the storage
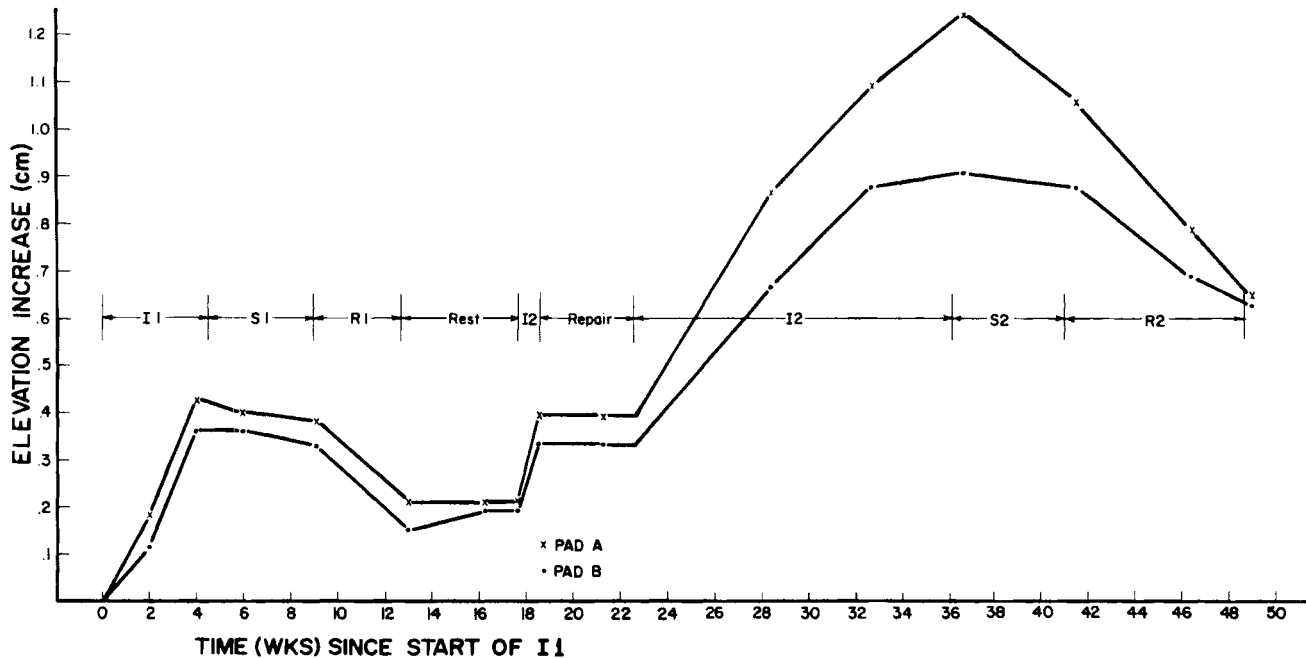
FIGURE 4.21. Land Surface Elevation as a Function of Time During Cycles
3-1 and 3-2
Note: Pads A and B are located near the injection-
production well as indicated in Fig. 4.4.

aquifer as well as radially outward from the wellbore. Pressure effects
due to injection appeared to cause negligible surface elevation changes.
The results of cycle 3-1 and 3-2 injections lend further support to this
viewpoint. Injection pressures were at least five times less than in
previous experiments, but land elevation changes were greater by a factor
of three due mainly to increased injection temperatures.

As mentioned previously, tracer experiments were performed during both
injection-storage-recovery cycles, and dispersivity estimates were made as
described in Section 3.0. Breakthrough curves obtained in an observation
well 15 m from the injection well and screened in the middle 1.5 m of the

4.25

storage aquifer (Well #15) resulted in an apparent local dispersivity average of 6.3 cm, which is among the lowest values ever measured in the field (Gelhar and Axness 1981). Analysis of cycle 3-1 recovery data at well #15 indicated a larger apparent dispersivity that was definitely less than 3 m and probably less than 1 m. The precise interpretation of this latter data was made difficult by the fact that free thermal convection occurred during the storage and recovery portions of the experiment. Field results similar to ours were obtained previously in a sandy aquifer by Pickens, Merritt and Cherry (1977).

During cycle 3-2 injection it became increasingly evident that many of the thermistors located in the hotter zones of the storage aquifer were becoming defective. Two thermistor strings were recovered and detailed laboratory examination of several failed thermistors confirmed that the problem resided in the body of the thermistor itself. No mechanical damage could be detected, so it was concluded tentatively that the problem was chemical in nature, probably due to unexpectedly rapid water migration through the epoxy barrier used to isolate the thermistor from the surrounding ground water. Evidently, such migration is accelerated significantly by temperatures above 60°C.

The thermistor manufacturers agreed with our tentative conclusions and suggested that future thermistor temperature probes be sealed in neoprene. This was the most impervious, readily usable material that they had been able to locate. On December 21, 1981 five new strings of neoprene-sealed thermistor probes were installed at the Mobile site. The new probes are able to operate up to a maximum of 100°C.

4.4 SUMMARY AND CONCLUSIONS

The first two injection-storage-recovery cycles of the third set of aquifer storage experiments conducted by Auburn University at the Mobile, Alabama field test facility were described. A 3-month cycle (cycle 3-1) followed by a 7.3-month cycle (cycle 3-2) constituted the main experiment.

The injection volumes were 25,402 m^3 and 58,063 m^3 at average temperatures of 58.5°C and 81°C, respectively. During both cycles, Br tracer concentrations were monitored in several observation wells and relative land surface elevation changes were recorded.

Cycle 3-1 production temperature was lower than expected, which resulted in a thermal energy recovery of 56% in a volume of water equal to the injection volume. There was distinct tracer and temperature profile evidence that free thermal convection in the storage aquifer contributed to the relatively low energy recovery. However, the measured ground-water temperature distributions also indicated the existence of high permeability zones in the aquifer, which could have contributed to unexpected mixing between the injected and native waters. With this situation, there is a possibility for synergistic effects between free thermal convection and nonhomogeneities.

At the higher injection temperature (81°C) of cycle 3-2, free thermal convection was more pronounced, and the initial recovery temperature was only 55.1°C. By 2 weeks into the production period, water above 45°C had migrated to the top half of the storage aquifer. At this time it was decided to modify the recovery well in an attempt to improve energy recovery. The bottom half of the well was filled with sand and a figure-k packer was placed above the sand. After this modification was complete, pumping resumed, and the energy ultimately recovered in a volume of water equal to the injection volume was 45.2%. Based on linear extrapolations of the temperature curve segments before and after modification, it was estimated that the energy recovery would have been 40% if modifications had not been made and 46 to 47% if modifications had been made prior to initiation of the production period. Thus, an additional 7% of the injected energy would have been obtainable with the modifications that were made. It would have been possible to recover additional energy if the effective penetration of the recovery well had been reduced significantly below 50%. In all practical cases, however, recovery factors less than 0.51 are projected based on computer simulations. Therefore, it must be concluded that

partially penetrating recovery wells alone are significantly incapable of overcoming the negative effects of free thermal convection in ATES.

A positive result realized during both cycles was the absence of injection well clogging due to clay particle swelling, dispersion and migration. In past experiments this phenomenon was a major technical problem. Absence of the problem during the current set of experiments is attributed to the fact that the cation concentration in the supply water used for injection was equal to or slightly greater than that in the native ground water.

By the end of cycle 3-1 injection, the land surface 4.6 m from the injection well had risen 0.43 m. The maximum elevation increase of 1.24 cm was recorded near the end of cycle 3-2 injection. Such a surface elevation change is not negligible and its potential effect on foundations would have to be considered, especially if an aquifer thermal energy storage system were being designed in an urban environment. Depending on local stratigraphy, injection temperature (assumed <100°C) and injection volume, it is estimated that elevation changes of 2 or 3 cm or more are possible.

In previous studies it was concluded that the observed surface elevation changes were due to thermal expansion of low permeability, water-saturated clays and not due to expansion of the storage aquifer matrix or injection pressure. The current results further support this conclusion. Injection pressures were smaller than those in previous experiments by at least a factor of five, but land elevation changes were greater by a factor of three due mainly to the increased injection temperature.

The portion of our tracer studies dedicated to estimating longitudinal dispersivity provided inconclusive information. Data expected to yield a relatively representative value for aquifer dispersivity was confounded by thermal convection effects. Early data collected 15 m from the injection well yielded an apparent local dispersivity average of 6.3 cm, which is almost certainly not representative of the overall aquifer.

5.0 DESCRIPTION AND RESULTS OF THE THIRD INJECTION-STORAGE-RECOVERY CYCLE

After the free thermal convection problem and its negative effect on recovery temperature were considered, it was concluded that a dual recovery well system might result in improved energy recovery. The two wells would be located as close together as possible, with one well screened in the upper half of the storage aquifer and the other screened in the lower half. Upon initiation of recovery pumping, both wells would be pumped simultaneously. In a thermally stratified and homogeneous storage aquifer, this arrangement would maintain radial flow approximately, with colder water entering the lower screen and warmer water entering the upper screen. The colder water could then be reinjected or wasted at an appropriate location. The effect of nonhomogeneities known to exist at the Mobile site cannot be predicted in detail but would probably act to reduce the effectiveness of a dual well system.

At the Mobile site, construction of a dual recovery well system was completed on April 1, 1982. This section reports the resulting cycle 3-3 data and discusses the effectiveness of the dual recovery well system. Some of the third cycle results are then compared with those of previous cycles and previous experiments.

5.1 DESCRIPTION OF EXPERIMENTS

Wells I2 and R1 constitute the dual recovery well system shown schematically in Figure 5.1. During recovery, I2 is called the production well and R1 is called the rejection well. The wells are separated horizontally by 1.8 m, with I2 screened in the top 9.1 m of the storage aquifer. The rejection well screen is also 9.1 m in length and begins 1.5 m below the bottom of the upper screen.

Cycle 3-3 injection began on April 7, 1982 and continued intermittently until July 14, 1982 when a total of 56,680 m^3 of water had been
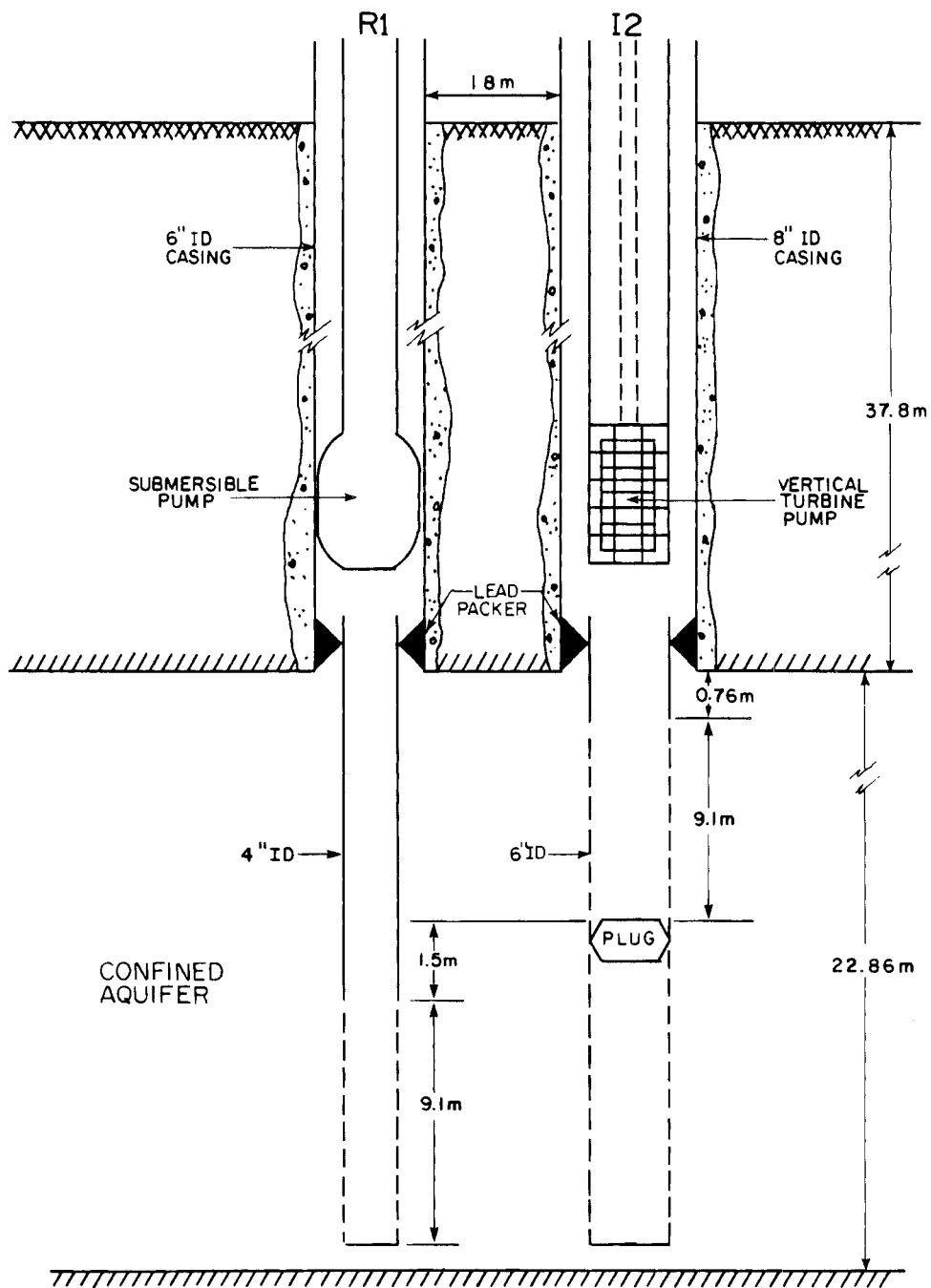
FIGURE 5.1. Dual Recovery Well System Constructed at the Mobile Site

5.2
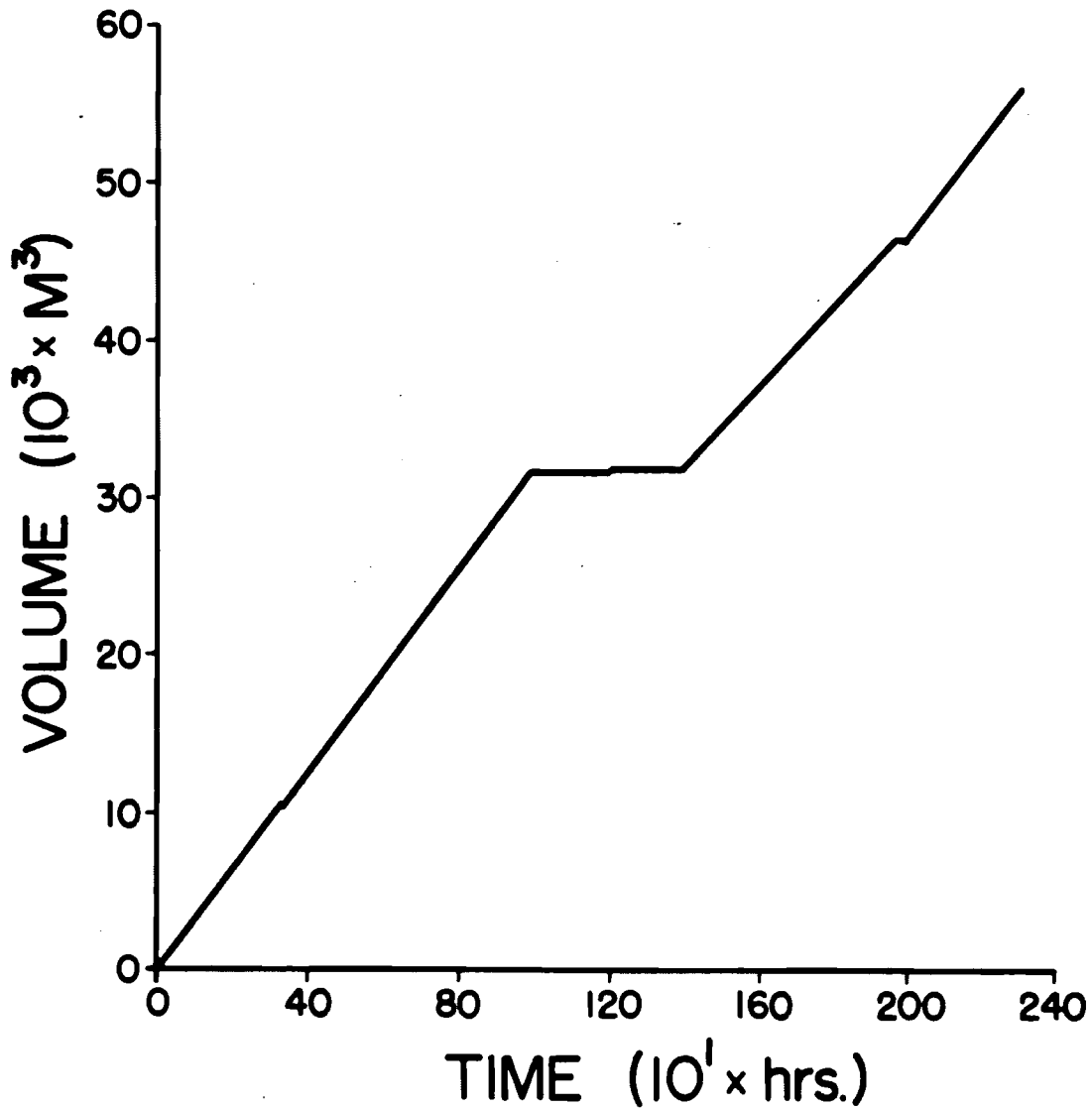
FIGURE 5.2. Cumulative Injection Volume versus Time for Cycle 3-3
Note: The long horizontal segment was due to failure
of the boiler fuel pump.

injected. The average injection temperature was 79°C. Shown in Figures
5.2 and 5.3, respectively, are the cumulative injection volume and the
injection temperature as functions of time. Injection proceeded smoothly
except for failure of a fuel pump (large horizontal segment in Figure 5.2)
at about 1000 hours into the experiment. A 52-day storage period ended on

5.3
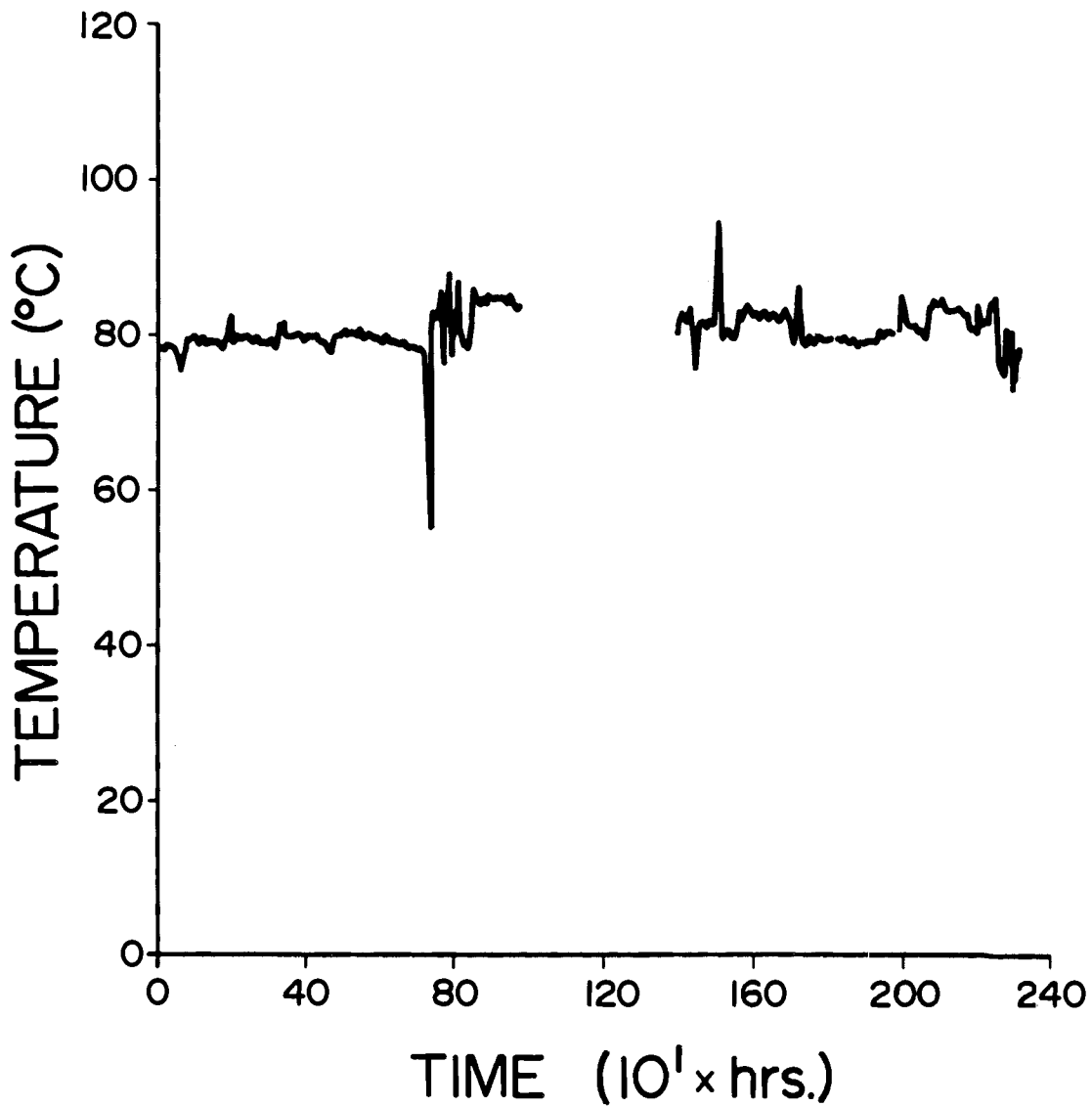
FIGURE 5.3. Injection Temperature Versus Time for Cycle 3-3

September 9, 1982, and production pumping with the dual recovery system began. Plots of cumulative production and rejection volumes versus time are shown in Figures 5.4 and 5.5, respectively. Recovery pumping was officially ended on November 16, 1982. At this time, 64,140 m^3 of water had been produced and 19,300 m^3 rejected.
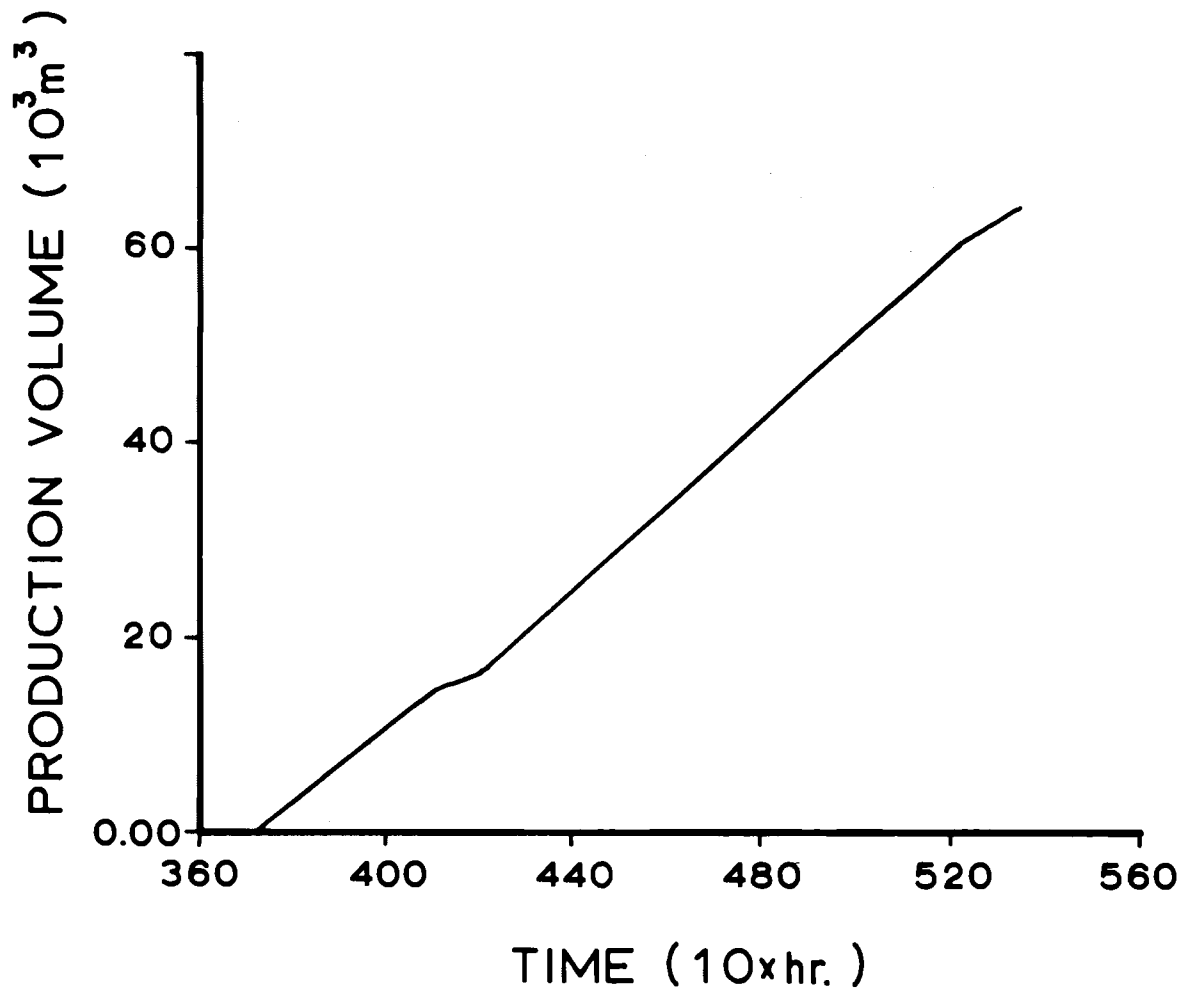
FIGURE 5.4. Cycle 3-3 Cumulative Production Pumping Volume as a Function of Time

At regular intervals during cycle 3-3, careful level measurements were made so that data could continue to be obtained on land surface elevation changes caused by ATES (Molz, Parr and Anderson 1981). As described in Section 4.0, two reference pads, two measurement pads and one observation pad were constructed of reinforced concrete with surveying markers embedded in the center of each. A level was placed on the observation pad; from this location, relative elevations of the markers on the reference and measurement pads were recorded.
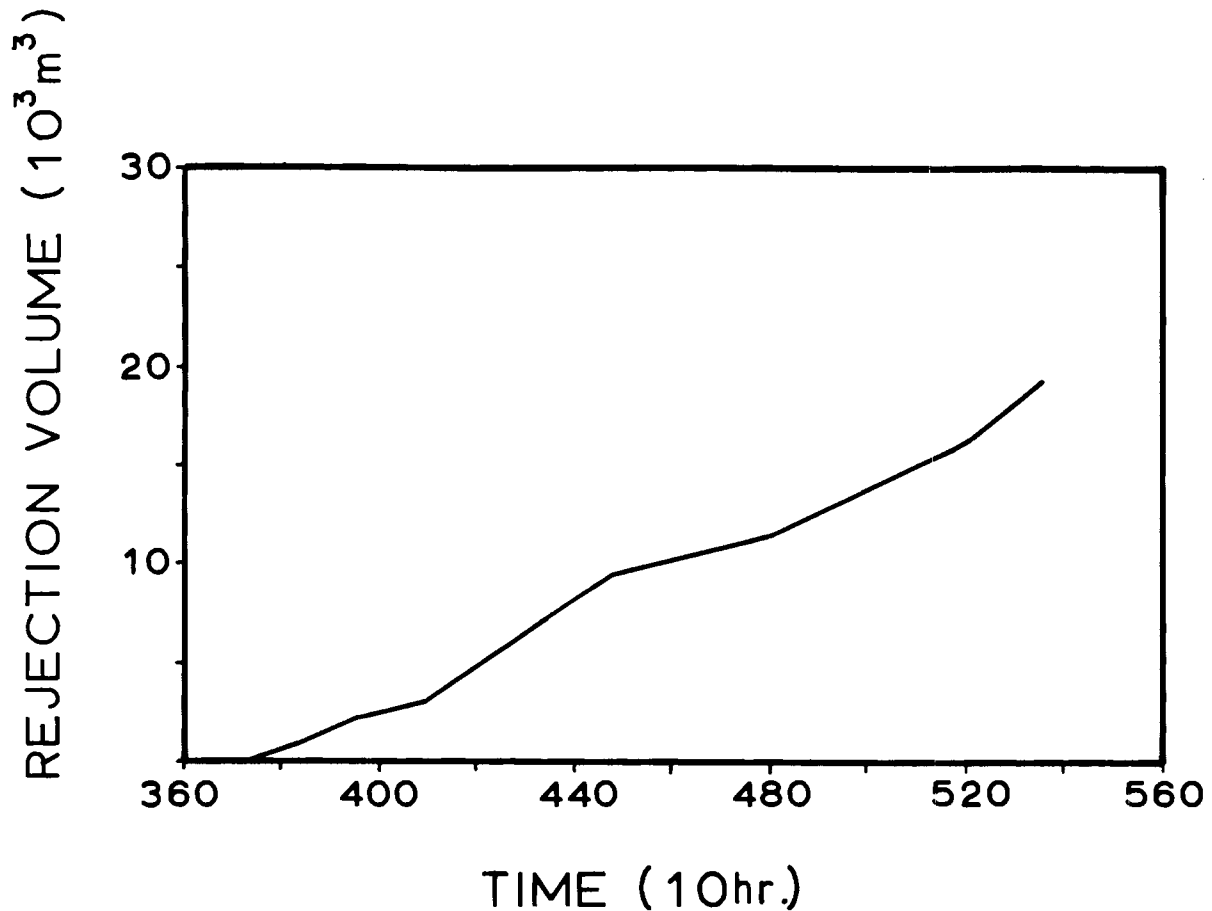
FIGURE 5.5. Cycle 3-3 Cumulative Rejection Pumping Volume as a Function of Time

5.2 RESULTS AND DISCUSSION OF CYCLE 3-3

The temperature history of the production and rejection wells during recovery pumping is shown in Figure 5.6. After a few minutes of pumping, the production temperature stabilized at 51.5°C, which is well below the average injection temperature of 79°C. It was soon discovered that variations in the rejection pumping rate had very little effect on the production temperature. Evidently, the nonhomogeneity in the storage aquifer was exerting a dominant influence on the velocity distribution. Further evidence for the significant effect of heterogeneous and temperature-dependent hydraulic conductivity in the storage aquifer can be obtained by examining the vertical temperature distribution curves obtained from the 15-m
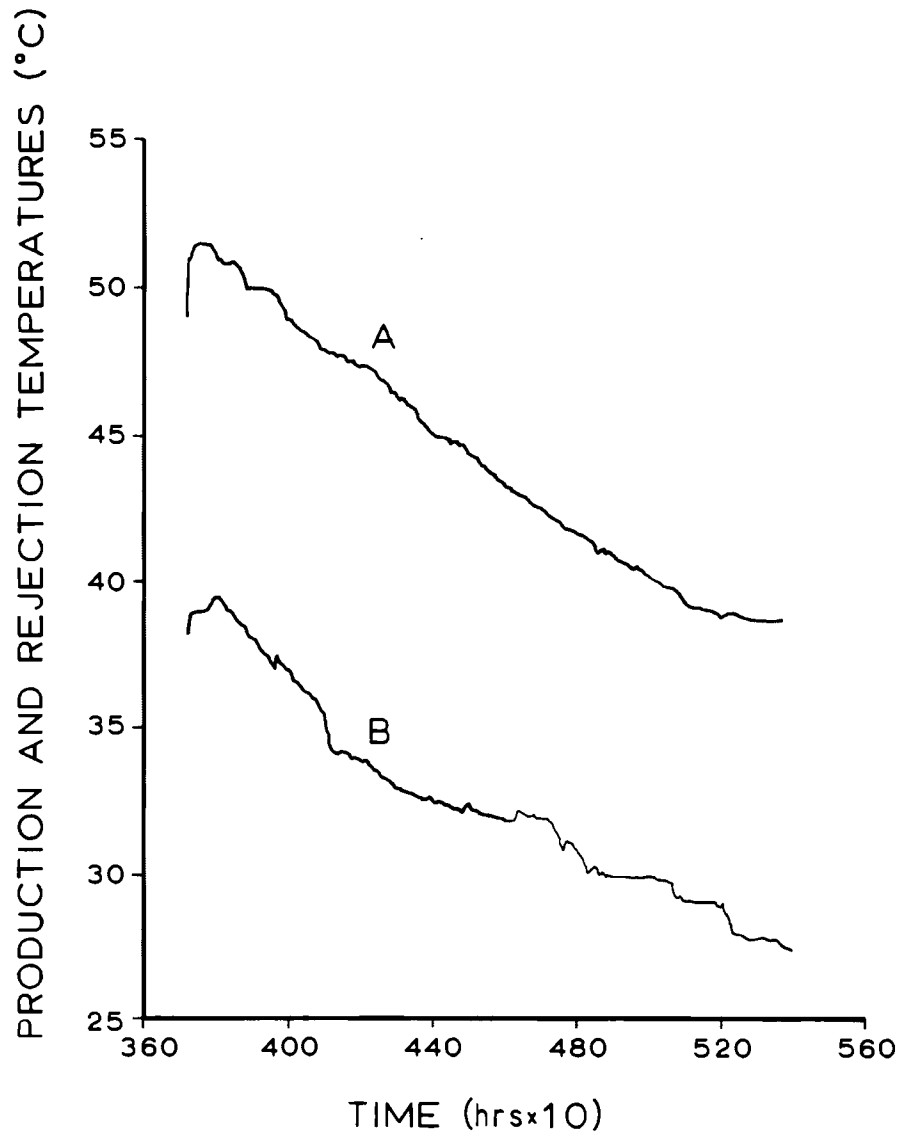
FIGURE 5.6. Production Temperature (curve A) and Rejection Temperature (curve B) versus Time for Cycle 3-3
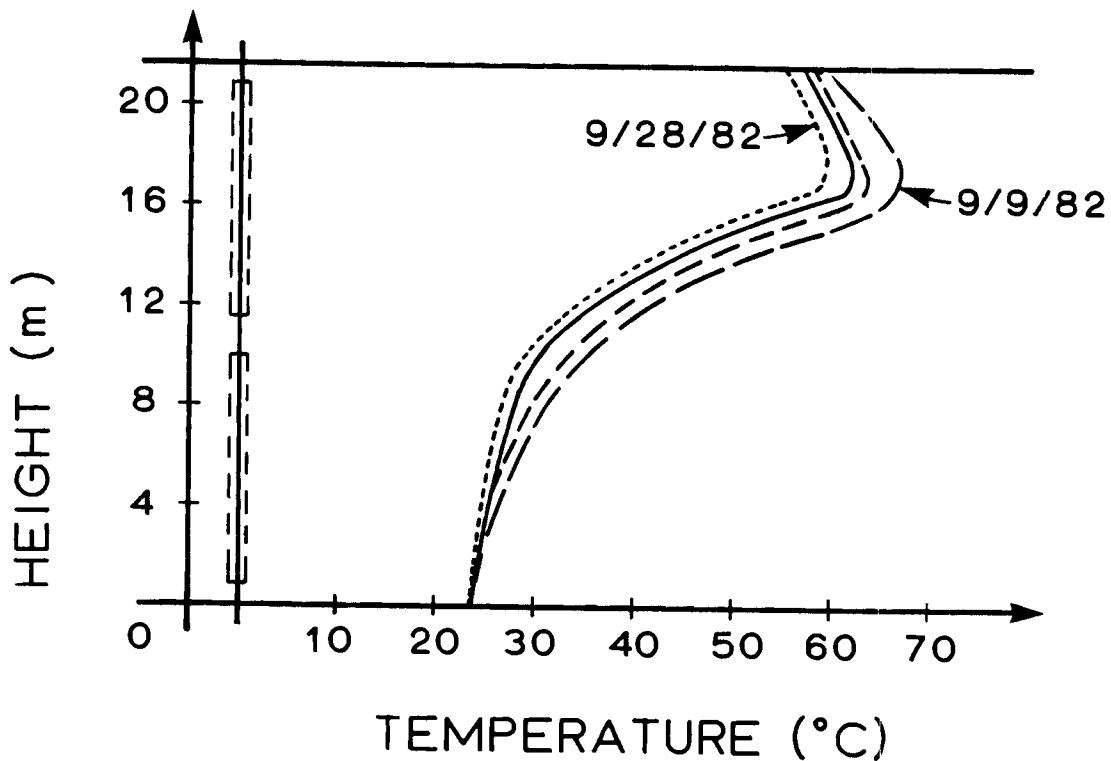
FIGURE 5.7. Vertical Temperature Profiles at the 15-m Observation Well During the First 3 Weeks of Recovery Pumping

observation well (#4) and shown in Figure 5.7. At various times, if one calculates the average temperature in the upper 50% to 60% of the aquifer, one comes within a degree or two of the production temperature. However, the average temperature in the bottom half of the aquifer is 10°C to 12°C below the observed rejection temperature. These data imply a preferential flow in the upper half of the aquifer, at least within a 15-m radius of the production well. Such a flow would be induced by the high intrinsic permeability zone somewhere near the center of the aquifer and a temperature-induced permeability increase (kinematic viscosity of water decreases by 50% between 30°C and 70°C) due to hotter water in the upper part of the aquifer. The magnitude of a temperature-induced permeability change is comparable to the intrinsic permeability differences selected by Buscheck, Doughty and Tsang in their 1983 simulations of cycles 3-1 and 3-2.

The previously mentioned relationship between average aquifer tempera-
ture, production temperature and rejection temperature held even when the
production pumping rate was five times greater than the rejection rate.
Pumping the rejection well at a higher rate relative to the production well
resulted in simply raising the rejection temperature, with little or no
effect on the production temperature. It appears, therefore, that both
wells are pulling water from the middle to upper portion of the storage
aquifer where the high intrinsic permeability zone exists (see Figures 4.15
and 4.16) and the hottest water resides. Relatively little water is moving
horizontally through the bottom third of the aquifer in the vicinity of the
rejection well where the intrinsic permeability is lower and the water vis-
cosity is higher due to lower temperatures.

It is important to note that the degree of aquifer nonhomogeneity
indicated by the current experiments was not observed in experiment set #2
(cycles 2-1 and 2-2), which utilized a zone of the aquifer approximately
109 m from the present storage zone. Examination of Figures 7, 8, and 9 of
Molz et al. (1979) indicates a relatively symmetric temperature distribu-
tion. For comparison, an average radial section of the isotherms at the
end of cycle 2-1 injection is shown in Figure 5.8 along with an isothermal
plot for a vertical aquifer cross section at the end of cycle 3-1 injec-
tion. The central fingering apparent at the new location during cycle 3-1
was not observed during cycle 2-1 at the old location. While still playing
an important role, the effects of the nonhomogeneity on the temperature
isotherms were not as apparent during cycles 3-2 and 3-3 (Figure 5.9)
because the buoyancy flow at the higher injection temperatures smears out
the obvious effect of the nonhomogeneity, according to Buscheck, Doughty
and Tsang.

The inferred differences in storage aquifer hydraulic properties
at two locations only 109 m apart have important implications for testing
programs whose purpose is to select aquifers suitable for ATES. Often, it
may not be sufficient to simply measure average horizontal hydraulic con-
ductivity, the sought-for results from standard pumping tests. It is not
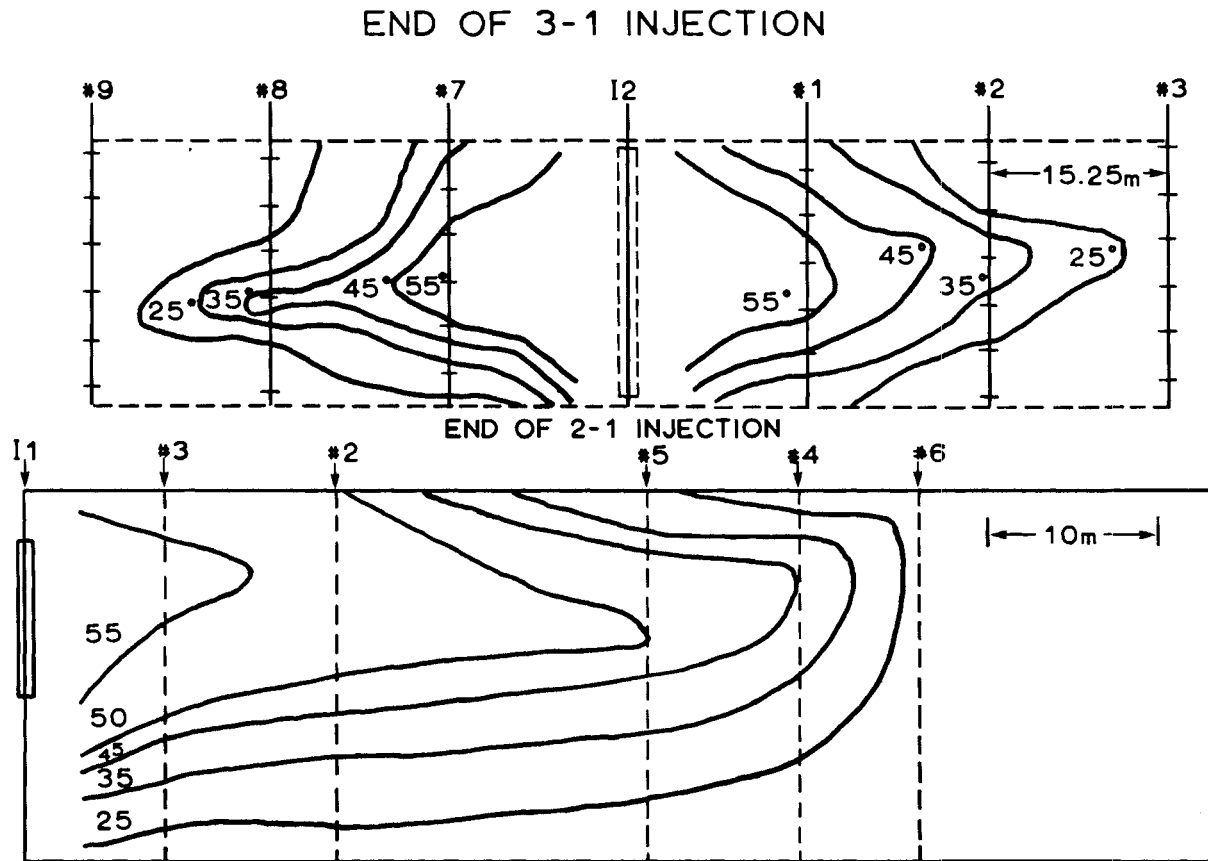
FIGURE 5.8. Comparison Plot of Isotherms on a Vertical Aquifer
Cross Section at the End of Injection for Cycles 2-1
and 3-1

easy to detect layering without variable screen length pumping tests or
tracer tests, and these procedures can be tedious. Simulation models are
useful, but only after good data have been obtained. It may be that
moderate-scale hot water injection testing will be an economical procedure
for making an overall and final evaluation of an aquifer's suitability for
ATES.

RADIAL ISOTHERMS

END OF INJECTION (CYCLE 3-2)

END OF INJECTION (CYCLE 3-3)

END OF STORAGE (CYCLE 3-3)
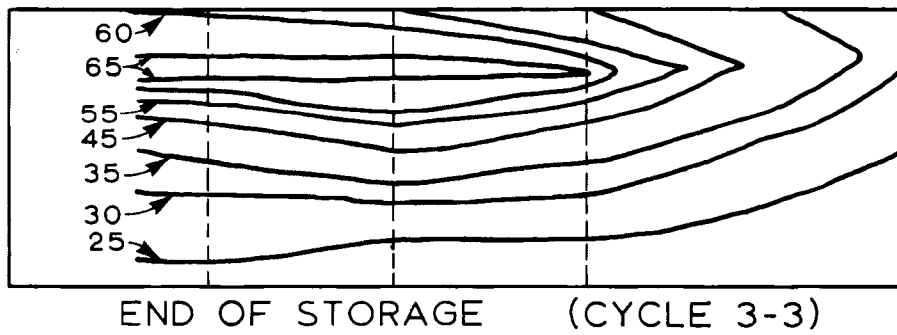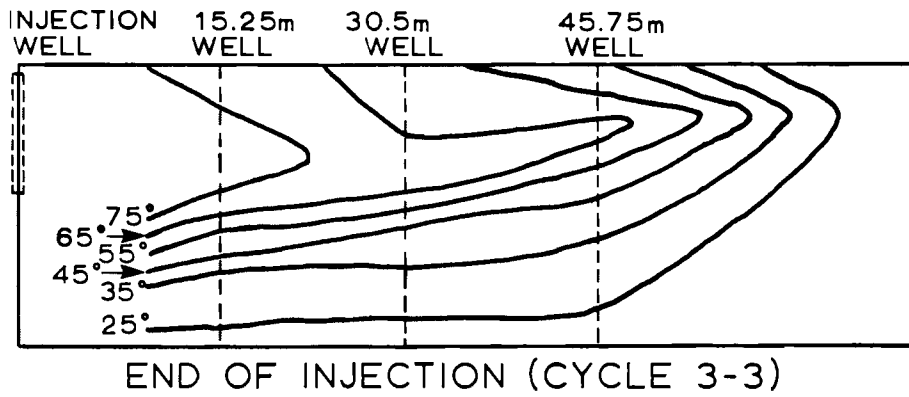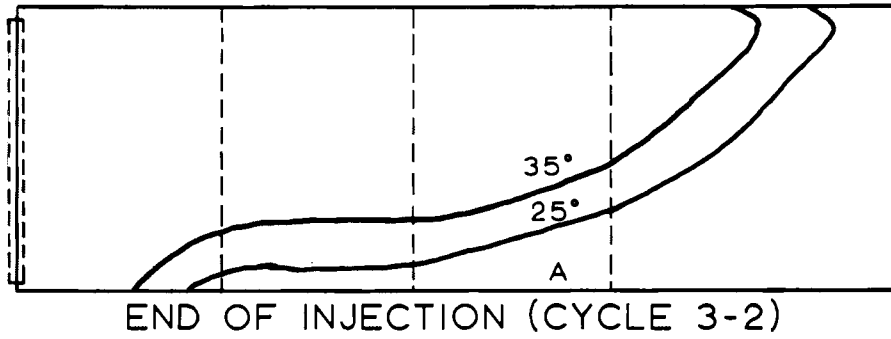
FIGURE 5.9. Radial Isotherms on a Vertical Aquifer Cross Section at the End of Injection of Cycles 3-2 and 3-3 and at the End of Cycle 3-3 Storage

Radial isothermal plots of the aquifer temperature distribution at the end of injection and storage, shown in Figure 5.9, provide clear visual evidence of free thermal convection during the storage period. Based on a more detailed version of Figure 5.9 and a simple numerical integration scheme, it is possible to estimate the percentage of stored heat that was lost due to convection and conduction from various zones of the aquifer during the storage period. The result indicated that 45% of the thermal energy stored in a cylinder of aquifer concentric with the injection well and of 15.25 m radius was lost from that zone during storage. An estimate based on average injection temperature and initial production temperature alone would have been 47%.[a] This energy loss is quite large and little or nothing can be done during storage to counteract it. Heat losses in similar aquifer volumes of 30.5 m radius and 45.7 m radius were estimated to be 32% and 22%, respectively.

Obviously, free thermal convection occurred during cycle 3-3 just as it did during cycle 3-2. The dual well recovery system was beneficial but not highly effective in counteracting negative convection effects. Shown in Figure 5.10 are plots of recovery fraction versus cumulative recovery volume with (curve A) and without (curve B) the dual well system. (Curve B was obtained by combining the heat flows and pumping volumes from the production and rejection wells as if they were a single well.) With the dual well system operating, we obtained a recovery factor of 0.42. A single production well would have yielded an estimated recovery factor of about 0.40. A summary of recovery factors and related data for all three sets of experiments performed at the Mobile site over a 7-year period is presented in Table 5.1.

Further understanding of the thermo-hydrodynamics at the Mobile site may be obtained by examining the radial isotherm plots at the end of the various recovery periods displayed in Figure 5.11. These plots show the

---

[a]This estimate was calculated as [(79-20)-(51.5-20)]/(79-20).
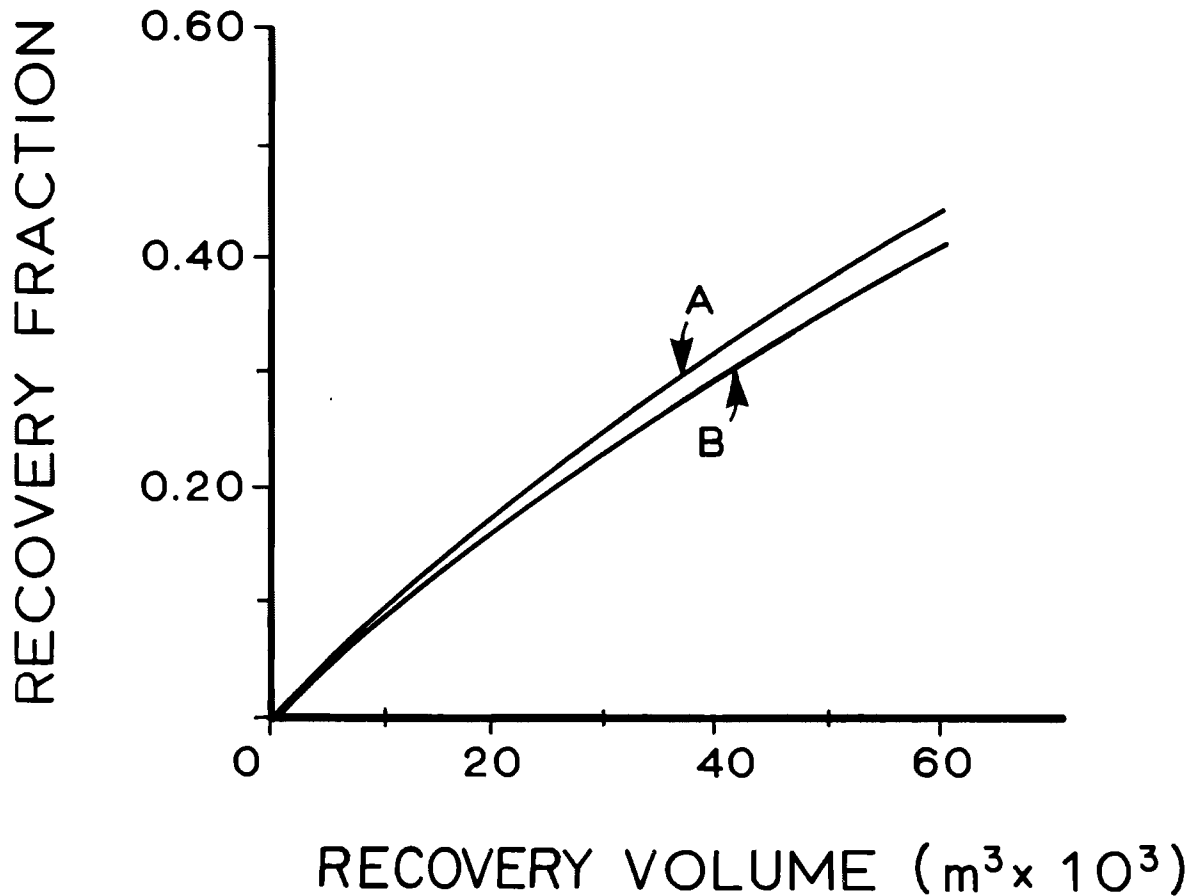
FIGURE 5.10. Cycle 3-3 Energy Recovery Fraction as a Function of Recovery Volume

Note: Curve A indicates the dual recovery well result and Curve B is the predicted result for a single equivalent well.

progressive effects of free thermal convection and emphasize the role played by the high intrinsic permeability zone near the center of the aquifer.

At the end of cycle 3-1 recovery, there is a large difference in temperature between the bottom and top of the storage aquifer. For the homogeneous case without buoyancy flow, the hottest water would be located symmetrically along the upper and lower aquitards. Even cycle 3-1 with a 58.5°C injection temperature deviates dramatically from this pattern, with 40°C water located at the very top of the aquifer and 22°C water at the

TABLE 5.1. Summary of Six Injection-Storage-Recovery Experiments Performed
at the Mobile Site

Cycle No.	Injection Duration, days	Injection Volume, m³	Injection °C	Storage Duration, days	Recovery Duration, days	Recovery Factor, %
1-1	17	7,570	37	37	31	0.53
2-1	79	54,800	55	51	41	0.66
2-2	64	58,010	55	63	48	0.68
3-1	33	25,402	58.5	30	26	0.56
3-2	110[a]	58,063	81	34	54	0.45
3-3	98	56,680	79	57	68	0.42

[a] 27 days of early downtime subtracted to facilitate comparison.

bottom. Cycle 3-2 recovery ended with a production temperature of 39.5°C. At this time, the temperature in the upper third of the aquifer varied from 50°C to about 62°C at the top. The temperature near the aquifer bottom was only 2 or 3 degrees above ambient (20°C). Due to the high permeability zone near the aquifer center, a relatively steep temperature gradient of about 9°C/m is created at the top of the middle third of the storage aquifer. Presumably, this is due to a relatively high discharge of cooler water carrying away heat from the upper third of the aquifer. By the end of cycle 3-3 recovery, the aquifer is almost perfectly stratified thermally within a 45-m radius of the injection well. The upper portion of the aquifer is cooler compared to cycle 3-2 because of the longer storage period and lower injection temperature. However, the steep temperature gradient zone is still evident.

Based on the temperature distributions shown in Figure 5.11 and the measured injection and recovery energies, it is possible to develop an energy budget for the third set of experiments. This budget, which is listed in Table 5.2, reflects the gross energy distribution and heat storage changes throughout the third set of experiments. The most interesting
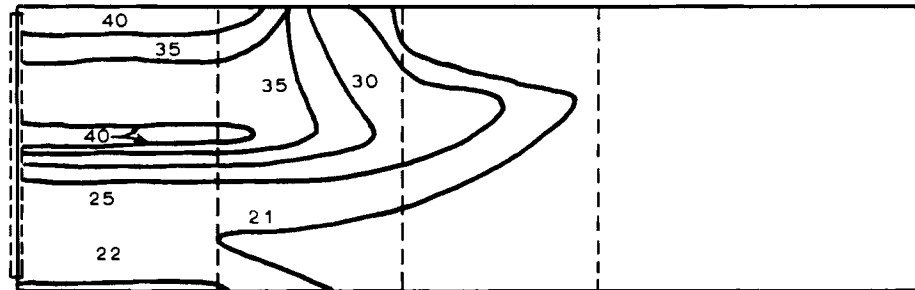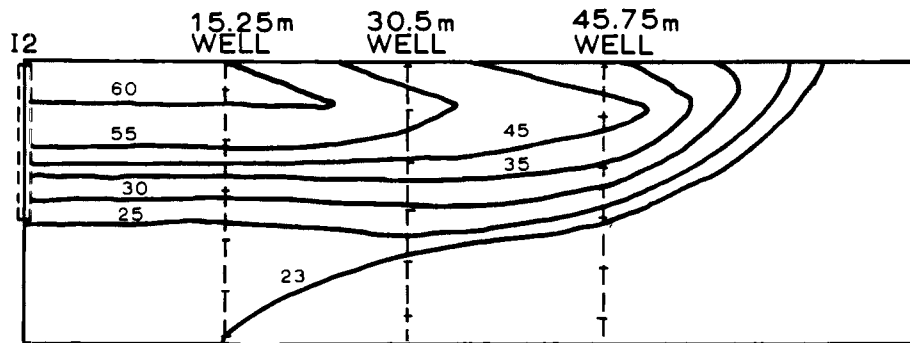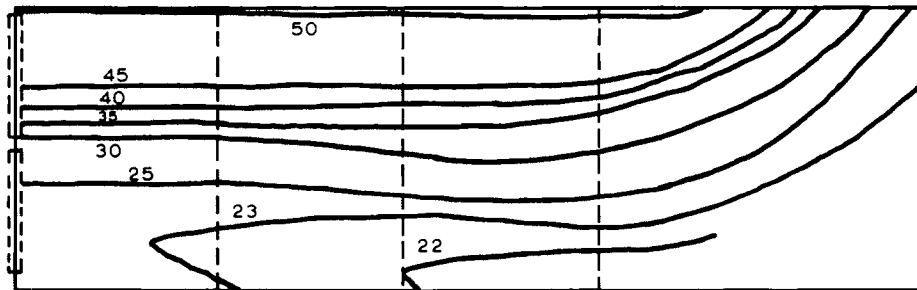
FIGURE 5.11. Comparison of Isotherms on a Vertical Aquifer Cross Section at the End of Production for Cycles 3-1, 3-2, and 3-3

figures relate to heat storage in the aquitards. Probably 95% or more of this energy resides in the upper aquitard, and by the end of cycle 3-3 recovery (i.e., when the production plus rejection volumes were equal to the injection volume), the cumulative heat content increase of the caprock was nearly equal to the total energy injected during the cycle. Due to the interaction of buoyancy flow and nonhomogeneities, heat conduction into the caprock thus emerges as a major energy loss mechanism at the Mobile site.

TABLE 5.2. Energy Budget for the Third Set of Experiments

Cycle No.	Energy Injected, J	Energy Recovered, J	Cumulative Energy[a] Left, J Aquifer	Aquitards	Energy Added, J Aquifer	Aquitards
3-1	4.02×10^{12}	2.25×10^{12}	8.77×10^{11}	8.93×10^{11}	8.77×10^{11}	8.93×10^{11}
3-2	1.44×10^{13}	6.48×10^{12}	3.90×10^{12}	5.79×10^{12}	3.02×10^{12}	4.90×10^{12}
3-3	1.38×10^{13}	5.51×10^{12}	5.78×10^{12}	1.22×10^{13}	1.88×10^{12}	6.41×10^{12}

[a]The cumulative energy left behind in the aquifer was calculated by numerical integration of the temperature distributions shown in Figure 5.11.

Use of a partially penetrating injection well during cycle 3-3 did not have a significant effect on the overall aquifer temperature distribution when compared to cycle 3-2, in which a fully penetrating well was employed. Shown in Figure 5.9 are radial isothermal plots at the end of injection for cycles 3-2 and 3-3. A complete comparison cannot be made because of thermistor failures at higher temperatures during cycle 3-2 (Section 4.0). However, the 25°C and 35°C isotherms are quite similar, indicating no gross differences within 50 m of the injection well. This observation is also consistent with the proposed high intrinsic

permeability zone. Flow from both the partially and fully penetrating injection wells would tend to follow the high permeability nonhomogeneity.

At the end of cycle 3-3 injection, it was decided to perform additional water chemistry analyses to determine if the flushing of heated water through the storage aquifer had caused changes in the concentrations of various dissolved materials. Accordingly, samples were taken on July 12, 1982, from wells S2 and 22. The water obtained from well 22 was at 62°C and had been flushed through the storage zone during cycle 3-2 and 3-3. That obtained from S2 was closer to a sample of the native groundwater but still subject to some flushing. Analyses results of both samples along with the previous measurements utilizing native ground water are displayed in Table 5.3. These data support the conclusion that there were no major changes in the chemical constituents of the ground water during the third set of experiments.

The best overall measure of change is probably the total dissolved solids (TDS), and the data in Table 5.3 indicate a trend from 274 to 284 to 299 mg/l. Throughout most of the experiment, TDS at the injection/production well was measured weekly. During cycle 3-1 the TDS averaged 280 mg/l. This average held for cycle 3-2 injection, but during production the average TDS increased to 320 mg/l. During cycle 3-3 injection the average increased again to 333 mg/l. Most likely, this increase was due to minor dissolution of the aquifer matrix by the hotter water during cycles 3-2 and 3-3. Also, by cycle 3-2 recovery, the hot water had been in contact with the aquifer matrix for an extended period of time.

Land surface elevation measurements relative to a benchmark approximately 70 m away were performed during the later part of cycle 3-3; the results are shown in Figure 5.12. At the end of injection, the relative elevation increase peaked at 1.39 cm, and then began a steady fall during storage and recovery. The maximum elevation gradient between pads A and B occurred at the end of cycle 3-2 injection and was 0.00023. The maximum average gradient between pad A and the reference pads was 0.0002 at the end of cycle 3-3 injection. Such elevation changes are not negligible and

5.17

TABLE 5.3. Results of Chemical Analyses Made During the ATES
          Experiments at the Mobile Site.

Parameter	Well S2 (7/12/82)	Well 22 (7/12/82)	Well I1 (6/20/78)
pH	7.38	7.38	7.38
dissolved solids (mg/l)	284	299	274
Ca^{2+} (mg/l)	4	4	2
Mg^{2+} (mg/l)	0	0	---[b]
alkalinity (mg/l as $CaCO_3$)	170	191	176
hardness (mg/l as $CaCO_3$)	9.6	11.6	---
Na^+ (mg/l)	85[a]	85[a]	9.4
NH_4^+-N (mg/l)	0.2	0.7	---
NO_3^--N (mg/l)	0.5	0.6	---
Fe^{3+} (mg/l)	<0.1	<0.1	<0.1
Mn^{2+} (mg/l)	<0.05	<0.05	---
SO_4^{2-} (mg/l)	<1.0	<1.0	---
K^+ (mg/l)	0.6	1.2	---
COD (mg/l)	12	8	---
Cl^- (mg/l)	21	18	---
Zn^{2+} (mg/l)	<0.1	<0.1	---
Cu^+ (mg/l)	<0.1	<0.1	---
Si (mg/l)	5	8	10
Br (mg/l)	10[a]	9.5[a]	<0.4

[a]Elevated levels due to NaBr tracer injection during cycles 3-1 and 3-2.

[b]No data.

their potential effect on foundations would have to be considered, espe-
cially if an ATES system were being designed for an urban environment.
Depending on local stratigraphy, injection temperature (assumed <100°C) and
injection volume, elevation changes two or three times greater than those
observed at the Mobile site seem possible.
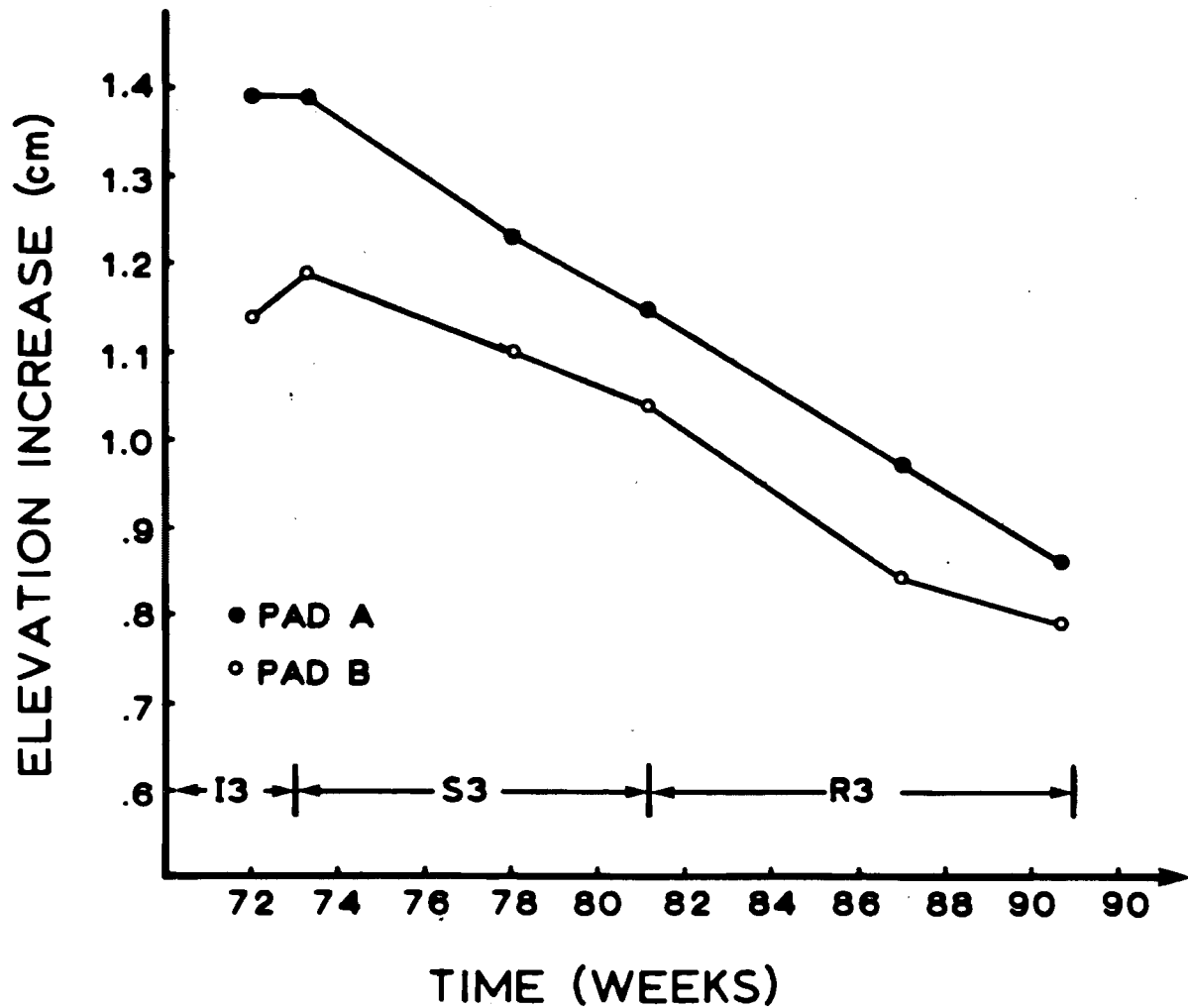
FIGURE 5.12. Increase in Land Surface Elevation Near the Injection Well
as a Function of Time.

5.3 SUMMARY AND CONCLUSIONS

Using a partially penetrating well, cycle 3-3 injection began on April 7, 1982. Ninety-eight days later a total of 56,680 m^3 of water at an average temperature of 79°C had been injected. After a 57-day storage period, production began with a dual recovery well system. The objective was to pull the hotter water in the upper portion of the storage aquifer into the production well, and the colder water in the bottom portion into the rejection well. By varying the pumping rates of the two wells, it was hoped that a near-optimal energy recovery from a thermally stratified aquifer could be achieved.

Shortly after production began, it became obvious that the dual recovery well system was not going to work as well as had been intended. The inadequate control was due to the following interacting effects:

1. During injection, much of the flow occurred near the center of the aquifer, which caused significant lateral spreading of the injected volume.

2. During storage, thermal convection in and above the high permeability zone was dramatic, causing increased lateral spreading of the heat.

3. Hot water in the top of the aquifer, having spread over a large area, allowed for maximum conductive heat loss to the upper confining layer.

4. Although estimated to have increased the recovery factor from 0.40 to 0.42, the selective recovery system did not have a dramatic effect because the aquifer anisotropy and nonhomogeneity controlled the velocity distribution to a significant extent.

Because of the above phenomena, the initial production temperature was 51.5°C, well below the average injection temperature of 79°C. During storage, approximately 45% of the thermal energy stored in a cylinder of aquifer of 15.25 m radius was lost.

The degree of aquifer nonhomogeneity inferred at the location of the current experiments was not apparent during previous experiments at a location only 109 m away. Therefore, aquifers with the same transmissivity can behave quite differently in a thermal energy storage sense. Vertical variations of horizontal hydraulic conductivity are difficult to detect, and moderate-scale hot water injection testing along with computer simulation may be an economical procedure for making an overall and final evaluation of an aquifer's suitability for ATES.

Chemical analyses of water samples over the course of the Mobile experiments indicated that there were no major changes in the chemical constituents during the third set of experiments. However, due to the flushing of heated water through the system, the average total dissolved solids content increased from 280 mg/l to 333 mg/l.

At the end of cycle 3-3 injection, the land surface near the injection well had risen 1.39 cm with respect to bench marks located 70 m away. The average elevation gradient was 0.0002. Depending on local stratigraphy, injection temperature (assumed <100°C) and injection volume, elevation changes two or three times greater than those observed at the Mobile site seem possible.

As mentioned previously, it is safe to say that the various experiments at the Mobile site have demonstrated the technical feasibility of low-temperature ATES but not necessarily the economic feasibility. However, several applications of ATES technology currently underway in Canada, Denmark, Sweden and other locations in Europe will soon contribute to resolution of the economic question. Some of the more interesting approaches involve the use of heat pump systems to extract heat from warm aquifer water and produce a useful temperature for space heating, water heating and other applications.

With the combined aid of field tests and computer modeling techniques that have been perfected over the past decade, it is now relatively

straightforward to develop the initial design of an ATES system. However, the useful lifetime and long-term maintenance costs are more difficult to define. The most subtle problems are chemical in nature. They result mainly from mixing waters having different temperatures and chemical properties (pH, ion concentration, etc.) during the injection process. This will occur to some degree even when the supply and injection wells are located in the same aquifer. Deleterious geochemical and/or colloid chemical effects can be immediate and dramatic, seriously impairing injection within a few days, or they can be of a very gradual, long-term nature. For obvious reasons, the latter situation has received the least amount of study.

REFERENCES

Bear, J., Dynamics of Fluids in Porous Media, American Elsevier Publishing Co., New York, 1972.

Bear, J., Hydraulics of Groundwater, McGraw-Hill, Inc., New York, NY, 1979.

Bostrom, K., Some pH-controlling redox reactions in natural waters, in Equilibrium Concepts in Natural Water Systems, ACS, 286, 1967.

Bouwer, H. Groundwater Hydrology, McGraw-Hill Book Company, 1978.

Brown, D. L., and W. D. Silvey, Artificial recharge to a freshwater-sensitive brackish-water sand aquifer, Norfolk, Virginia, U.S. Geological Survey Professional Paper 939, U.S. Government Printing Office, Washington, DC 1977.

Buscheck, T., C. Doughty and C. F. Tsang, Prediction and analysis of a field experiment on a multi-layered aquifer thermal energy storage system with strong buoyancy flow, Submitted for publication to Water Resources Research, 1983.

Davis, S. N., G. N. Thompson, H. W. Bentley, and S. Gary, Groundwater tracers-a short review, Ground Water, 18, 18-23, 1980.

Doughty, C., G. Hellstrom, C. F. Tsang and J. Claesson, A dimensionless parameter approach to the thermal behavior of an aquifer thermal energy storage system, Water Resources Research, 18, 571-587, 1982.

Ferris, J. G., D. B. Knowles, R. H. Browne, and R. W. Stallman, Theory of aquifer tests, U.S. Geological Survey, Water-Supply Paper 1536-E, 174 p., 1962.

Garrels, R. M. and C. L. Christ, Solutions, Minerals, and Equilibria, Harper & Row, NY, 1965.

Gelhar, L. W., and C. L. Axness, Stochastic analysis of macrodispersion in three dimensionally heterogeneous aquifers, Rept. No. H-8, Geophysical Research Center, New Mexico Institute of Mining and Technology, Socorro, NM, 140p., 1981.

Gupta, S. K., R. E. Batta, and R. N. Pandey, Evaluating hydrodynamic dispersion coefficients, Journal of Hydrology, 47, 369-372, 1980.

Hantush, M. S., Drawdown around a partially penetrating well, American Society of Civil Engineers Proceedings, 87, HY4, 83-98, 1961.

Helfferich, F., Ion Exchange, McGraw-Hill, 1962.

Hoopes, J. A., and D. R. F. Harleman, Dispersion in radial flow from a recharge well, Geophysical Research, 72, 3595-3607, 1967.

Jacob, C. F., Flow of groundwater, in Engineering Hydraulics, edited by H. Rouse, John Wiley, New York, 367-371, 1950.

Kramer, J. R., Equilibrium models and composition, in Equilibrium Concepts in Natural Water Systems, ACS, 255, 1967.

Krauskopt, K. B., Introduction to Geochemistry, McGraw-Hill, 1967.

Mathey, B., Development and resorption of a thermal disturbance in a phreatic aquifer with natural convection, Journal of Hydrology, 34, 315-333, 1977.

Meyer, C. F., The Johnson Driller's Journal, 1982, (First Quarter), 4.

Mitchell, J. K., and C. K. Tsung, Measurement of soil thermal resistivity, ASCE Journal of the Geotechnical Engineering Division, 104 (#10), 1307-1320, 1978.

Molz, F. J., and L. C. Bell, Head gradient control in aquifers used for fluid storage, Water Resources Research, 13, 795-798, 1977.

Molz, F. J., A. D. Parr, P. F. Andersen, V. D. Lucido, and J. C. Warman, Thermal energy storage in a confined aquifer: experimental results, Water Resources Research, 15, 1509-1514, 1979.

Molz, F. J., A. D. Parr, and P. F. Andersen, Thermal energy storage in a confined aquifer: second cycle, Water Resources Research, 17, 641-645, 1981.

Molz, F. F., J. C. Warman, and T. E. Jones, Aquifer storage of heated water: part I - a field experiment, Ground Water, 16, 234-241, 1978.

Neuman, S. P., and P. A. Witherspoon, Field determination of the hydraulic properties of leaky multiple aquifer systems, Water Resources Research, 8 (5), 1284-1298, 1972.

Nix, G. H., R. I. Vachon, G. W. Lowery, and T. A. McCurry, The line-source method: procedure and iteration scheme for combined determination of conductivity and diffusivity, Proceedings of 8th Conference on Thermal Conductivity, Plenum Press, NY, 1969.

Papadopulos, S. S., and S. P. Larson, Aquifer storage of heated water: Part II - numerical simulation of field results, Ground Water, 16, 242-248, 1978.

Pickens, J. F., W. F. Merritt and J. A. Cherry, Field determination of physical contaminant transport parameters in a sandy aquifer, Proceedings of the IAEA Advisory Group Meeting, Poland, 1977.

Reddell, D. L., R. R. Davison, and W. B. Harris, Cold water aquifer storage, Proceedings of Fourth Annual Thermal Energy Storage Review Meeting, DOE Publication CONF-791232, Washington, DC, 1979.

Reilly, R. W., A Descriptive Analysis of Aquifer Thermal Energy Storage, Prepared for U.S. Dept of Energy by Pacific Northwest Laboratory, PNL-3298, U6-94a, 1980.

Sauty, J. P., A. C. Gringarten, H. Fabris, D. Thiery, A. Menjoz, and P. A. Landel, Sensible heat storage in aquifers 2. field experiments and comparison with theoretical results, Water Resources Research, 18, 253-265, 1982.

Stern, L. I., Conceptual design of aquifer thermal energy storage system demonstration, Proceedings of Mechanical, Magnetic, and Underground Energy Storage 1980 Annual Contractors' Review, Conf-801128, NTIS, Springfield, VA, 28-33, 1980.

Stottlemyre, J. A., Equilibrium geochemical modeling of a seasonal thermal energy storage aquifer field test, Proceedings of Fourth Annual Thermal Energy Storage Review Meeting, DOE Publication CONF-791232, Washington, DC, 1979.

Stottlemyre, J. A., C. H. Cooley, and Gary J. Banik, Physicochemical properties analyses in support of the seasonal thermal energy storage program, Proceedings of the Mechanical, Magnetic, and Underground Energy Storage 1980 Annual Contractor's Review, NTIS, Conf-801128, 90-95, 1980.

Sykes, J. F., R. B. Lantz, S. B. Pahwa, and D. S. Ward, Numerical simulation of thermal energy storage experiment conducted by Auburn University, Ground Water, 20, 569-576, 1982.

Todd, D. K., Groundwater Hydrology, John Wiley and Sons, New York, NY, 2nd Edition, 1980.

Tsang, C. F. (Ed.), Seasonal Thermal Energy Storage Newsletter, Earth Sciences Div., Lawrence Berkeley Laboratory, Berkeley, CA, 94720, 1981/ 1982.

Tsang, C. F., T. Buscheck, and C. Doughty, Aquifer thermal energy storage- a numerical simulation of Auburn University field experiments, Water Resources Research, 17, 647-658, 1981.

U.S. Department of Energy, Proceedings of the International Conference on Seasonal Thermal Energy Storage and Compressed Air Energy Storage, NTIS, CONF-811066, Vols. 1 and 2, 1981.

van der Held, EFM and F. G. van Drunen, A method for measuring the thermal
conductivity of liquid, Physics, 15, 1949.

Van Olphen, H., An Introduction to Clay Colloid Chemistry, John Wiley and
Sons, New York, NY, 1963.

Weeks, E. P., Determining the ratio of horizontal to vertical permeability
by aquifer test analysis, Water Resources Research, 5 (1), 196-214, 1969.

Werner, D., and W. Kley, Problems of heat storage in aquifers, Journal of
Hydrology, 34, 35-43, 1977.

Whitehead, W. R., and E. J. Langhetee, Use of bounding wells to counteract
the effects of pre-existing groundwater movement, Water Resources
Research, 14, 273-280, 1978.

Yokoyama, T., H. Umemiya, T. Teraoka, H. Watanabe, K. Katsuragi, and K.
Kasahara, Seasonal thermal storage in aquifer for utilization, Bulletin,
Japanese Society of Mechanical Engineers, 23, 1646-1654, 1980.

APPENDIX

WELL FIELD GEOMETRY AT THE MOBILE SITE

1980-1983 EXPERIMENTS

CYCLES 3-1, 3-2, AND 3-3

WELL FIELD COORDINATES

Well No.	x ft.	(m)	y ft.	(m)	r ft.	(m)
1	.025	(.0076)	49.09	(14.96)	49.09	(14.96)
2	.267	(.081)	98.12	(29.91)	98.12	(29.91)
3	0	(0)	146.64	(44.70)	146.64	(44.70)
4	48.85	(14.89)	-.38	(-0.12)	48.86	(14.89)
5	97.10	(29.60)	-.78	(-0.24)	97.10	(29.60)
6	145.69	(44.41)	7.16	(2.18)	145.87	(44.46)
7	4.98	(1.52)	-49.09	(-14.96)	49.34	(15.04)
8	.22	(0.067)	-98.53	(-30.03)	98.53	(30.03)
9	.04	(0.012)	-146.83	(-44.75)	146.83	(44.75)
10	-48.80	(-14.87)	.56	(0.17)	48.80	(14.87)
11	-97.41	(29.69)	-.20	(-0.06)	97.41	(29.69)
12	-145.79	(-44.44)	-.64	(-0.20)	145.79	(44.44)
13	-34.39	(-10.48)	34.65	(10.56)	48.81	(14.88)
14	33.94	(10.34)	34.86	(10.63)	48.65	(14.83)
15	37.18	(11.33)	-37.34	(-11.38)	52.70	(16.06)
16	104.48	(31.85)	-104.39	(-31.82)	147.69	(45.02)
17	-66.45	(-20.25)	-68.71	(-20.94)	95.58	(29.13)
18	-143.55	(-43.75)	-143.25	(-43.66)	202.80	(61.81)
19	-197.63	(-60.24)	-.16	(-0.049)	197.63	(60.24)
20	-134.95	(-41.13)	165.95	(50.58)	213.90	(65.20)
21	105.96	(32.30)	185.62	(56.58)	213.73	(65.14)

Well No.	x ft.	(m)	y ft.	(m)	r ft.	(m)
22	54.19	(16.52)	94.38	(28.78)	108.83	(33.17)
23	107.26	(32.69)	-184.84	(-56.34)	213.71	(65.14)
24	-273.58	(-83.39)	.02	(.006)	273.58	(83.39)
25	-346.05	(-105.48)	-11.95	(-3.64)	346.26	(105.54)
26	-472.95	(-144.16)	-1.10	(-0.34)	472.95	(144.16)
27	-571.53	(-174.20)	-4.09	(-1.25)	571.55	(174.21)
28	-694.53	(-211.69)	-.92	(-0.28)	694.53	(211.69)
29	-857.99	(-261.52)	-1.48	(-0.45)	857.99	(261.52)
S1	-402.31	(-122.62)	63.56	(19.37)	407.30	(124.15)
S2	-798.08	(-243.25)	-.53	(-0.16)	798.08	(243.25)
I2	0	(0)	(0)	(0)	(0)	(0)
R1	4.18	(1.27)	4.18	(1.27)	5.90	(1.80)

LAND SURFACE PAD COORDINATES

Pad	x ft.	(m)	y ft.	(m)	r ft.	(m)
A	-2.18	(-0.82)	-14.91	(-4.54)	15.17	(4.62)
B	46.77	(14.26)	-16.22	(-4.94)	49.50	(15.09)
C	10.72	(3.27)	-141.60	(-43.16)	142.01	(43.28)
D	-56.87	(17.33)	-245.76	(-74.91)	252.25	(76.89)
E	74.85	(22.81)	-255.81	(-77.97)	266.54	(81.24)

WELL NO. I2

TOF (top of formation)

a

b

aquifer
c — probes

d

e

f

BOF (bottom of formation)

POSITION	ELEVATION (M) Ft.		
	M	Ft.	
TOF	37.92	(124.4)	Datum is a spike
Top of screen	38.88	(128.9)	located in an
b	_____	( )	electrical power
c	_____	( )	pole
d	_____	( )	
e	_____	( )	
Btm of screen	60.02	(196.9)	
BOF	60.76	(199.4)	

WELL NO. I2
(After 12/16/81)

TOF (top of formation)

a

b

aquifer
c

Packer

d — Sand

e

f

BOF (bottom of formation)

POSITION	ELEVATION (M) Ft.		
	M	Ft.	
TOF	37.92	(124.4)	Datum is a spike
Top of Screen	38.88	(128.9)	located in an
b	_____	( )	electrical power
Top of Packer	50.41	(165.4)	pole
d	_____	( )	
e	_____	( )	
Btm. of Screen	60.02	(196.9)	
BOF	60.76	(199.4)	

A.3

WELL NO. I2

After 4/1/82

TOF (top of formation)

aquifer

Packer

a
b
c
d
e
f

BOF (bottom of formation)

POSITION   ELEVATION (M) Ft.

	M	Ft.
TOF	37.92	(124.4)
Top of screen	38.66	(126.9)
b		( )
Top of packer	47.78	(156.8)
d		( )
e		( )
f		( )
BOF	60.78	(199.4)

Datum is a spike
located in an
electrical power
pole

WELL NO. S2

TOF (top of formation)

aquifer

a
b
c — probes
d
e
f

BOF (bottom of formation)
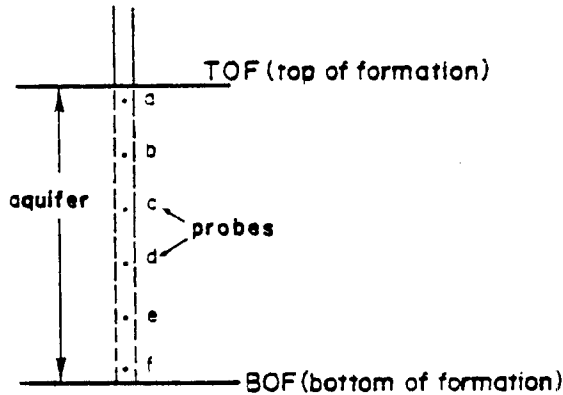
POSITION   ELEVATION (M) Ft.

	M	Ft.
TOF	43.36	(142.3)
a		( )
b		( )
c		( )
d		( )
e		( )
f		( )
BOF	53.82	(196.3)

Datum is a spike
located in an
electrical power
pole

A.4

WELL NO. R1

After 4/1/82

POSITION   ELEVATION (M) Ft.
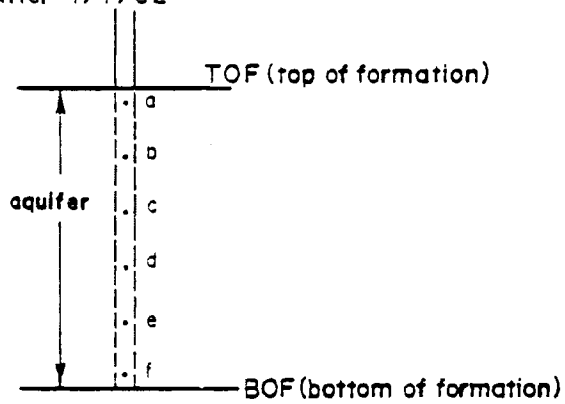
POSITION	M	Ft.	
TOF	37.92	(124.4)	Datum is a spike
a		( )	located in an
b		( )	electrical power
c		( )	pole
Top of Screen	49.28	(161.7)	
e		( )	
Btm. of Screen	58.38	(191.5)	
BOF	60.78	(199.4)	

WELL NO. 1

POSITION   ELEVATION (M) Ft.
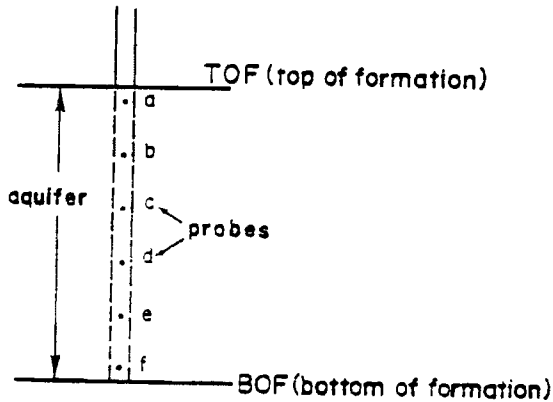
POSITION	M	Ft.	
TOF	39.50	(129.6)	Datum is a spike
a	37.67	(123.6)	located in an
b	41.57	(136.4)	electrical power
c	45.46	(149.2)	pole
d	49.38	(162.)	
e	53.28	(174.8)	
f	57.18	(187.6)	
BOF	61.14	(200.59)	
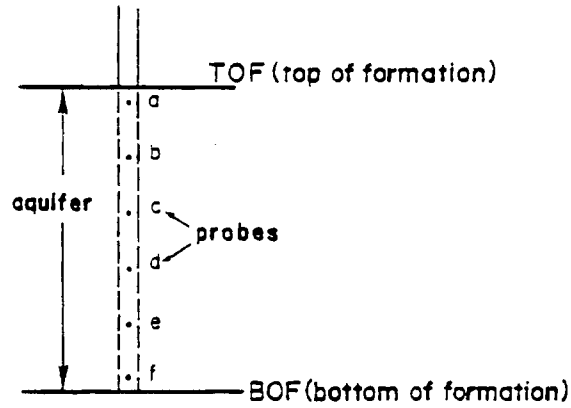
WELL NO. 2

POSITION	ELEVATION (M) Ft.		
	M	**Ft.**	
TOF	39.25	(128.8)	
a	41.39	(135.8)	Datum is a spike
b	45.29	(148.6)	located in an
c	49.19	(161.4)	electrical power
d	53.10	(174.2)	pole
e	57.00	(187.)	
f	60.90	(199.8)	
BOF	61.19	(200.8)	
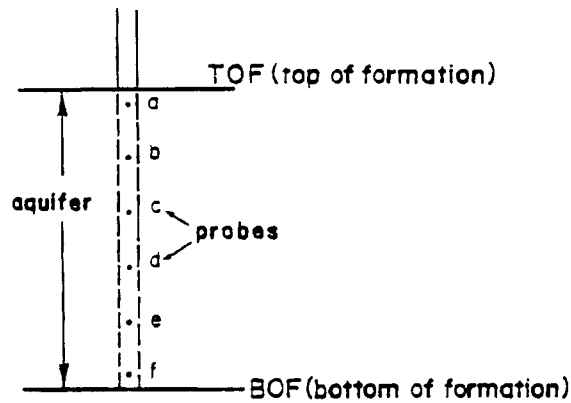
WELL NO. 3

POSITION	ELEVATION (M) Ft.		
	M	**Ft.**	
TOF	39.20	(128.6)	
a	40.11	(131.6)	Datum is a spike
b	44.01	(144.4)	located in an
c	47.91	(157.2)	electrical power
d	51.82	(170.)	pole
e	55.72	(182.6)	
f	59.62	(195.6)	
BOF	60.84	(199.6)	
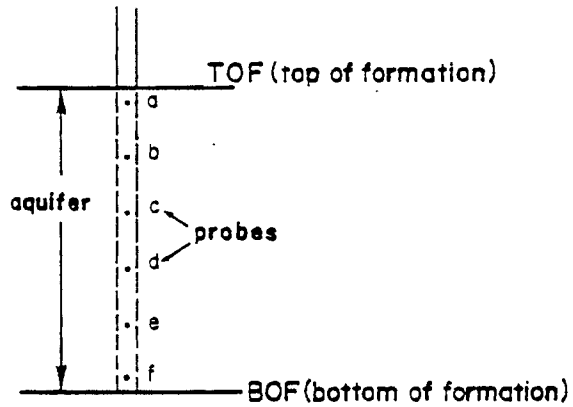
WELL NO. 4

POSITION	ELEVATION (M) Ft.	
	M	Ft.
TOF	39.90	(130.91)
a	40.81	(133.9)
b	44.71	(146.7)
c	48.62	(159.5)
d	52.52	(172.3)
e	56.42	(185.1)
f	60.32	(197.9)
BOF	61.54	(201.9)

Datum is a spike located in an electrical power pole

WELL NO. 4
(After 12/22/81)
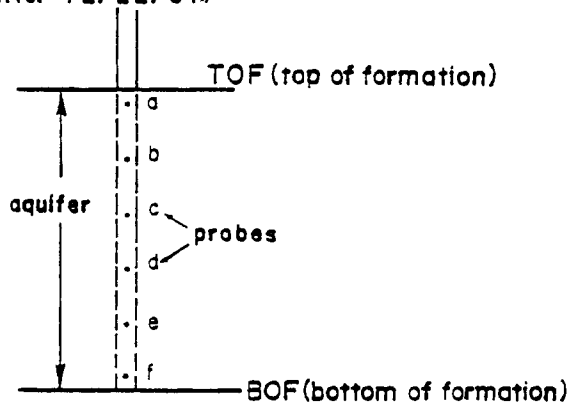
POSITION	ELEVATION (M) Ft.	
	M	Ft.
TOF	39.90	(130.91)
a	41.12	(134.9)
b	45.02	(147.7)
c	48.92	(160.5)
d	52.82	(173.3)
e	56.72	(186.1)
f	60.62	(198.9)
BOF	61.54	(201.9)

Datum is a spike located in an electrical power pole

WELL NO. 5

TOF (top of formation)

aquifer — probes

a
b
c
d
e
f

BOF (bottom of formation)

POSITION	ELEVATION (M) Ft.		
	M	Ft.	
TOF	38.92	(127.7)	
a	38.31	(125.7)	Datum is a spike
b	42.21	(138.5)	located in an
c	46.12	(151.3)	electrical power
d	50.02	(164.1)	pole
e	53.92	(176.9)	
f	57.82	(189.7)	
BOF	60.85	(199.7)	

WELL NO. 5
(After 12/22/81)

TOF (top of formation)

a
b
aquifer c — probes
d
e
f

BOF (bottom of formation)

POSITION	ELEVATION (M) Ft.		
	M	Ft.	
TOF	38.92	(127.7)	
a	38.83	(127.4)	Datum is a spike
b	42.73	(140.2)	located in an
c	46.63	(153.)	electrical power
d	50.54	(165.8)	pole
e	54.44	(178.6)	
f	58.34	(191.4)	
BOF	60.85	(199.7)	

WELL NO. 6

TOF (top of formation)

aquifer

probes

a
b
c
d
e
f

BOF (bottom of formation)
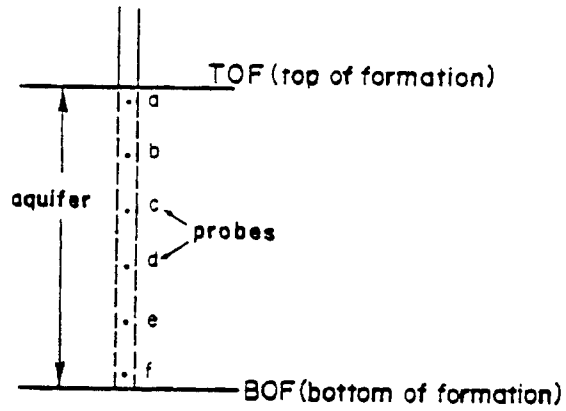
POSITION	ELEVATION (M) Ft.		
	M	Ft.	
TOF	38.04	(124.8)	
a	41.70	(136.8)	Datum is a spike
b	45.60	(149.6)	located in an
c	49.50	(162.4)	electrical power
d	53.40	(175.2)	pole
e	57.30	(188.)	
f	61.20	(200.8)	
BOF	62.42	(204.8)	

WELL NO. 6
(After 12/22/81)

TOF (top of formation)

aquifer

probes

a
b
c
d
e
f

BOF (bottom of formation)
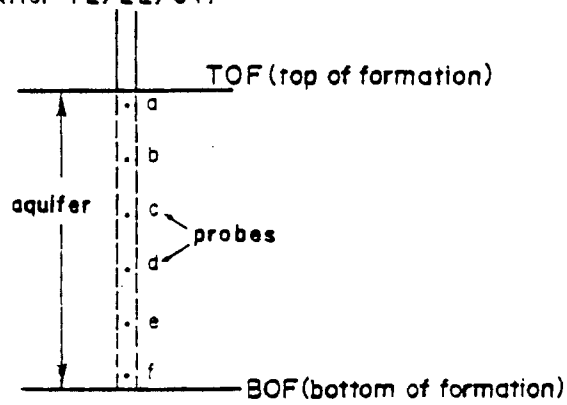
POSITION	ELEVATION (M) Ft.		
	M	Ft.	
TOF	38.04	(124.8)	
a	38.19	(125.3)	Datum is a spike
b	42.09	(138.1)	located in an
c	45.99	(150.9)	electrical power
d	49.90	(163.7)	pole
e	53.80	(176.5)	
f	57.70	(189.3)	
BOF	62.42	(204.8)	
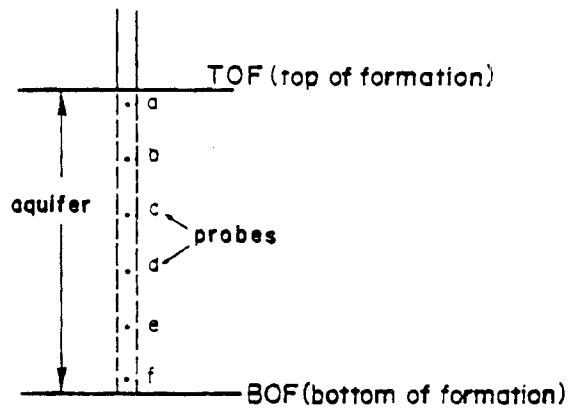
WELL NO. 7

POSITION	ELEVATION (M) Ft.		
	M	**Ft.**	
TOF	38.15	(125.2)	⎫
a	38.77	(127.2)	⎬ Datum is a spike
b	42.67	(140)	located in an
c	46.57	(152.8)	electrical power
d	50.47	(165.6)	pole
e	54.38	(178.4)	
f	58.28	(191.2)	
BOF	59.80	(196.2)	⎭
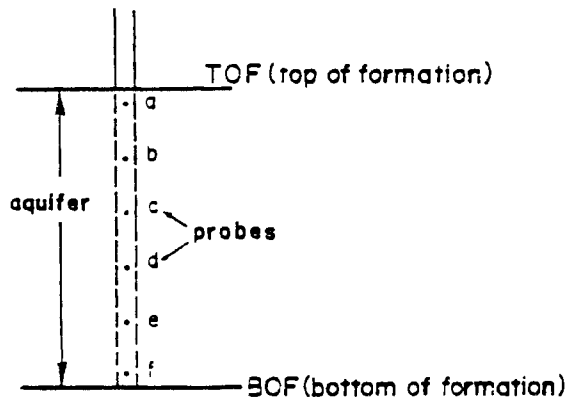
WELL NO. 8

POSITION	ELEVATION (M) Ft.		
	M	**Ft.**	
TOF	38.55	(126.3)	⎫
a	40.08	(131.5)	⎬ Datum is a spike
b	43.98	(144.3)	located in an
c	47.88	(157.1)	electrical power
d	51.79	(169.9)	pole
e	55.69	(182.7)	
f	59.59	(195.3)	
BOF	60.49	(198.5)	⎭
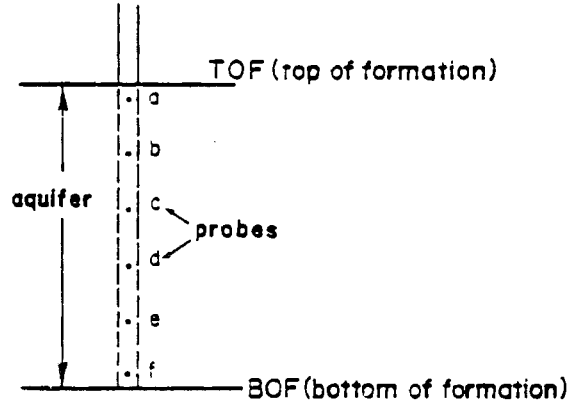
WELL NO. 9

POSITION	ELEVATION (M) Ft.		
	M	Ft.	
TOF	36.40	(126.)	
a	39.32	(129.)	Datum is a spike
b	43.22	(141.8)	located in an
c	47.12	(154.6)	electrical power
d	51.02	(167.4)	pole
e	54.92	(160.2)	
f	58.83	(193.)	
BOF	60.34	(196.)	
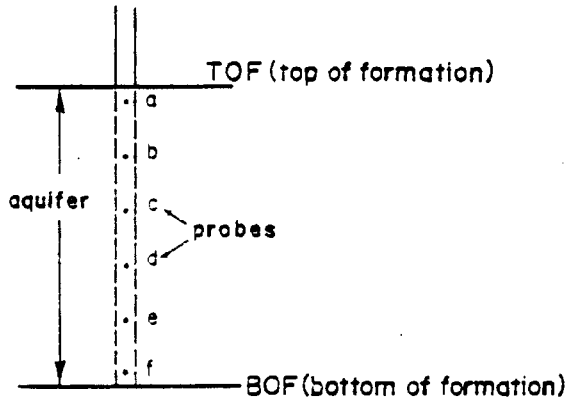
WELL NO. 10

POSITION	ELEVATION (M) Ft.		
	M	Ft.	
TOF	38.80	(127.3)	
a	35.45	(116.3)	Datum is a spike
b	39.35	(129.1)	located in an
c	43.25	(141.9)	electrical power
d	47.15	(154.7)	pole
e	51.05	(167.5)	
f	54.96	(160.3)	
BOF	60.44	(196.3)	

WELL NO. 11

TOF (top of formation)

aquifer

a
b
c — probes
d

e
f

BOF (bottom of formation)
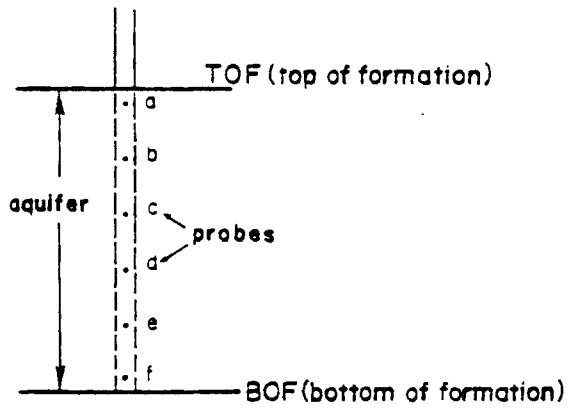
POSITION	ELEVATION (M) Ft.		
	M	Ft.	
TOF	38.92	(127.7)	
a	39.84	(130.7)	Datum is a spike
b	43.74	(143.5)	located in an
c	47.64	(156.3)	electrical power
d	51.54	(169.1)	pole
e	55.44	(181.9)	
f	59.34	(194.7)	
BOF	59.96	(196.7)	

WELL NO. 11
(After 12/22/81)

TOF (top of formation)

aquifer

a
b
c — probes
d

e
f

BOF (bottom of formation)
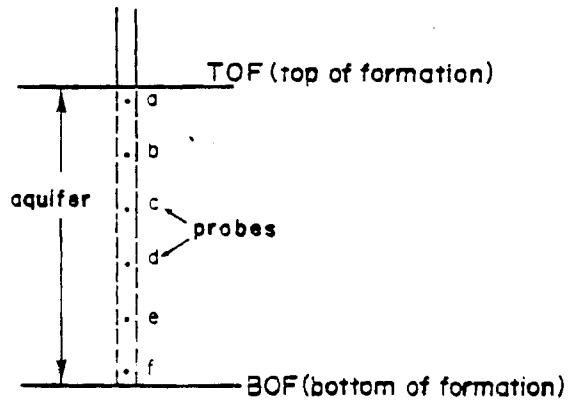
POSITION	ELEVATION (M) Ft.		
	M	Ft.	
TOF	38.92	(127.7)	
a	39.75	(130.4)	Datum is a spike
b	43.65	(143.2)	located in an
c	47.55	(156.)	electrical power
d	51.45	(168.8)	pole
e	55.35	(181.6)	
f	59.25	(194.4)	
BOF	59.95	(196.7)	

A.12

WELL NO. 12

POSITION   **ELEVATION (M) Ft.**

POSITION	M	Ft.	
TOF	39.03	(128.1)	
a	40.26	(132.1)	Datum is a spike
b	44.17	(144.9)	located in an
c	48.07	(157.7)	electrical power
d	51.97	(170.5)	pole
e	55.87	(183.3)	
f	59.77	(196.1)	
BOF	60.67	(199.1)	

WELL NO. 12
(After 12/22/81)

POSITION   **ELEVATION (M) Ft.**

POSITION	M	Ft.	
TOF	39.03	(128.1)	
a	40.05	(131.4)	Datum is a spike
b	43.95	(144.2)	located in an
c	47.85	(157.)	electrical power
d	51.76	(169.8)	pole
e	55.66	(182.6)	
f	59.56	(195.4)	
BOF	60.67	(199.1)	

WELL NO. 13

TOF(top of formation)

aquifer

BOF(bottom of formation)
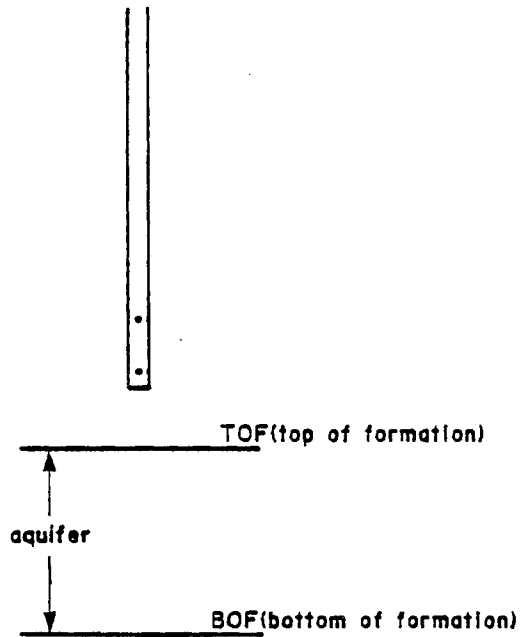
POSITION	ELEVATION (M) Ft.		
	M	Ft.	
a	33.25	(109.1)	Datum is a spike
b	34.78	(114.1)	located in an
TOF	39.04	(128.1)	electrical power
BOF	60.69	(199.1)	pole

WELL NO. 14

TOF(Top of formation)

aquifer

BOF(Bottom of formation)

a

b
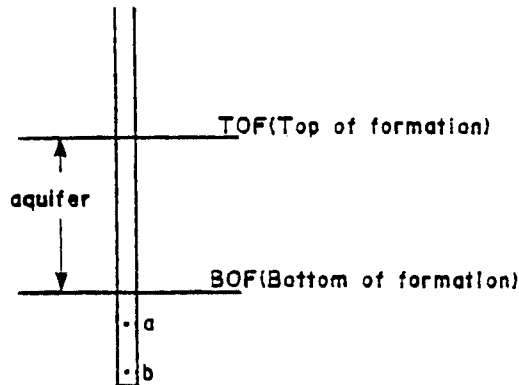
POSITION	ELEVATION (M) Ft.	
	M	Ft.
TOF	39.29	(128.9)
BOF	61.23	(200.9)
a	62.76	(205.9)
b	64.29	(210.9)

WELL NO. 15

TOF (top of formation)

aquifer

a
b
c — probes
d
e
f

BOF (bottom of formation)
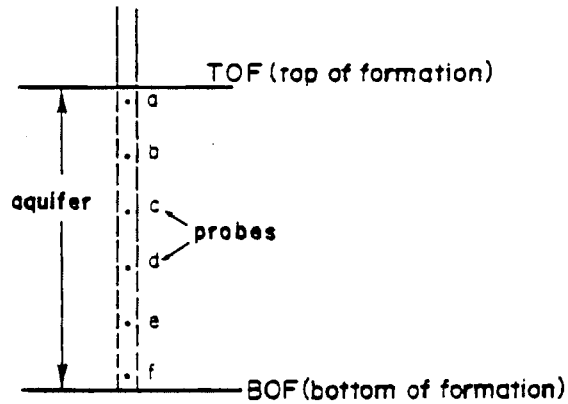
POSITION	ELEVATION (M) Ft.		
	M	**Ft.**	
TOF	**36.88**	(127.6)	⎫
a	_____	( )	⎪ Datum is a spike
b	_____	( )	⎬ located in an
c	_____	(.)	⎪ electrical power
d	_____	( )	⎪ pole
e	_____	( )	⎪
f	_____	( )	⎪
BOF	**60.52**	(198.6)	⎭

WELL NO. 16

TOF (top of formation)

aquifer

a
b
c — probes
d
e
f

BOF (bottom of formation)
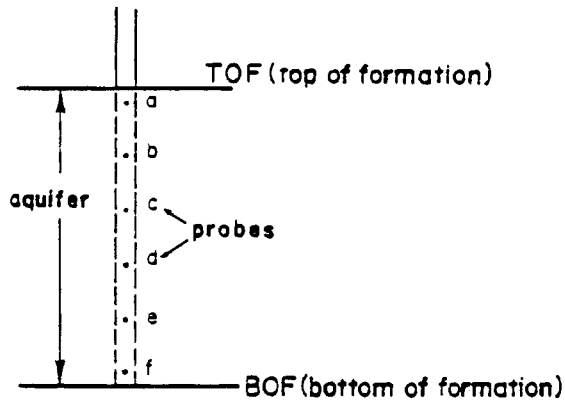
POSITION	ELEVATION (M) Ft.		
	M	**Ft.**	
TOF	**39.03**	(128.1)	⎫
a	_____	( )	⎪ Datum is a spike
b	_____	( )	⎬ located in an
c	_____	( )	⎪ electrical power
d	_____	( )	⎪ pole
e	_____	( )	⎪
f	_____	( )	⎪
BOF	**60.67**	(199.1)	⎭
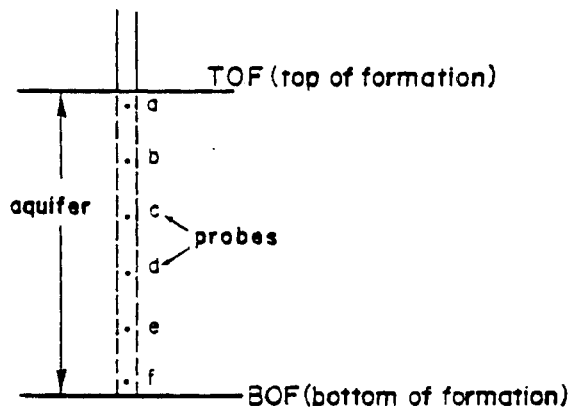
WELL NO. 17

POSITION	ELEVATION (M) Ft.		
	M	**Ft.**	
TOF	38.78	(127.2)	Datum is a spike
a	_____	( )	located in an
b	_____	( )	electrical power
c	_____	( )	pole
d	_____	( )	
e	_____	( )	
f	_____	( )	
BOF	60.40	(198.2)	

WELL NO. 18

POSITION	ELEVATION (M) Ft.		
	M	**Ft.**	
TOF	38.83	(127.4)	Datum is a spike
a	_____	( )	located in an
b	_____	( )	electrical power
c	_____	( )	pole
d	_____	( )	
e	_____	( )	
f	_____	( )	
BOF	_____	(197.4)	

WELL NO. 19

TOF (top of formation)

aquifer — probes

BOF (bottom of formation)
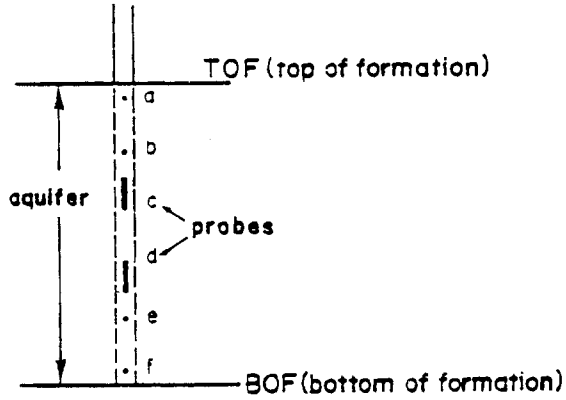
POSITION		ELEVATION (M) Ft.		
		M	Ft.	
TOF		38.78	(127.2)	} Datum is a spike
a			( )	located in an
b			( )	electrical power
c	Top sampler →	46.70	(153.2)	pole
d	Bottom sampler →	52.79	(173.2)	
e			( )	
f			( )	
BOF		60.73	(199.2)	

WELL NO. 20

TOF (top of formation)

aquifer — probes

BOF (bottom of formation)
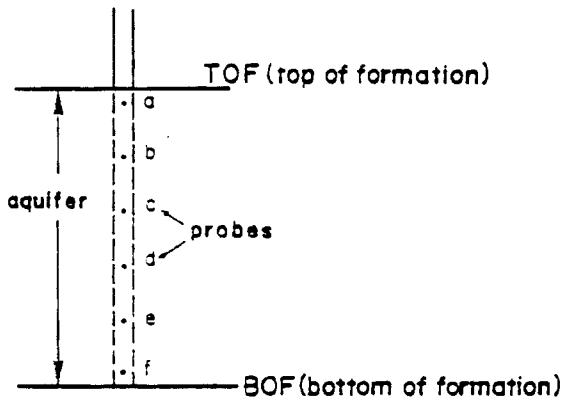
POSITION	ELEVATION (M) Ft.		
	M	Ft.	
TOF	38.48	(126.3)	} Datum is a spike
a		( )	located in an
b		( )	electrical power
c		( )	pole
d		( )	
e		( )	
f		( )	
BOF	60.73	(199.3)	
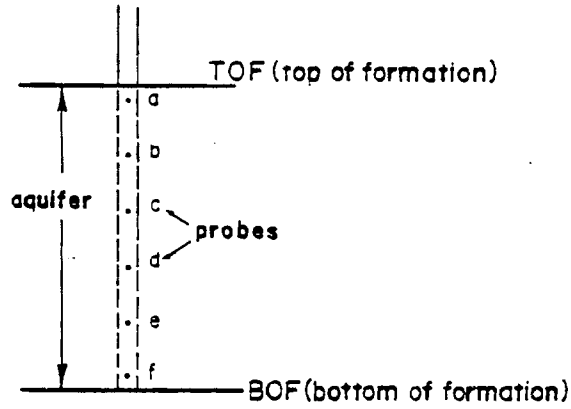
WELL NO. 21

POSITION	ELEVATION (M) Ft.		
	M	Ft.	
TOF	40.16	(131.8)	Datum is a spike located in an electrical power pole
a	_____	( )	
b	_____	( )	
c	_____	( )	
d	_____	( )	
e	_____	( )	
f	_____	( )	
BOF	61.5	(201.8)	

WELL NO. 22

POSITION	ELEVATION (M) Ft.		
	M	Ft.	
TOF	39.61	(129.9)	Datum is a spike located in an electrical power pole
a	_____	( )	
b	_____	( )	
c	_____	( )	
d	_____	( )	
e	_____	( )	
f	_____	( )	
BOF	60.94	(199.9)	

WELL NO. 23

TOF (top of formation)

aquifer · a
· b
probes · c
· d
· e
· f

BOF (bottom of formation)
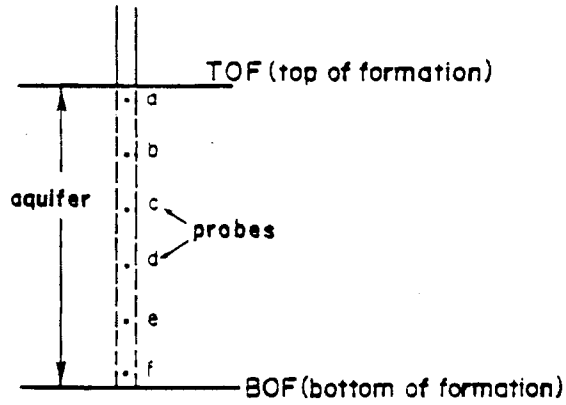
POSITION	ELEVATION (M) Ft.	
	M	**Ft.**
TOF	39.08	(125.2)
a	_____	( )
b	_____	( )
c	_____	( )
d	_____	( )
e	_____	( )
f	_____	( )
BOF	50.41	(198.2)

Datum is a spike located in an electrical power pole

WELL NO. 24

TOF (top of formation)

aquifer · a
· b
· c
probes · d
· e
· f

BOF (bottom of formation)
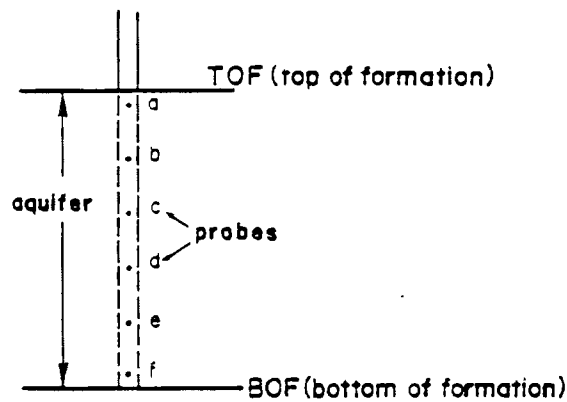
POSITION	ELEVATION (M) Ft.	
	M	**Ft.**
TOF	40.05	(131.4)
a	_____	( )
b	_____	( )
c	_____	( )
d	_____	( )
e	_____	( )
f	_____	( )
BOF	62.00	(203.4)

Datum is a spike located in an electrical power pole

WELL NO. 25
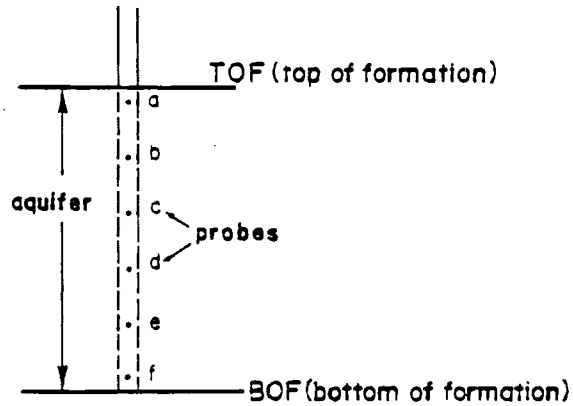
POSITION   ELEVATION (M)Ft.

POSITION	M	Ft.	
TOF	38.82	(127.4)	
a	———	( )	Datum is a spike
b	———	( )	located in an
c	———	( )	electrical power
d	———	( )	pole
e	———	( )	
f	———	( )	
BOF	60.15	(197.4)	
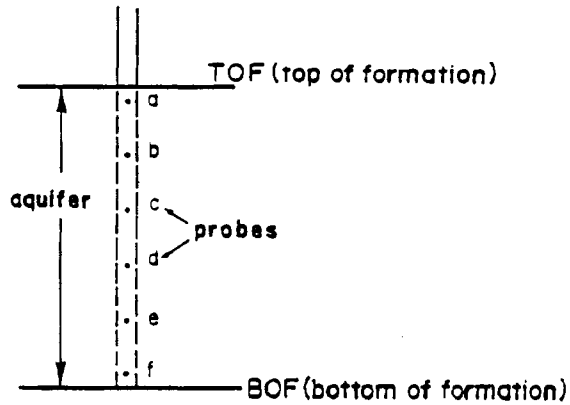
WELL NO. 26

POSITION   ELEVATION (M)Ft.

POSITION	M	Ft.	
TOF	39.11	(128.3)	
a	———	( )	Datum is a spike
b	———	( )	located in an
c	———	( )	electrical power
d	———	( )	pole
e	———	( )	
f	———	( )	
BOF	60.75	(199.3)	
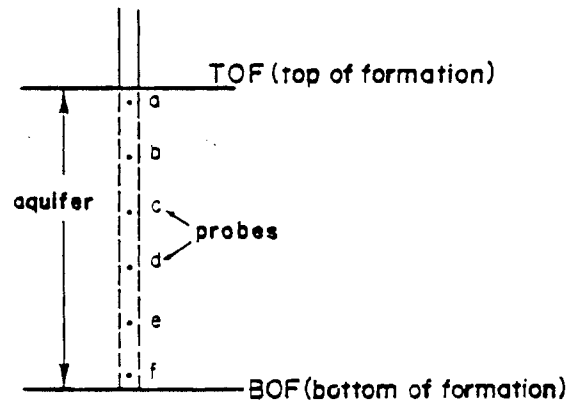
WELL NO. <u>27</u>

POSITION	ELEVATION (M) Ft.	
	M	**Ft.**
TOF	<u>40.74</u>	(133.7)
a	_____	( )
b	_____	( )
c	_____	( )
d	_____	( )
e	_____	( )
f	_____	( )
BOF	<u>60.86</u>	(199.7)

Datum is a spike located in an electrical power pole

WELL NO. <u>28</u>
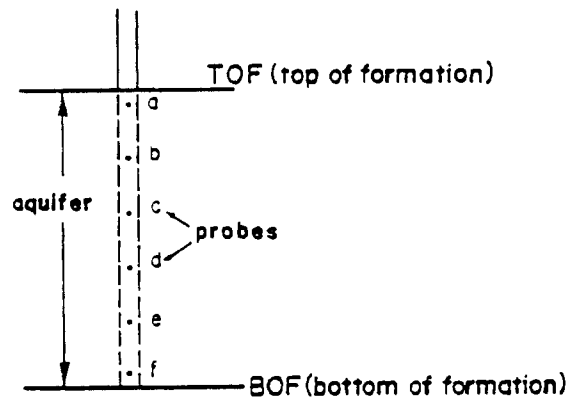
POSITION	ELEVATION (M) Ft.	
	M	**Ft.**
TOF	<u>43.53</u>	(142.8)
a	_____	( )
b	_____	( )
c	_____	( )
d	_____	( )
e	_____	( )
f	_____	( )
BOF	<u>58.07</u>	(193.8)

Datum is a spike located in an electrical power pole

WELL NO. 29
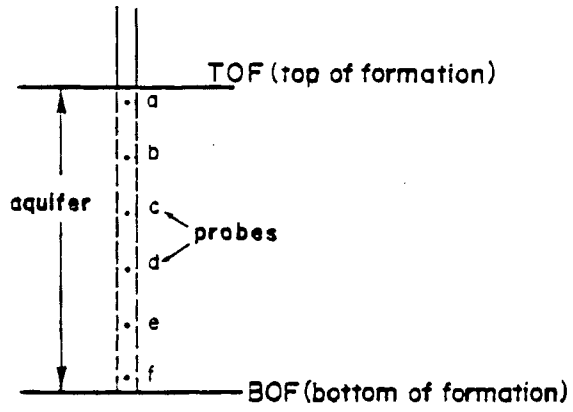
POSITION	ELEVATION (M) Ft.		
	M	Ft.	
TOF	43.71	(143.4)	
a	_____	( )	Datum is a spike
b	_____	( )	located in an
c	_____	( )	electrical power
d	_____	( )	pole
e	_____	( )	
f	_____	( )	
BOF	61.09	(200.4)	

WELL GEOMETRY AND MATERIALS

WELL	SIZE Casing/ Screen	CASING	PIPE	SCREEN	COMMENTS
I2	8"/6"	130 (ft) steel	10 (ft) steel	70 (ft) steel	L-R lead seal, packer installed for recovery
S2	8"/6"	130	10	70	L-R lead seal
I1	8"/6"	139	--	30	
S1	8"/6"	82	--	32	Supply water from upper formation in earlier experiments.
1	4"/2"	131	12 PVC	65 PVC	Backfilled, figure K L-R packer
2	4"/2"	131	15.2	65.3	Backfilled, figure K L-R packer
3	4"/2"	131.3	5.3	65.5	Backfilled, figure K L-R packer
4	4"/2"	131	11	65.5	PVC collar with 2" RH PVC female pickup, backfilled for thermistors
5	4"/2"	131	6	65.5	PVC collar with 2" RH PVC female pickup, backfilled for thermistors

WELL	SIZE Casing/ Screen	CASING		PIPE		SCREEN		COMMENTS
6	6"/4"	131 (ft)	PVC	-- (ft)	PVC	65.5 (ft)	PVC	Backfilled, a well from earlier experiment
7	4"/2"	131	steel	5.3	PVC	65.5	PVC	Rag packer, 2" RH female PVC pick-up, backfilled for thermistors
8	4"/2"	131		10		65		PVC collar, 2" RH female PVC pick-up, backfilled
9	4"/2"	131		5.3		65.5		PVC collar, 2" RH female PVC pick-up, backfilled
10	4"/2"	131		5.3		65.5		PVC collar, 2" RH female PVC pick-up, backfilled
11	6"/4"	131	PVC	--		65.5		Backfilled, a well from earlier experiment
12	4"/2"	131	steel	5.6	PVC	65.5	PVC	PVC collar with 2" RH female PVC pickup, back-filled
13	4"/2"	106		15.5		5.2		2" figure K LR packer, back-filled
14	4"/2"	207		21		5		2" figure K LR packer, back-filled
15	4"/2"	131		40	steel	5	steel	Lead seal with L-R thread, back-filled around 1" fiberglass perfo-rated tube in the 5' sampling sect.

WELL	SIZE, Casing/ Screen	CASING		PIPE		SCREEN		COMMENTS
16	4"/2"	131 (ft) steel		40 (ft) steel		5 (ft) steel		Lead seal with L-R thread, back-filled around 1" fiberglass perfo-rated tube in the 5' sampling sect.
17	4"/2"	131		60		10		Upper sampling zone, 134.6 ft to 139.6 ft; lower zone, 190.3 ft to 195.3 ft; backfilled around 1" perforated fi-berglass tube in the two sampling sections; LR lead seal
18	4"/2"	131		60		10		Upper sampling zone, 135 ft to 140 ft; lower zone, 190 ft to 195 ft; R-R lead seal
19	6"/4"	131	PVC	--		10	PVC	Barcad samplers installed at 153.2 ft and 173.2 ft, back-filled, a well from an earlier experiment
20	6"/4"	131		--		10	PVC	A well from an earlier experi-ment
21	4"/2"	131	steel	5	steel	66.3	steel	L-R lead seal

A.25

WELL	SIZE Casing/ Screen	CASING	PIPE	SCREEN	COMMENTS
22	4"/2"	131 (ft) steel	5 (ft) steel	66.3 (ft) steel	L-R lead seal, tracer sampling taken in middle of aquifer
23	4"/2"	131	5.3	66.3	L-R lead seal
24	6"/4"	--	--	--	Well from previous experiment
25	6"/4"	131	--	66.3 PVC	Well from earlier experiment
26	6"/4"	131	5.3	66.3	Well from earlier experiment
27	6"/4"	131	5.3	66.3	Well from earlier experiment
28	4"/2"	131	18	61 steel	L-R lead seal
29	4"/2"	131	15.7	61	R-R lead seal
R1	4"/2"	--	--	--	Screened from 161.7 ft to 191.5 ft, submersible pump used for rejection pumping

DISTRIBUTION

No of
Copies

No of
Copies

OFFSITE

US Department of Energy
Attn: J. Brogan
Office of Energy Systems Res.
Forrestal Bldg, CE-141 5E-052
Washington, DC 20585

US Department of Energy
Attn: I. Gyuk
Office of Energy Systems Res.
Forrestal Bldg, CE-141 5E-052
Washington, DC 20585

US Department of Energy
Attn: R. Shivers
Office of Energy Systems Res.
Forrestal Bldg, CE-141 5E-052
Washington, DC 20585

US Department of Energy
Attn: Director, Policy and
  Planning
Office of Conservation and
  Solar Applications
Washington, DC 20545

27 DOE Technical Information
   Center

Argonne National Laboratory
Solar Thermal Storage Program
Attn: A. Michaels
Building 362
9700 S. Cass Avenue
Argonne, IL 60439

75 Auburn University
   Attn: F. J. Molz
   School of Engineering
   Auburn, AL 36830

Colorado School of Mines
Attn: Donald Langmuir
Dept of Chemistry and
  Geochemistry
Golden, CO 80401

GeoTrans Inc.
Attn: J. W. Mercer
PO Box 2550
Reston, VA 22090

Walter Hausz
4520 Via Vistosa
Santa Barbara, CA 93110

Lawrence Berkeley Laboratory
Attn: C. F. Tsang
University of California
Bldg. 90, Room 1012-H
1 Cyclotron Road
Berkeley, CA 94720

Lawrence Livermore Laboratory
Attn: Tech. Info. Dept, L-3
University of California
PO Box 808
Livermore, CA 94550

Charles F. Meyer
1141 Cima Linda Lane
Santa Barbara, CA 93108

Midwest Research Institute
Attn: Charles Lee
425 Volker Blvd.
Kansas City, MO 64110

Minnesota Geological Survey
Attn: M. Walton
319 15th Avenue S.E.
Minneapolis, MN 55455

National Aeronautics and
 Space Administration
Asst. Adm. for Energy Programs
Washington, DC 20546

National Science Foundation
Division of Advanced Energy
 Research and Technology
Room 1140
1800 G Street, NW
Washington, DC 20550

New York State Energy
  Research & Development
  Agency
Attn: Director
Rockefeller Plaza
Albany, NY 12223

New York State Energy
  Research & Development
  Agency
Attn: Gunnar Walmet
Rockefeller Plaza
Albany, NY 12223

Oak Ridge National Laboratory
Attn: J. F. Martin
PO Box Y
Oak Ridge, TN 37830

Office of Congressman
  Sid Morrison
Attn: Kevin Billings,
  Legislative Asst.
1330 Longworth Bldg.
Washington, DC 20515

Rocket Research
Attn: L. B. Katter
York Center
Redmond, WA 98052

Sandia Laboratories
Attn: L. Radosevich
PO Box 969
Livermore, CA 94550

Sandia Laboratories
Technical Library Div. 3141
Albuquerque, NM 87185

Sandia Laboratories
Attn: William G. Wilson
PO Box 969
Organization 8453
Livermore, CA 94550

Solar Energy Research Inst.
Attn: Director
1536 Cole Blvd.
Golden, CO 80401

Tennessee Valley Authority
Attn: William Waldrop
Asst. Branch Chief
Water Systems Develop. Branch
Division of Water Management
PO Drawer E
Norris, TN 37828

Terra Tek, Inc.
Attn: C. Cooley
University Research Park
400 Wakara Way
Salt Lake City, UT 84108

TRW Energy Systems Group
Attn: E. Berman
Technical Library
7600 Colshire Drive
McLean, VA 22101

Union Carbide Corporation
Nuclear Division
Attn: Library
Y-12 Plant
PO Box Y
Oak Ridge, TN 37830

University of Minnesota
Attn: W. E. Soderberg
Program Director, ATES
Physical Plant Operations
200 Shops Bldg.
319 15th Avenue S.E.
Minneapolis, MN 55455

US Army Corps of Engineers
Attn: Library
PO Box 59
Louisville, KY 40202

US Department of Interior
Attn: Natural Resources
  Library, Lucy Howton
Serials Branch (G/E)
Washington, DC 20240

FOREIGN

Bengt Hidemark Gosta Danielson
 Arkitekter SAR
Attn: A. Boysen
Jarntorget 78
S-11 29 Stockholm
Sweden

Public Works of Canada
Attn: E. L. Morofsky
C456 Sir Charles Tupper Bldg.
Riverside Dr. and Heron Rd.
Ottawa, Ontario
K1A 0M2 Canada

ONSITE

DOE Richland Operations Off.

H. E. Ransom/D. R. Segna

33 Pacific Northwest Laboratory

S. C. Blair
W. Deutsch
T. J. Doherty
L. D. Kannberg (20)
C. T. Kincaid
J. R. Raymond
L. Vail
Technical Information (5)
Publishing Coordination (2)